A STUDY ON THE EFFECT OF THMC CONDITIONS ON SCRATCH TEST MEASUREMENTS

BY

MOHAMMAD RASHEED KHAN

A Thesis Presented to the
DEANSHIP OF GRADUATE STUDIES

KING FAHD UNIVERSITY OF PETROLEUM & MINERALS

DHAHRAN, SAUDI ARABIA

In Partial Fulfillment of the
Requirements for the Degree of

MASTER OF SCIENCE

In

PETROLEUM ENGINEERING

APRIL 2019

KING FAHD UNIVERSITY OF PETROLEUM & MINERALS
DHAHRAN- 31261, SAUDI ARABIA
DEANSHIP OF GRADUATE STUDIES

This thesis, written by **MOHAMMAD RASHEED KHAN** under the direction of his thesis advisor and approved by his thesis committee, has been presented and accepted by the Dean of Graduate Studies, in partial fulfillment of the requirements for the degree of **MASTER OF SCIENCE IN PETROLEUM ENGINEERING**.

Dr. Dhafer A. Al Shehri
Department Chairman

Dr. Salam A. Zummo
Dean of Graduate Studies

21/4/19
Date

Dr. Guenther Glatz
(Advisor)

Dr. Devon Chikonga Gwaba
(Member)

Dr. Shirish Patil
(Member)

This thesis is dedicated to my beloved parents and wife who encouraged me to pursue grad-school and have been the greatest source of inspiration in all things great and small.

ACKNOWLEDGMENTS

First, I would like to thank Allah, The Almighty for his blessings, which made this thesis completion possible.

I am extremely grateful to my advisor Dr. Guenther Glatz for his continuous support and encouragement throughout my MSc. study and research. His inspiration, passion, and vast knowledge played a big role in timely completion of my degree. Dr. Glatz provided expert guidance right from day one of the degree program until the writing of this thesis report. I could not have envisioned having a superior coach and advisor for my MSc. thesis.

In addition to Dr. Glatz, I express honest thankfulness to the thesis committee: Dr. Devon C. Gwaba and Dr. Shirish Patil, for their incredible help and expert direction, which helped me to improve throughout the course of my thesis.

Special gratitude to Dr. Gallyam Aidagulov, Research Scientist at Schlumberger, for providing critical insight in to the theoretical concepts and taking out his valuable time to help me in improving this thesis report.

I would like to convey appreciation to Schlumberger Dhahran Carbonate center for Research headed by Dr. Mohamed Badri who introduced me to the research being conducted and provided a chance to be part of a collaboration between SLB and KFUPM. Furthermore, credit goes to Dr. Mustapha Abbad, Program Manager Production and Completion group who made it possible to work under his group during my internship with them.

I would also like to praise the efforts of the staff at the Petroleum Engineering labs at KFUPM including Mr. Assad, Mr. Abdul-Sumed, Mr. Eassa, and Mr. Ammar who provided utmost technical assistance whenever it was required. Special thanks to Mr. Mobeen Murtaza for introducing me to key laboratory procedures and guiding me during experimental work. Furthermore, the researchers at Center for Integrative Petroleum Research (CIPR), KFUPM were helpful in giving key inputs and allowed me to use their facilities. Worth mentioning here would be Mr. Sarmad, Mr. Rizwan, Mr. Redha, and Mr. Hani.

Sincere gratitude to all my friends and colleagues at KFUPM for supporting me throughout the degree program.

This section would be incomplete without mentioning my family. My parents were the force behind my decision to pursue higher education and without their support it would never have been possible to achieve the success which I have today. In addition, my beloved wife deserves special thanks for her love and encouragement that kept me motivated and provided purpose to progress towards my goals. Finally, my siblings deserve credit for always being there to cheer on my accomplishments.

TABLE OF CONTENTS

LIST OF TABLES

LIST OF FIGURES

LIST OF ABBREVIATIONS

API	:	American Petroleum Institute
BB	:	Berea Buff
BG	:	Berea Grey
CT	:	Computed Tomography
DOC	:	Depth of Cut
DP	:	Desert Pink
ILS	:	Indiana Limestone
ISE	:	Intrinsic Specific Energy
KDE	:	Kernel Density Estimate
LEFM	:	Linear Elastic Fracture Mechanics
QEMSCAN	:	Quantitative Evaluation of Minerals by Scanning Electron Microscopy
SEL	:	Size Effect Law
SEM	:	Scanning Electron Microscope
SPHB	:	Split Hopkinson Pressure Bar
THMC	:	Thermal-Hydrological-Mechanical-Chemical
UCS	:	Unconfined Compressive Strength
XRD	:	X Ray Diffraction
XRF	:	X Ray Fluorescence

ABSTRACT

Full Name : Mohammad Rasheed Khan
Thesis Title : A Study on the Effect of THMC Conditions on Scratch Test Measurements
Major Field : Petroleum Engineering
Date of Degree : April 2019

Rock strength determination from scratch test allows correlation of the cutting specific energy to the uniaxial compressive strength (UCS) without completely destroying the specimen. The continuous nature of the scratch test helps to identify sections of interest within a core making it a valuable decision-making tool in core analysis workflows. Ideally, rock strength is measured in situ. Currently, however, no commercial technology exists allowing to perform a continuous scratch test directly at the reservoir formation of interest. Also, any in situ technique based on the principle of cutting specific energy would collect measurements with the rock being in a wetted and loaded state at reservoir temperatures. Conventionally, laboratory scale scratch tests are executed on a dry and unloaded sample at room temperature. If an in situ scratch test tool, however, existed, correlations are needed to translate logging data into standardized measurements to be used in, e.g., drilling mud design for ensuring wellbore stability. Accordingly, we investigate the effect of the wetting state of specimens on the UCS data derived from scratch tests. Particularly, we age outcrop samples under defined temperature and fluid saturations to elucidate the impact of reservoir conditions on UCS measured. This study provides quantifiable evidence of change in rock strength characteristics at conditions closer to reservoir conditions. Experimental weakening as a consequence of saturation and aging of

the rock samples was observed. This points to a methodical overestimation of in situ strength if results of testing at ambient (room temperature and dry sample) conditions are to be extrapolated to the field scale. The novelty of this research stems from the fact that the investigation of the UCS utilizing the scratch test has not been conducted at varying Thermo-Hydro-Mechanical-Chemical (THMC) conditions.

ملخص الرسالة

الاسم الكامل: محمد رشيد خان

عنوان الرسالة: دراسة عن تأثير شروط THMC على قياسات اختبار الخدش

التخصص: هندسة البترول

تاريخ الدرجة العلمية: أبريل 2019

يسمح تحديد قوة الصخور من اختبار الخدش بربط الطاقة المعينة بالقطع و قوة الضغط أحادية المحور (UCS) دون إتلاف العينة. تساعد الطبيعة المستمرة لاختبار الخدش على تحديد المقاطع ذات الاهتمام داخل العينات مما يجعلها أداة قيمة لاتخاذ القرارات في سير عمل تحليل العينات. من الناحية المثالية يتم قياس قوة الصخور في الموقع الاصلى ومع ذلك لا توجد تكنولوجيا تجارية تسمح بإجراء اختبار خدش مستمر مباشرة في طبقات الخزان. أيضا فإن أي تقنية في الموقع تعتمد على مبدأ قطع الطاقة المحددة من شأنها جمع القياسات مع وجود الصخور في حالة رطبة ومحملة في درجات حرارة الخزان. تقليديا يتم تنفيذ اختبارات خدش على نطاق المختبر على عينات جافة و مفرغة في درجة حرارة الغرفة. في حالة وجود أداة اختبار خدش في الموقع ستكون هناك حاجة إلى الارتباطات لترجمة بيانات تسجيل الدخول إلى قياسات موحدة لاستخدامها على سبيل المثال تصميم طين الحفر لضمان استقرار حفرة البئر. وفقًا لذلك فإننا نتحرى تأثير حالة ترطيب العينات على بيانات UCS المستمدة من اختبارات الخدش. على وجه الخصوص قمنا بتفريغ عينات النتوء تحت درجة حرارة محددة وتشبع السوائل لتوضيح تأثير ظروف الخزان على UCS المقاسة. تقدم هذه الدراسة دليلًا عمليًا على التغير في خصائص قوة الصخور في ظروف أقرب إلى ظروف الخزان. وقد لوحظت نتيجة للتجربة إضعاف التشبع والشيخوخة من عينات الصخور. هذا يشير إلى المبالغة في تقدير القوة في الموقع الطبيعي إذا كانت نتائج الاختبار في الظروف المحيطة يجب استقراءها. تنبع الجدة من هذا البحث من حقيقة أن محاولة خدش اختبار الصخور بالقرب من ظروف الخزان لم يتم إجراؤها من قبل.

CHAPTER 1

INTRODUCTION

1.1 Unconfined Compressive Strength

The accurate estimation of rock mechanical parameters play a critical role in designing and evaluating drilling, reservoir, and production engineering related programs (Aadnøy and Looyeh 2011; Roegiers 1993). Geomechanical parameters including strength, and elastic moduli are essential for a plethora of wellbore completion challenges ranging from sand production to hydraulic fracture efficiency (Gatens et al. 1990).

Unconfined Compressive Strength (UCS) is a measure of rock strength. It is conventionally defined as the maximum axial compressive stress that a sample can bear under no confining stress. UCS is also known as uniaxial compressive strength as the nature of applied stress is limited to the longitudinal direction. It is an important geomechanical property, critical for many design applications in petroleum reservoirs, mining, and civil engineering projects (Gunsallus and Kulhawy 1984). Several petroleum engineering decisions are dependent on accurate estimation of UCS, for example:

- Wellbore stability during underbalanced drilling;
- Sand production prediction.

Standardized UCS test procedures have been outlined by ASTM D-2938 (1995) and ISRM (2015). These test procedures have been validated and reported by various researchers. A comprehensive discussion on UCS testing is found in a book chapter, “Uniaxial Strength

Testing" (Pells 1993). Different authors (Fener et al. 2005; Kahraman 2001; Tsiambaos and Sabatakakis 2004) have employed the standard test procedure for evaluating correlations to determine UCS from indirect methods. Modifications to UCS testing have also been reported with regards to load application (Sheshde and Cheshomi 2015). Also, test procedures for earth bricks (Aubert et al. 2016) and corrections for granite sample size (Yin et al. 2017) have been reported.

1.1.1 UCS Test Drawbacks

UCS tests have been carried out for the past many decades. Lately, indirect solutions for the determination of unconfined compressive strength values have emerged. The direct UCS test procedure being time-consuming and expensive led to the invention of an index system for UCS values of mining rocks (Laubscher 1990). UCS testing involves extensive and accurate sample preparation. In addition, high level of technical expertise in determining proper plug selection from core samples is required (Hack and Huisman 2002). Comparing direct UCS tests with other simpler index systems for compressive strength determination, it was found that the latter provided accurate estimation without the drawbacks (Hack and Huisman 2002). Another shortcoming of UCS testing is an underestimation of strength caused by premature failure due to the presence of microcracks/fractures (Khaksar et al. 2009). Using a height to diameter ratio less than 2.5 (Ulusay 2015) for the test specimen can lead to failure initiating from pre-existing cracks, misrepresenting the actual compressive strength (Farmer and Rakowski 1991; Dey and Halleck 1981). Additionally, improper end-face grinding can result in non-uniform loading and premature specimen failure inducing dispersion in experimental data (Liu et al. 2017). The specimen length to diameter aspect ratio for testing must be in a reasonable range. Too

small ratios will introduce end-effects as stated previously. Very large ratios, however, would lead to development of micro-cracks and defects during the loading process and, hence effecting the results. Non-repeatability is another disadvantage of UCS tests. Presence of micro-cracks, beddings, and fractures in heterogeneous cores, leads to tensile stress concentration even under pure compressional regimes, hence affecting rock failure (Marinos and Hoek 2001; Lan et al. 2010).

1.1.2 Indirect UCS Estimation

Due to the complexity and drawbacks of conventional direct UCS test procedures, researchers have conceived numerous alternatives to indirectly quantify the compressive strength of rock samples, like, point load tests (Broch and Franklin 1972), indentation/impact tests (Aydin and Basu 2005; Hill et al. 1989), and scratch tests (Detournay et al. 1997, 1995). To reduce the need for conducting time consuming and costly rock-mechanical experiments, researchers have started investigating the applicability of artificial intelligence techniques to determine rock mechanical parameters. Using extreme machine learning Liu et al. (2015) indirectly estimated UCS and reported results within tolerable error limits. The authors employed rock mineralogical content and structural properties as inputs for their algorithms. Tariq et al. (2017) utilized neural network to predict UCS of carbonate rocks. In this case, database of compressive strength values was employed to generate a correlation. Mohamad et al. (2015) The PSO-ANN hybrid predictive model was applied to estimate UCS. They utilized UCS database to train the basic model along with other basic rock tests and parameters such as bulk densities. Armaghani et al. (2016) applied the Imperialist Competitive Algorithm (ICA) as the optimization tool for ANN model to predict UCS of sandstone samples. Schmidt Hammer

Rebound Number, point load test, p-wave velocity, and UCS of 108 samples was incorporated into a database to generate model for the prediction. Having discussed the application of artificial intelligence techniques, however, it is important to mention that this only helps in investigating and improving correlations between UCS and other measurements. For computational intelligence methods to work, it is imperative that they have large sets of past experimental data.

The introduction of index tests (Deere and Miller 1966) was crucial in an effort to better define the reservoir strength characteristics. Strength tests conducted on plug samples are unable to capture effect of the whole reservoir section that is provided by a continuous log of strength. Indirect tests have the advantage of being quick, simple to perform, and partially or completely non-destructive as opposed to conventional UCS test. Also, indentation indices can provide UCS by testing even smallest of the specimen. Schmidt hammer and scratch tests can be deployed in the field to test freshly cored samples. Indirect testing, however, has its own inherent drawbacks. Schmidt hammer tests involve using a predefined energy to hit the sample with a loaded-mass (Aydin and Basu 2005). Depending on the energy of the loaded-mass, the rock sample may be prone to fractures or cracks (Brown 1981). As the name suggests, a point load test is not capable of providing a continuous log of strength (Broch and Franklin 1972). In addition, it was found that for certain experiments the measurements are poorly correlated with UCS (Fener et al. 2005). The Brinell/Rockwell hardness test (Vlis 1970) relies on a force provided by a standard size metallic ball which can result in unexpected failure in brittle rocks. Furthermore, it is slow to conduct on long cored intervals (Khaksar et al. 2009a). Indirect testing methodologies are marred by various external factors which impact their correlation to

UCS such as the shape of rock specimen along with the moisture content (Hucka 1965; Tsiambaos and Sabatakakis 2004), and degree of surface roughness among other factors (Tsur-Lavie and Denekamp 1982).

This research focusses on utilizing a scratch machine developed in 1997 by Detournay et al. (1997) at the University of Minnesota. The equipment was originally designed to investigate the action of a PDC cutter on a rock sample. The interaction between cutter and rock gives rise to forces that can be used to determine the angle of internal friction along with the unconfined compressive strength (Adachi et al. 1996; Richard et al. 1998; Almenara and Detournay 1992; Detournay et al. 1995). Experimental evidence shows that the derived intrinsic specific energy (ISE) is directly correlated to UCS (Richard et al. 2012). The concept behind cutting tests has been the focus of several studies where it is employed to determine the compressive strength of rocks (He et al. 2017; Ferreira et al. 2014; Germay and Richard 2014; Suarez-Rivera et al. 2003; Dagrain et al. 2004; Schei et al. 2000). Various authors have also proposed the use of real-time drilling data to determine compressive strength utilizing the underlying principle of scratch tests (Kalantari et al. 2018; Reddish and Yasar 1996).

The scratch test is a common component of many core analysis workflows in the industry. In the Middle East, the scratch test was utilized in the fracturing design stage to determine optimum frac points in tight reservoirs by providing strength profile which is correlated to logs (Spain et al. 2015; Noufal et al. 2015). Scratch tests were used in the geomechanical characterization of unconventional shale oil reservoirs in Argentina (Varela et al. 2016).

Utilization of scratch test, however, has not gone beyond the conventional (i.e. testing under lab conditions) mode of acquiring the compressive strength profile. Accordingly, the primary objective of this thesis is to investigate the effect of aging and saturation dependent changes in rock compressive strength in a first effort to study the potential influence between reservoir and lab conditions. Ultimately, this would assist in determining the strength profile reflecting in situ conditions which are of more relevance in designing field operations demanding geomechanical properties. The necessity to determine in situ parameters is emphasized by:

1. The majority of empirical correlations are developed and tested under dry conditions (Chang et al. 2006). Their applicability to in situ conditions maybe limited given that existence of fluids in the pore space potentially affects bulk rock properties (Cargill and Shakoor 1990).
2. Petrophysical properties like porosity, permeability, and density of rocks change with varying saturation values, elevated temperatures, and pressures that have been reported to decrease mechanical integrity in some cases (Berckhemer et al. 1997; Holt 2001).
3. The samples required for UCS testing must be of ‘good’ quality. Macroscopic fractures/cracks, joints, and vuggy pores, however, may not be adequately captured under lab conditions (Khaksar et al. 2014; Germay and Richard 2014; Naeimipour et al. 2018).
4. The need for correlations/data to support potential commercialization of a conceptualized in situ geomechanical tool (see patent by Schlumberger) (Badri and Taherian 2013).

5. Deployment of miniature disc cutter tool in situ requires data under reservoir conditions. (Naeimipour et al. 2018).

1.1.3 The Scratch Test

The typical scratch tester consists of a sample holder with a loading fixture along with a movable cutter providing the rock scratching action. The main components of the device are shown in Fig. 1 and described below:

I. A detachable sample holder with clamps to keep the sample in place during operation (1)

II. A movable frame (2) consisting of the vertical positioning system (3),

III. Load cell (4), and the cutting element holder (5).

IV. Movement of the frame is controlled by a motor operated through the computer (6) by driving a horizontal motion screw (7) via a drive assembly (8).

V. LVDT (10) indicates the depth of cut, adjusted manually with the positioning system (9).

VI. The vertical motion is locked (11) against the frame, to provide a constant depth of cut during the scratch operation.

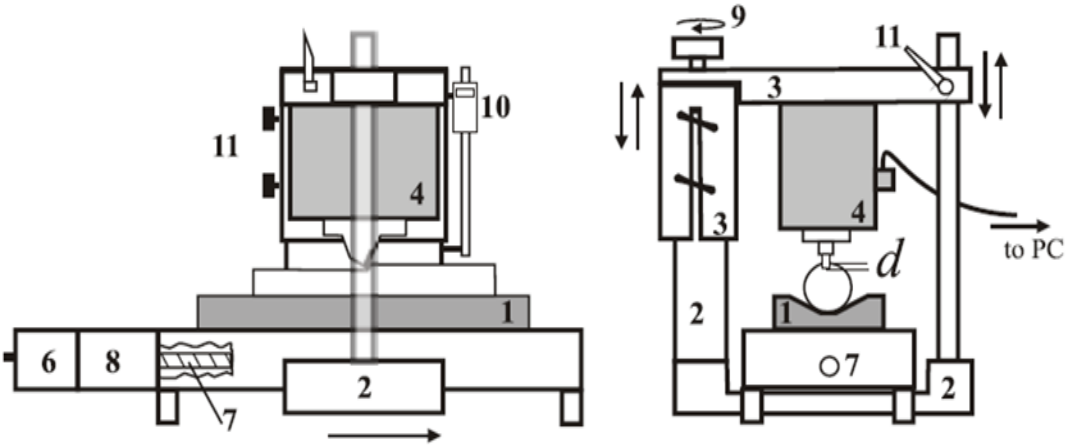

Figure 1: Sketch of a typical scratch machine (Dagrain et al. 2004.).

While scratching, there are two force components; horizontal, parallel to the direction of cutting and vertical, normal to the cutting surface. Both are measured by the load cell. The whole setup is computer controlled which allows for automatic system control, real-time data acquisition (RTA), and auto-control of the cutter velocity (Khaksar et al. 2009b). The software provides automatically rock UCS results.

A sharp cutter is dragged from one end of the core sample to the other at a predefined cutter depth. Rock-fragmentation ahead of the cutter face and frictional contact between the cutter and rock surface are processes occurring simultaneously as the cutter moves (Detournay and Defourny 1992). During the cutting action, two distinct failure mechanisms can occur depending on cutting depth:

1. Ductile mode
2. Brittle mode

The mode of interaction or failure is defined by a critical depth of cut (d*). For depths smaller than d*, ductile mode prevails else brittle mode occurs. Experiments indicate that this critical depth is dependent on rock fracture toughness and compressive strength among other factors (Richard et al. 1998). For sedimentary rocks, this ranges from 0.5 – 2 mm (Richard et al. 1998).

Plastic flow occurs in the ductile mode. In this case, the failure regime caused by the cutter, that can be characterized as a “flow” of failed rock material ahead of the cutter. Ductile mode is achieved as the rock is completely sheared in front of the cutter and crushed at the tip, shown in Fig. 2a. During this mode, the energy spent is associated with the volume of rock removed, consequently, indicating rock compressive strength (He and Xu 2015). The brittle mode is also termed as “chipping”. At the cutter tip, cracks are formed

which propagate further upwards. Once the cracks reach the specimen surface, a chip is formed that is subsequently removed by the moving cutter. This is shown in Fig. 2b. In this mode, however, dissipated energy is associated to the chipping effect (He et al. 2017). As a result, this energy is correlated to mode I fracture toughness yielding tensile strength (Richard et al. 2012).

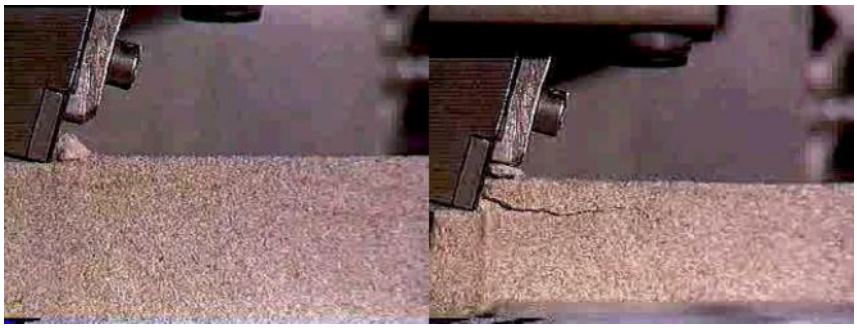

Figure 2: (a) Ductile failure mode (left) (b) Brittle failure mode (right) (He and Xu 2015).

Distinct relationships exist for both the failure mechanisms. The variables governing these relationships are the tangential component of cutting force, F_s, and the cutter depth, d. For ductile mode, at a constant cutter width, F_s is proportional to cutter depth. In the brittle mode, however, the proportionality does not hold as d increases. This is due to more energy used up for the chipping effect related to the surface of the crack. Accordingly, this gives rise to the conceptual explanation regarding energy consumption during the two modes leading to critical cutter depth, d^* (Richard et al. 1998). Greater energy is required for greater cutter depths owing to the chipping action. The opposite, however, is true for the ductile regime.

The existing scratch test model is based on the ductile regime (Detournay and Defourny 1992). The following three aspects independent of cutter wear are critical to rock/cutter interaction:

1. The forces on the cutter (averaged over a larger distance in comparison to cuter depth) is proportional to the cross-sectional area of the traced cut.
2. The angle of inclination of the averaged-out (resultant) force is consistent throughout the process.
3. Frictional contact exists at the rock-cutter interface.

Consequently, three parameters define this phenomenological model (Adachi et al. 1996), namely:

1. ε – *Intrinsic Specific Energy* (ISE) required for the cutting action.
2. ζ – number characterizing ratio of the drag to normal force acting on the cutter.
3. μ - friction coefficient actuated over the wear flat.

The resultant force acting on the cutter is a result of the cumulative effect of a force acting on the cutter face and another acting on the wear-flat rock surface. Components of these forces acting tangentially and normally to the cutting motion are illustrated in Fig. 3. Also shown is the back-rake angle, Θ that the cutter face makes with the vertical axis. The force components are described as:

$$\mathbf{F_s} = \boldsymbol{\varepsilon} \times \mathbf{A} \tag{1}$$

$$\mathbf{F_n} = \boldsymbol{\zeta} \times \boldsymbol{\varepsilon} \times \mathbf{A} \tag{2}$$

Where,

$$\mathrm{A} = \text{width of cut x depth of cut}$$

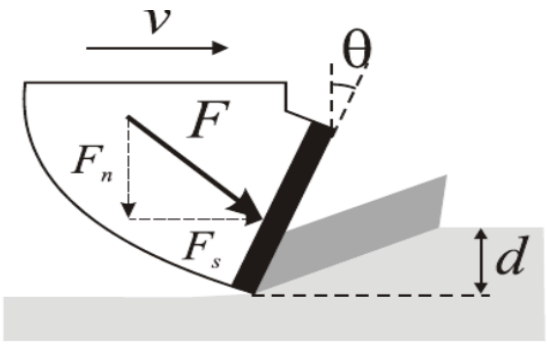

Figure 3: Force resolution at the cutter (Dagrain et al. 2004).

The model for scratch test interpretation assumes that intrinsic specific energy is independent of depth of cut and is a constant parameter defining an aggregate of cutter configuration and rock (Richard et al. 1998). It is imperative, however, to differentiate ISE from specific energy (SE). The former quantity, accounts only for the energy consumed to crush the rock neglecting any frictional dissipation related to cutter wear/bluntness. Conversely, SE characterizes the energy spent in cutting the rock and the energy consumed due to friction between rock and cutter surface. Based on the phenomenological model, therefore, the determination of rock strength employing scratch machines should be performed at a depth of cut where ductile regime is dominant (Richard et al. 2012). This is also reflected by a constant ISE value (Schei et al. 2000). By observing vertical and lateral forces that are established to sustain a particular cutter-depth, it is possible to estimate the intrinsic specific energy which is determined to be well correlated to the unconfined compressive strength (Richard et al. 2012; Detournay et al. 1995). Another reason for employing a model that is based on the ductile regime is due to the assumption that in direct UCS test, the sample fails in ductile mode rather than in brittle. Although numerically equivalent to the energy per unit volume, ISE is generally expressed as MPa due to its expected relation with UCS.

For a fixed cutter width, the tangential component of the force acting on the cutter is proportional to the depth of cut. Evidence of this is shown by Richard et al. (2012) by conducting experiments on a wide range of rock types. They plotted the tangential force with the depth of cut and performed a linear best fit for the set of data for each rock type. Using equations 1 and 2, the intrinsic specific energy can be inferred by using the slope divided by the cutter width.

1.2 Problem Statement

Scratch tests are not carried out under different THMC conditions. Currently UCS measurements are carried out at ambient conditions. Different THMC conditions, however, will impact the UCS values which are measured. This effect is not captured in the current techniques used to measure geomechanical properties.

A study of the THMC effects on rocks can have application in various fields:

- Petroleum Engineering
    - Wellbore stability
    - Sand production
- Geothermal Energy
- Mining
- Civil Engineering
- Nuclear Waste Disposal

Focusing on the Petroleum Engineering aspect, conclusions/data from this study will provide a stepping stone in developing the conceptualized geomechanical logging tool (patent by Dr. Badri from SLB) (Badri and Taherian 2013).

1.3 Objectives

The objective of this thesis is to elucidate the effect of various wetting states, and aging procedures, on measured geomechanical properties, particularly UCS. We seek to investigate the missing link that would help in mapping dry state lab measurements to in situ conditions and vice versa. This work aims to provide data mimicking in situ conditions that will aid in improving critical decisions concerning e.g., wellbore stability analysis. Particularly, conclusions from this investigation would support the development of borehole geomechanical logging tool technology as described in the patent by Schlumberger (Badri and Taherian 2013). In addition, interpretation model for technology capable of in situ data measurement in the field of mining would be possible (Naeimipour et al. 2018). The objectives can be broken down into the following distinct stages:

1. Investigate the effect of saturation and temperature conditions on unconfined compressive strength derived from scratch test for various carbonate and sandstone samples.
2. Morphological analysis of scratch generated powder
3. Developing best practices to carry-out scratch tests as no standard exists

CHAPTER 2

LITERATURE REVIEW

The literature survey is divided into two main parts. The first part discusses the effect of fluid saturation on rock strength, followed by temperature effects in the second part.

2.1 Factors Affecting Geomechanical Properties

It is well established that rock mineralogical composition and rock texture influence geomechanical parameters. Investigation on sandstone samples concluded that rock texture and contact controls strength and deformability characteristics (Dyke and Dobereiner 1991). Intact rock mechanical characteristics are dependent upon grain, crystal, and cementing material composition, in addition to, grain and crystal size, shape, orientation, distribution, and pore structure (Hawkes and Mellor 1970). Extrinsic factors also play a critical role in affecting the outcome of UCS testing. Specimen preparation, size, and testing methodology has been studied with respect to the effect on strength and other rock mechanical properties (Darlington et al. 2011). Sygala et al. (2013) reported that temperature has significant impact on geomechanical rock characteristics and the extent of this impact is governed by different rock properties. Water and moisture content is another parameter that has been extensively investigated for its outcome on the strength characteristics (Bauer 1980; Barton et al. 2008; Vásárhelyi and Ván 2006). In the context of rock engineering, several studies have been carried out reporting the effect of water-weakening on different rock types (Colback and Wiid 1965; Naghadehi et al. 2010; Risnes et al. 2005; Demarco et al. 2007).

2.1.1 Effect of the Coring Process

Reliable core analysis is highly dependent upon the extent of mechanical damage to the sample. Mechanical damage causes irreversible changes in properties even if the core is brought back to in situ conditions. This can potentially occur over the course of core drilling and during core retrieval (Santarelli and Dusseault 1991; Holt et al. 1994). During drilling, induced fractures and vibrations can have an adverse effect on sample quality. In addition, many rock properties might change during the tripping operations due to release of stress, pore fluid pressure, and temperature (Hettema et al. 2002). Fast decompression of cores due to high tripping rates may lead to creation of tensile fissures and micro-cracks in the center of the core, thus, damaging them internally (Ashena et al. 2018). Rosen et al. (2007) reported that the viscous forces created during rapid expansion and expulsion of gas are responsible for such damage. This phenomenon is particularly severe in the case of very low-permeability samples (McPhee et al. 2015). Various companies according to their experience have implemented safe tripping rates for core retrieval. These rates, however, are for specific cases and cannot be applied generally (Ashena and Thonhauser 2018).

2.1.2 Effect of Water

Before discussing the pore water effect on geomechanical properties, it is imperative to describe different terms used to define quantity of water absorbed by the test specimen. ‘Water saturation’ and ‘water content’ are two terms used in literature. Theoretically, the latter shows the absolute volume of water contained in the rock. This value is non-negative and can be greater than 1. The former term, whereas, shows the degree of saturation ranging from 0-1. The lower limit indicates completely dry rock, while the upper limit implies 100% water saturated rock. Fully saturated rocks have also been described in terms of

‘water absorption’ in the literature. Lack of pore communication may never give fully saturated conditions. Therefore, care should be practiced when interpreting results stating 100% saturation. Laboratory procedures for determining water content, absorption, saturation, and sample preparation should be given adequate attention at the beginning of the investigation. For example, water absorption determination using immersing techniques has been reported differently by investigators. In addition, weighing saturated sample which is surface dried is different. An early study reported significant variation among mechanical properties of air-dried and fresh sandstone samples (Burshtein 1969). It was recommended to avoid using these results to carry-out in situ rock behavior predictions based on dry samples. Rock preparation needs attention prior to core testing for geomechanical calculations. Price (1960) observed compelling differences between compressive strength of saturated, air-dried, and oven-dried sandstone. It is emphasized that usage of terms characterizing various states of rocks should be done accurately (Hawkes and Mellor 1970). These include, ‘saturated’, ‘oven-dried’, and ‘air-dried’.

2.1.2.1 Sandstone

Mann and Fatt (1960) investigated the effect of water saturation on the elastic properties namely; Young’s modulus, Poisson’s ratio, and bulk compressibility of sandstone. They concluded that the effect was dependent on amount of clay minerals present. Up to 20% decrement in the Young’s modulus and 30% increment in bulk compressibility of the wet samples was observed. The results with respect to Poisson’s ratio were inconclusive. Bauer (1984) reported that application of point-load tests on anisotropic sediments did not yield accurate results for UCS. Incorporation of a moisture content index, however, greatly improved compressive strength estimates. Reportedly, the reduction in rock strength is not

dependent on the total amount of water present but rather on the effective saturation (Bell 1978). It was also found that the percentage reduction in compressive strength decreased with samples of higher UCS when they were saturated. Ojo and Brook (1990) point out that test results should state the value of water/moisture content as this has resulted in reduction of both the tensile and compressive strength of rocks. Investigations on Pennant sandstone conclude that the geological micro-structure, and grain-matrix link (clayey matrix) affects the extent of reduction in strength due to water (Hadizadeh and Law 1991). A study claiming that the strength and deformability of weaker sandstones is more sensitive to water content (Dyke and Dobereiner 1991) was refuted in 1992 by another investigation. Hawkins and McConnell (1992) reported that a stronger variety of sandstone is more prone to strength reduction and this is more reliant on mineral content rather than the rock micro-structure. The effect of cyclic wetting-drying has also been extensively studied, resulting in mixed interpretations among researchers. One research pointed to no significant change in compressive strength even after 50 cycles of wetting-drying (Hale and Shakoor 2003). Deng et al. (2012), however, reported that the reduction in cohesion, compressive strength, and internal friction, after cycling through different states is significant. This is further challenged by a recent study (Zhao et al. 2017) which states that the reduction in strength is reinstated once the sample is brought back to the dry state. Contrary to several studies claiming the water-weakening effect, there are few investigations, which suggest the opposite. Conclusions from some studies suggest that this effect is non-existent in sandstone samples that contain a negligible amount of clayey minerals (Hadizadeh and Law 1991; Reviron et al. 2009).

2.1.2.2 Shale

The investigation of the compressive strength of shales should be looked upon with caution. Shales are type of formation that tend to deform and fail with time (Mishra and Verma 2015). Studies regarding the fluid saturation effect on shale compressive strength are available in the literature. Investigations on various shale rocks used as building stones found that dry samples exhibit the greatest compressive and shear strength in comparison to water saturated samples (Jumikis 1966). Investigation on coal mine shales revealed possible mechanisms of water-weakening. Increase in pore-water pressure, decrease in capillary tension, change in rock fabric, and a combination of chemical and corrosive degradation are responsible for strength reduction (Eeckhout 1976; Eeckhout and Peng 1975). Different researchers have come to similar conclusions that the reduction in strength is due to dissolution of certain minerals like chlorite or calcite due to water saturation. This increases the porosity, hence decreasing the rock strength (Silva et al. 2008; Anwar et al. 1998). Investigation on mud-shale, clay-shale, and mudstones found that upon saturation, strength reduction was up to 90% accompanied by a reduction of up to 84% in the modulus of elasticity (Lashkaripour and Ajalloeian 2000). In the same study, a negative-exponential correlation between compressive strength and water saturation was observed. Jiang et al. (2014) reported a decrease of about 89% in UCS from dry to saturated state in mudstone. They employed medical computer tomographic scanning to describe the weakening mechanism. Failure pattern initializes as micro-sized discontinuities followed by clay swelling giving rise to crack propagation.

2.1.2.3 Limestone

The geomechanical characteristics of carbonate reservoirs are of great interest due to the huge amounts of oil and gas reserves stored in them (Roehl and Choquette 1985). Some

estimates claim that conventional carbonate reservoirs make up 50-60% of global reserves (Burchette 2012). Many studies have suggested that water saturation can affect the mechanical characteristics of carbonates in a very strong manner. A study in 2005 suggested that in Miocene limestones the degradation in mechanical properties was evident and the relationship between dry and saturated values was linear in nature (Vasarhelyi 2005). Another study on limestone was carried out with regards to pore compressibility measurements (Carles and Lapointe 2005). It was concluded that compressibility measurements should be carried out under in situ saturation conditions to obtain accurate estimates for chalk reservoir modeling. This finding is supported by Sylte et al. (1999) through a study on the famous Ekofisk case, where compaction has been a huge problem. It was reported that water-weakening played a detrimental role in this chalk reservoir collapse and must be taken into account to revise the rock compressibility functions. Rajabzadeh et al. (2012) reported up to 70% decrease in the UCS value owing to water saturation of the limestone samples. Most of the work till date has focused on sandstones. In this work, however, the focus will also be on carbonate, which is the dominant reservoir rock type in Saudi Arabia.

2.1.3 Effect of Water on Tensile Strength

Tensile strength (TS) is also an important strength parameter. It is a critical input parameter in hydraulic fracture studies and fracture network modelling. Notably, water-weakening phenomenon on the TS of rocks has also been studied. Dube and Singh (1972) tested five types of sandstone samples with respect to the effect of atmospheric humidity on the tensile strength, yielding 48.6% decrease under completely saturated environment. Tensile strength decreased with an increase in porosity and humidity. During research on the effect

of moisture on various mechanical properties from sandstone samples in the United Kingdom, a reduction of 50% in tensile strength was observed (Ojo and Brook 1990). A study on Turkish sandstone specimen revealed a 63% reduction in tensile strength due to water saturation (Karakul and Ulusay 2013). The same study reported similar weakening effect on UCS. An investigation on limestones, concluded that the decline in tensile strength was related to a reduction in cohesive strength, which is affected by the interfacial free-energy (Parate 1973). Vutukuri (1974) investigated the effect of various liquids on the rock tensile strength of limestone samples. An exponentially decreasing relationship between strength and two parameters of the saturating liquids was determined; dielectric constant and surface tension. Vasarhelyi (2005) carried out a statistical analysis to determine the influence of water on the strength of Miocene limestone. A linear relation was established between dry and saturated rock tensile strength. In addition, an exponential relationship was reported between tensile strength and density of the samples.

2.1.4 Combined Effect of Water Saturation and Anisotropy

Numerous investigations focused on the effect of anisotropy and predicting the failure mechanism due to fissuring/jointing, stratification, foliation, bedding, and layering (Ghazvinian and Hadei 2012; Cho et al. 2012; Barla and Innaurato 1973; Nova 1980; Nova and Zaninetti 1990). Studies on the combined effect of fluid saturation and anisotropy are few in numbers. Notable works evaluating the effect of both factors on various geomechanical properties of majorly sedimentary rocks are compiled in Table 1. This table also includes information regarding the angle between the foliation plane and the direction of maximum applied stress. It is worth mentioning that the effect of anisotropy is more pronounced in shale rocks.

Table 1: Combined effect of fluid saturation and anisotropy on geomechanical properties.

Rock	Test/s Conducted	Φ (%)	UCS Loss (%)			Young's Modulus Loss (%)			Tensile Strength Loss (%)			Remarks
			0º	45º	90º	0º	45º	90º	0º	45º	90º	
Bituminous Coal	UCS	-	21.1	-	12.2	34.3	-	31.1	-	-	-	(White and Mazurkiewicz 1989)
Slate	Triaxial, UCS, and Brazilian	0.35	6	27	12	7	28	4	17.4	14.9	7.4	(Gholami and Rasouli 2014)
Beatrice Mine-Shale	Unconfined Compression Test	1 - 3	-	-	-	61.5	74.7	59.5	-	-	-	(Eeckhout and Peng 1975)
Matthews Mine-Shale			-	-	-	59	-	54.9	-	-	-	
Armco Mine-Shale			-	-	-	9.5	49.4	49.5	-	-	-	

2.1.5 Other Factors Effecting Rock Deformability

Reduction in rock strength and deformability characteristics of rocks are not only dependent on the water content. Several other internal and external factors have been identified to contribute to the reduction. Rock density, fabric/structure and porosity influence the weakening intrinsically. Whereas, strain rate, and characteristics of the saturating fluid (surface tension, dielectric constant etc.) affect rock strength extrinsically. Major correlations between different parameters have been summarized in Table 6 in the Appendix. The following general conclusions were drawn for the rock types studied:

1. Geomechanical properties exhibit a negative power or negative exponential relationship with water content, saturation degree, moisture content, and water absorption.

2. As rock density increases, UCS tends to increase as well. The relationship is reported to be exponential or power.
3. Porous rocks are found to have lower UCS values. This is reflected by a negative power correlation between porosity and unconfined compressive strength.
4. Investigation of saturating liquid properties were made on tensile strength only. An exponential relationship is observed between tensile strength and dielectric constant, and surface tension.
5. Strain rate and rock strength relationship has been observed to produce a power relationship. Some studies also show a linear relationship.

The water-weakening effect discussed and investigated in numerous articles has been summarized in Tables 7 - 9 presented in the Appendix.

2.1.6 Effect of Oil Saturation and Temperature on UCS

Investigations on the effect of oil saturation and temperature on geomechanical rock properties are rare. Chalk reservoirs have been examined with respect to a critical water saturation value. This value causes the behavior of the rock to change from ‘oil-like’ to ‘water-like’ (Schroeder 1995). Aforementioned shows a characteristic decrease in rock strength and deformability which is more prominent in water saturated samples (Homand and Shao 2000; Hoeg et al. 2000). Several studies come to contradicting conclusions regarding the effect of oil saturation on compressive strength. A scratch test study by Schei et al. (2000) found that oil saturation caused a greater effect on the strength correlations with scratch parameters. A recent study by Silva et al. (Silva et al. 2017), however, claimed that the effect of oil weakening on rock strength is significantly less pronounced than the effect of water. The literature survey points towards the lack of investigation on the effect

of oil saturation on rock strength characteristics. This phenomenon, therefore, requires further examination.

Another important aspect is the effect of temperature on compressive strength of geomaterials. The majority of the work aiming to quantify the influence of temperature has been for applications of nuclear waste disposal, construction materials, geothermal systems, and underground coal mining/gasification (Ranjith et al. 2012). Two main conclusions were drawn with respect to the influence of temperature. First, the strength increases with the increase in temperature in sandstones (Rao et al. 2007; Duclos and Paquet 1991). Second, there is evidence of a critical temperature after which this strengthening effect reverses (Zhang et al. 2009; Xu et al. 2008; Xiao-li et al. 2009; Mao et al. 2009). One study in particular reported that for carbonate rocks, the compressive strength decreases from the onset of the heating process (Sygała et al. 2013). Notably, though, previous work focused on mining applications where the rock types and conditions differ in comparison to conventional petroleum reservoirs. There has been limited work related to petroleum reservoirs. Closmann and Bradley (1979) reported that both tensile and compressive strength decreases with temperature for a given organic richness in oil shales. Similar trend was also observed for a given temperature with increasing organic content. Lisabeth and Zhu (2015) tested Indiana limestone up to elevated temperatures of 75 ^{o}C saturated with water using a triaxial setup. Their study reported significant weakening effect with saturation and temperature.

Investigations with respect to effect of oil saturation and temperatures on rock strength are not significant in number. The changes experienced in rock compressive

strength at elevated pressures, temperatures and variable fluid saturation needs to be further established.

CHAPTER 3

METHODOLOGY

3.1 Work Phases

The methodology for the experiments is divided into the following phases.

3.1.1 Core Sample Selection

Two types of sandstones and two types of limestones are tested in this project. The rock types and corresponding porosities are:

1. Berea Buff sandstone (Φ = 21.2 %)
2. Berea Grey sandstone (Φ = 18.8 %)
3. Indiana limestone (Φ = 19 %)
4. Desert Pink limestone (Φ = 20 %)

These rock types are considered homogeneous in nature (Churcher et al. 1991). Six samples of each rock type are used for the experiments. Each specimen has a diameter of 1.5 inches and length varies from 4 to 6 inches.

3.1.2 Baseline Scratch Test

In order to establish a UCS baseline reference for all the core samples, scratch tests are conducted under ambient conditions. This baseline will serve as a reference to compare the results of different processes applied to the samples.

The WOMBAT scratch machine by *Epslog* (Fig. 4) is used to carry-out the scratch tests throughout all the phases of this project. Cutter width of 10 mm, cutting velocity of

30 mm/s and depth of cut from 0.05 to 0.4 mm with 0.05 mm increments is used to perform the scratch tests.

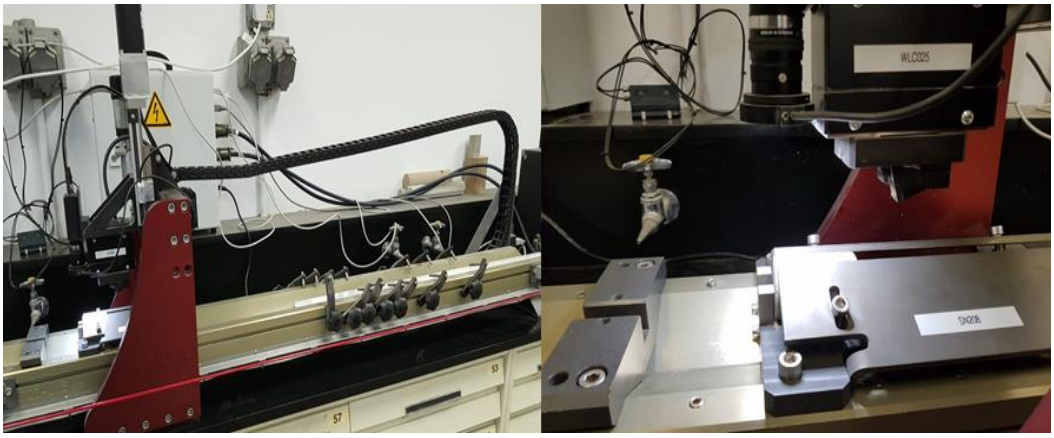

Figure 4: *Epslog's* The Wombat scratch machine side view (left). Zoomed in view of the side of the cutter (right).

Each sample is scratched thrice at different locations. This approach is employed primarily to establish a meaningful data set from a statistical point of view. Additionally, scratching at different locations along the core allows to capture potential variations in strength.

3.1.3 Core Saturation

The samples were completely saturated according to the *API RP 40* (API 1998). The steps carried out are as follows:

a) Measure dry weight of the samples
b) Place the weighed samples in chamber (vacuum desiccator and pressure saturator shown in Fig. 5)
c) Apply vacuum for 3 to 5 hours before introducing the liquid for saturation
d) Brine/distilled water to be used for saturation is introduced in to the evacuated chamber containing the core sample
e) Keep samples saturated for a set amount of time depending on the objective
f) Remove samples and after weighing them, wrap in cling film to avoid evaporation.

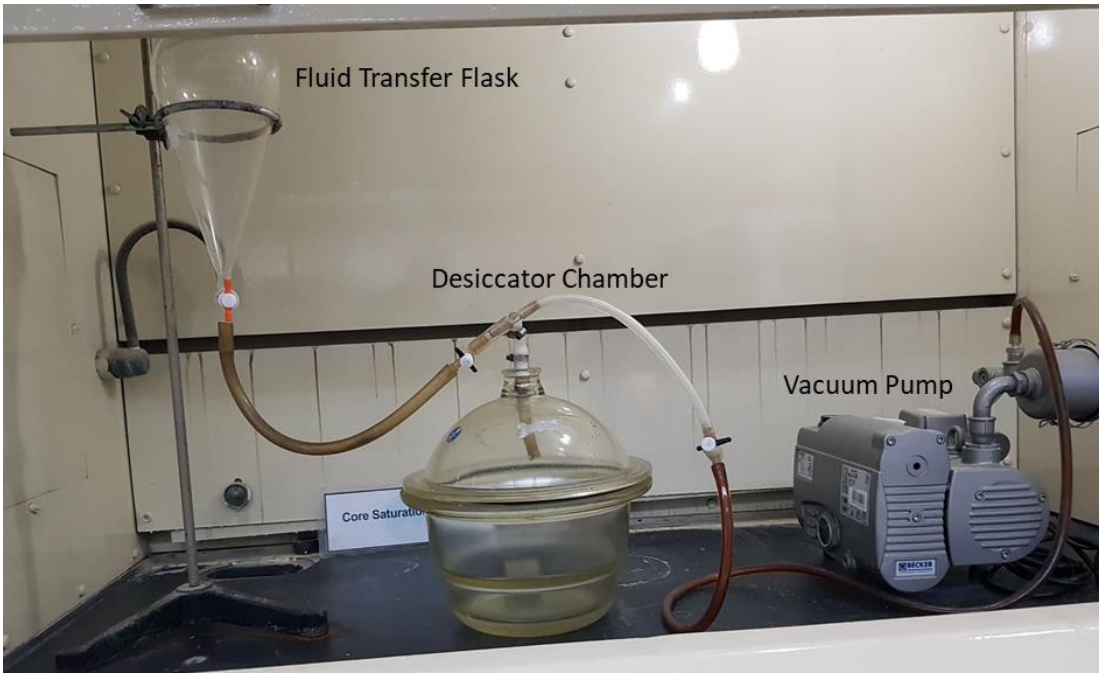

Figure 5: Setup used to saturate the core samples which includes a vacuum pump, transfer flask and desiccator.

The formation brine being used in this phase of the experiments has a composition similar to formation water found in Saudi Arabian reservoirs (Chen et al. 2017). The composition is summarized in Table 2. Yielding a salinity of about 213000 ppm.

Table 2: Actual formation water composition of a Saudi Arabian reservoir (Chen et al. 2017).

Ions	Concentration (ppm)
Sodium	59491
Calcium	19040
Magnesium	2439
Sulfate	350
Chloride	132060
Bicarbonate	354
TDS	213734

A *DCI*, USA transfer cell *4055-HC*, having a capacity of 1000 cubic centimeters and a pressure rating of 10000 psi, is utilized to saturate the samples in oil. The cell is shown in Fig. 6.

Figure 6: DCI, USA cell used to saturate samples in oil.

As per API RP 40 (API 1998), samples were saturated in crude oil according to the following steps:

a) Measure dry weight of the samples

b) Place samples in core holder

c) Apply vacuum for a set amount of time

d) Introduce oil and pressurize to pressures in excess of 2000 psi employing piston in the core holder to ensure maximum saturation as recommended in *API RP 40 Section 5.3.2.2.3.6* (API 1998)

e) Keep samples saturated for a period of one week

3.1.4 Scratch Test

The scratch test is conducted for the samples in the saturated state.

- Like baseline scratch, tests are done on multiple locations of the core to establish enough statistical data for conclusive results.
- Compare the obtained results of this step to previously acquired baseline scratch to observe the changes.

3.1.5 Core Aging

In conventional core analysis procedures, aging is the process used to restore wettability of the samples by introducing reservoir temperature, pressure and fluids to simulate in situ

conditions of the reservoir. In our case, however, we use a different definition of aging. We introduce high temperature and reservoir fluids to the core samples that are characteristic of in situ conditions. The pressure effect is not taken in to account as it has been reported to having negligible effect on the aging process (Hjelmeland and Larrondo 1986; Wang and Gupta 1995). The pressure applied is solely to ensure that the samples are fully saturated.

In order to have a representative time for aging, literature review was carried out to determine an optimum time. Jadhunandan and Morrow (1995) reported that for Berea sandstone, at temperatures ranging from 50 ^{o}C to 80 ^{o}C the optimum time was 10 days. Extending time to up to 40 days showed no significant differences. Graue et al. (1999) reported optimum times of about 2-3 weeks to observe maximum wettability alteration. Rao (1999) and Yi and Sarma (2012) reported that 3-4 weeks of aging time is considered to be adequate in most cases. Keeping in mind the usual times reported for aging, we conducted our experiments using aging times of 10 days for brine and 1 month for distilled water and oil.

A similar cell as utilized for oil saturation was used for aging the samples in oil. For aging in brine and distilled water, a *Coretest*, USA cell, model number *PA 81 79101C* with similar capacity and pressure rating, was used as shown in Fig. 7.

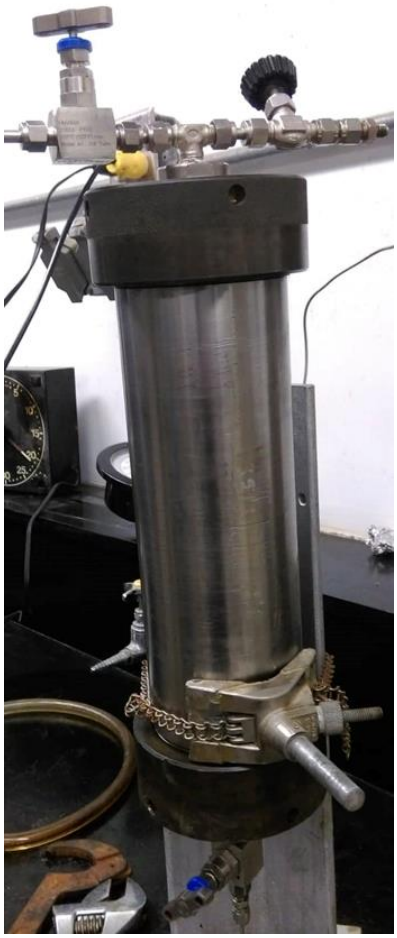

Figure 7: Coretest, USA cell used to saturate samples in brine and distilled water.

The following steps were followed to age the core samples:

a) Core samples are placed in the core holder.

b) Vacuum is applied before introducing fluid to ensure no air was trapped in the pore spaces.

c) Three different fluids are used in separate phases to age the core samples:

   1. Brine
   2. Oil
   3. Distilled Water

d) The core holder is pressurized to about 2000 psi to ensure maximum saturation

e) The core holder is placed in an oven at 150 ^{o}C for a set period.

Two main reasons encouraged this particular choice of temperature. Firstly, the global classification of a high temperature well starts from a temperature of 150 ^{o}C (Belani and Orr 2008). Secondly, there is evidence of existence of temperatures above 150 ^{o}C in wells in Saudi Arabia, with Khuff formation being a primary example (Turki 1991).

3.1.6 Scratch Test

The scratch test is conducted for the samples in the aged condition.

- Like baseline scratch, ensure that multiple scratches are done to establish enough statistical data for conclusive results.
- Compare the obtained results of this step to previously acquired baseline scratch to observe the changes.

3.2 Data Analysis Tools

It was decided to employ statistics rather than a single UCS value to study the results from the various samples and phases of the project. Statistical analysis is done because multiple UCS values are generated for a single sample by the scratch test.

3.2.1 Qualitative Analysis

Figure 8 shows the original form of data produced by the software bundled with the scratch machine. As UCS values are recorded at every centimeter making it difficult to compare the results from two different scratches. In addition, comparing results in such a manner can be misleading as each time the cutter sees a new piece of rock, which arguably can yield differences in strength. Therefore, keeping in view the complexity of reporting the results in such a manner, this graphical form of results will not be used in our analysis.

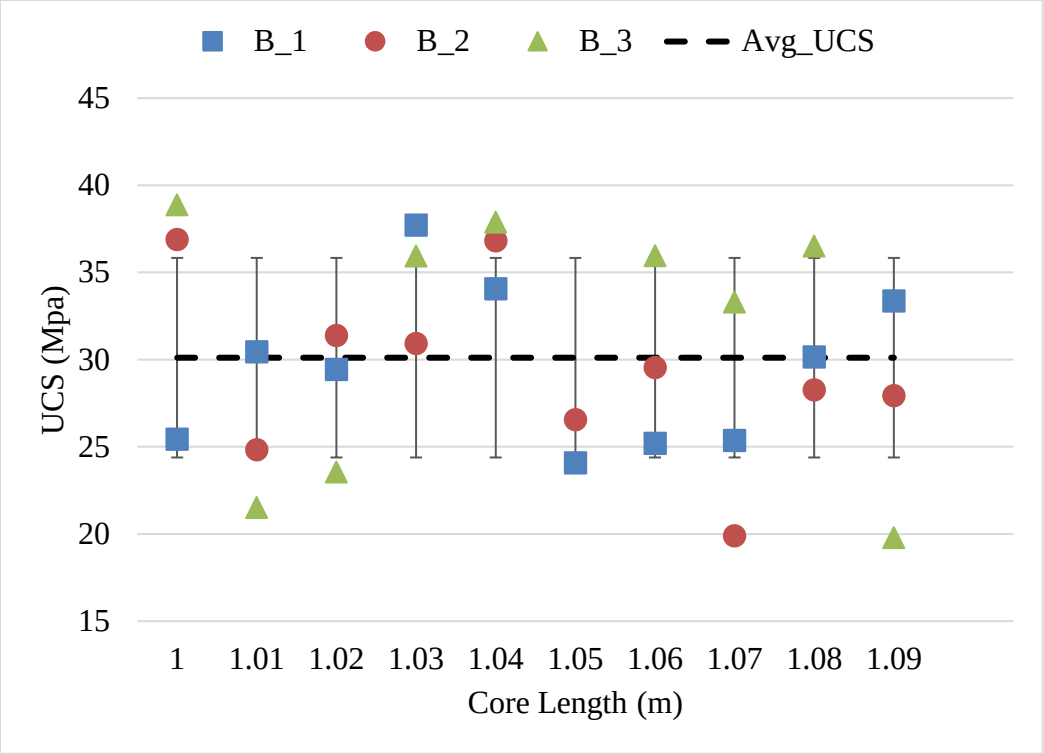

Figure 8: Log of UCS along the core length as generated by the scratch machine software. Error bars denote the standard deviation from the mean.

Another way of displaying the results is using histograms. Based on the data from one of our experiments, the empirical histograms is shown in Fig. 9. This does not yield any standard histograms like normal/Gaussian or lognormal but rather pathological distributions that cannot be described by known distribution families adequately. In addition, it can also be argued that the shape of the distribution is due to the lack of data rather than the underlying physical phenomena.

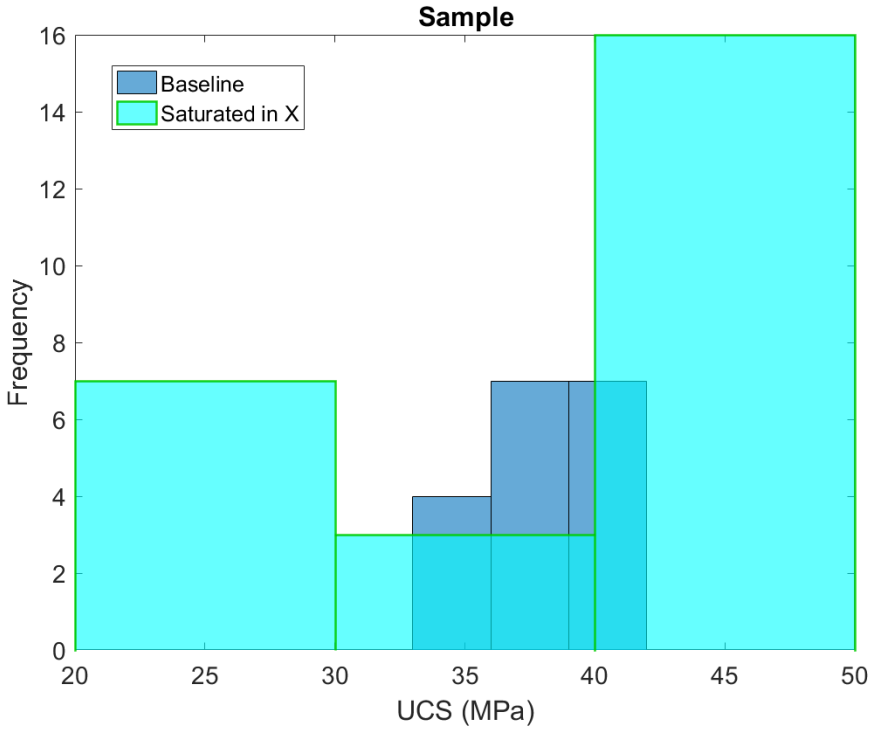

Figure 9: A sample histogram generated using data from an experiment.

Keeping in view the aspects of the histogram discussed above, they are in adequate to carry out comparative analysis in our case. Consequently, we have decided to use kernel density estimators to conduct analysis on our data sets generated using scratch tests.

Kernel density estimators (KDE) are part of a family of estimators called non-parametric density estimators. Parametric estimators have a fixed functional structure and the parameters of this function are the only required information. Non-parametric estimators, however, have no fixed structure and utilize all the data points to automatically understand the underlying distribution of the data. (Mishra 2016; Chen 2017)

The non-smoothness of the histogram mars its effectiveness in data interpretation. KDEs help to circumvent this issue by centering a kernel function at each data point. Using a smooth function results in a smooth density estimation. In other words, KDE are able to

smooth out the contribution of each data point over a local neighborhood of that point (Jenq-Neng Hwang et al. 1994).

3.2.2 Quantitative Analysis

Primarily, we utilized the non-parametric descriptive statistics using KDE to report our results. For quantitative analysis of the data, however, we have three statistical parameters to choose from:

1. Mean
2. Mode
3. Median

The data generated in our study does not necessarily follow normal distribution. Hence, the mean cannot be used to quantify changes in the data as it assumes data to be normally distributed. In addition, as the precision for the derived UCS is up to one decimal place, the UCS values recorded after each centimeter are, in most cases, non-repetitive. Moreover, where there is repetition, it is not representative of the data. As a result, using the mode will lead to erroneous assessment of the data due to reporting of non-representative UCS values. Arguably, median is the most appropriate parameter to report change in UCS for the data generated in the experiments because it more aptly describes the trend in the data.

3.3 Rock Characterization

All the core samples used in this project are outcrop samples sourced from *Kocurek* in the USA. As mentioned previously, four different rock types are being studied and have been chosen due to two main reasons. Firstly, they are said to be homogeneous in nature (Churcher et al. 1991; Schön 2015) allowing us to study the changes with respect to externally applied processes rather than inherent rock behavior. Secondly, extensive geological/mineralogical characterization exists already in the literature (Mohamed and Nasr-El-Din 2013).

Table 3 shows the XRD derived mineralogical composition of the rock types used in this project. As mentioned previously, the data was adapted from a vast collection of literature (Shehata and Nasr-El-Din 2014; M. Hassan and S. Al-Hashim 2016; Mahmoud and Al-Hashim 2018; Eliebid et al. 2018).

Table 3: Mineralogical composition of the rock types used in this study, compiled from literature.

Minerals	Gray Berea (wt.%)	Buff Berea (wt.%)	Indiana Limestone (wt.%)	Desert Pink Limestone (wt.%)
Quartz	89	91	0.158	
Calcite	0.08	-	97	95
Albite	1.47	-	-	-
Kaolinite	4.8	3	-	-
Illite	2.29	-	2.61	-
Chlorite	1.02	-	-	-
Ankerite	0.38		-	-
Microline	-	4	-	-
Muscovite	-	1	-	-
Smectite	-	1	-	-
Dolomite	-		-	5

CHAPTER 4

CRITICAL DEPTH OF CUT DETERMINATION

4.1 Objective and Scope

Accurate interpretation of scratch data is highly dependent on the failure mode being experienced by the rock. Determination of depth at which the transition from one failure mode to the other occurs is, therefore, crucial.

In this part of the study, our attempt is to conduct a comparative analysis between various approaches employed to determine the critical depth. The following methods will be utilized:

1. Force response analysis

Ductile and brittle mechanisms can be discerned based on the response (shape) of the force signal (Richard et al. 2012). In the ductile mode, the signal can be interpreted as a white noise as shown in Fig. 10a, provided the rock is homogeneous. On the contrary, brittle mode is indicated by a saw-tooth pattern (see Fig. 10b) which is attributed to the chipping action.

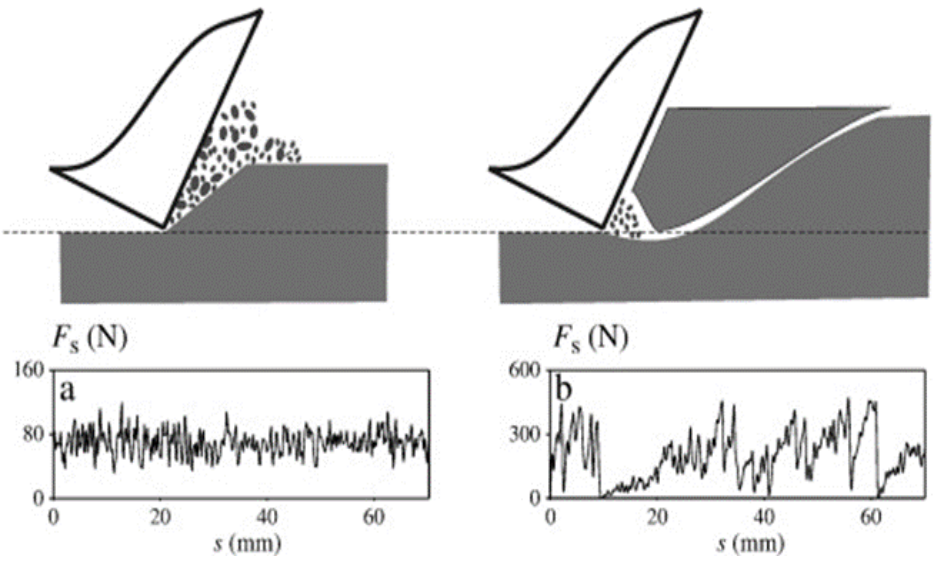

Figure 10: Schematic representation of the ductile and brittle failure modes. (a) Force response for ductile mode of failure like a white noise signal (b) Force response for brittle mode of failure like a saw-tooth pattern (Richard et al. 2012).

2. Force Inflection Point Analysis
3. The Size Effect Law (SEL) as proposed by Bazant (1984) and modified for the scratch test by Lin and Zhou (2014; 2013)
4. Scratch test particle morphological analysis

The aim of using this approach will be to correlate particle morphology with the mode of failure. It is expected that as the regime transitions from ductile to brittle, the particle size generated by the cut will increase. Helical micro-CT scanning is employed to characterize the particles. The idea is to use computed tomography to obtain a characterization of the particles and relate them to the failure regimes.

4.2 Methodology

The collection of scratch chips and data analysis is conducted utilizing the following methodology:

1. Scratch samples starting from the smallest possible depth of cut to the maximum achievable depth using the scratch machine.
2. Collect powder for each depth and store it for further analysis.
3. Conduct Micro-CT experiments.
4. Process the acquired data.
5. Data analysis.

4.3 Experimental Results

Scratch tests are carried out on Indiana Limestone with the cutter-rock interaction characterized by the following geometry:

- Cutter width, w = 10 mm
- Back rake angle, $\Theta = 15^{o}$

Both normal, F_n and tangential force, F_s components are measured during the cutting action. F_n and F_s are normal and parallel to direction of the cutting action respectively. Figure 11 shows a sketch of the rock-cutter interaction geometry. The sample is scratched in the range of 0.05 mm to 0.4 mm with increments of 0.05 mm. Three scratches for each depth of cut is done to establish statistical significance of the data set.

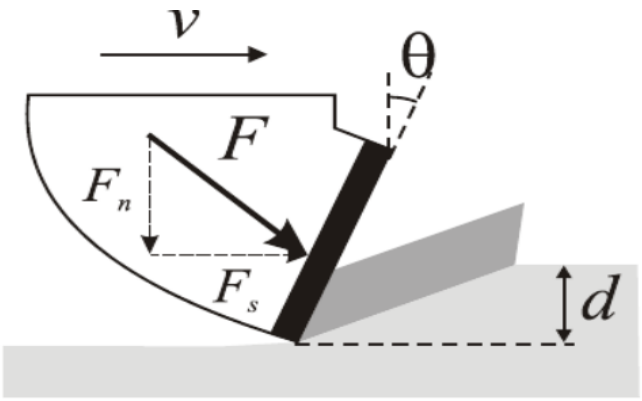

Figure 11: Force resolution and geometry of the cutter (Dagrain et al. 2004).

4.3.1 Method 1: Force Signal Analysis

Tangential force signals measured during the scratching process are plotted as a function of core length in Fig. 12. Observing this plot, we can filter out signals from the first three depths of cut, 0.05 mm – 0.15 mm (bottom three plots), because the response from these is constant and depicting that the regime is ductile during these depths. The force response plot without the first three depths of cut is shown in Fig. 13. For a more precise view, individual force signals are plotted to detect the regime change. In the brittle regime, also denoted as "chipping", cracks are initiated at the tip of the tool and propagate upwards while the force reaches a maximum value. Once the crack reaches the surface of the sample, a chip is formed, and, subsequently, removed by the cutter causing a decrease in the force signal. This action gives rise to a saw-tooth like force signal. Observing the signals in Fig. 13, however, it is not easy to pinpoint the depth where this exact change occurs. It seems that the chipping action exists to some extent at all depths. At d = 0.25 mm, however, it becomes more pronounced with maximum intensity being recorded at d = 0.35 mm.

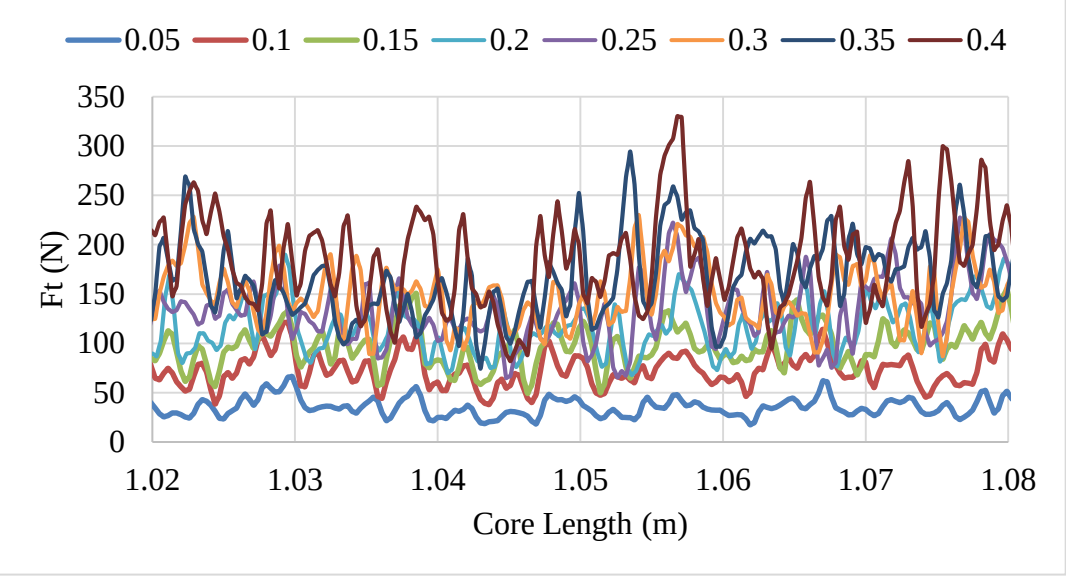

Figure 12: Tangential force signals plotted along the core length for all depths of cut. The depths of cut from 0.05-0.15 show a white noise response and can be removed from further analysis.

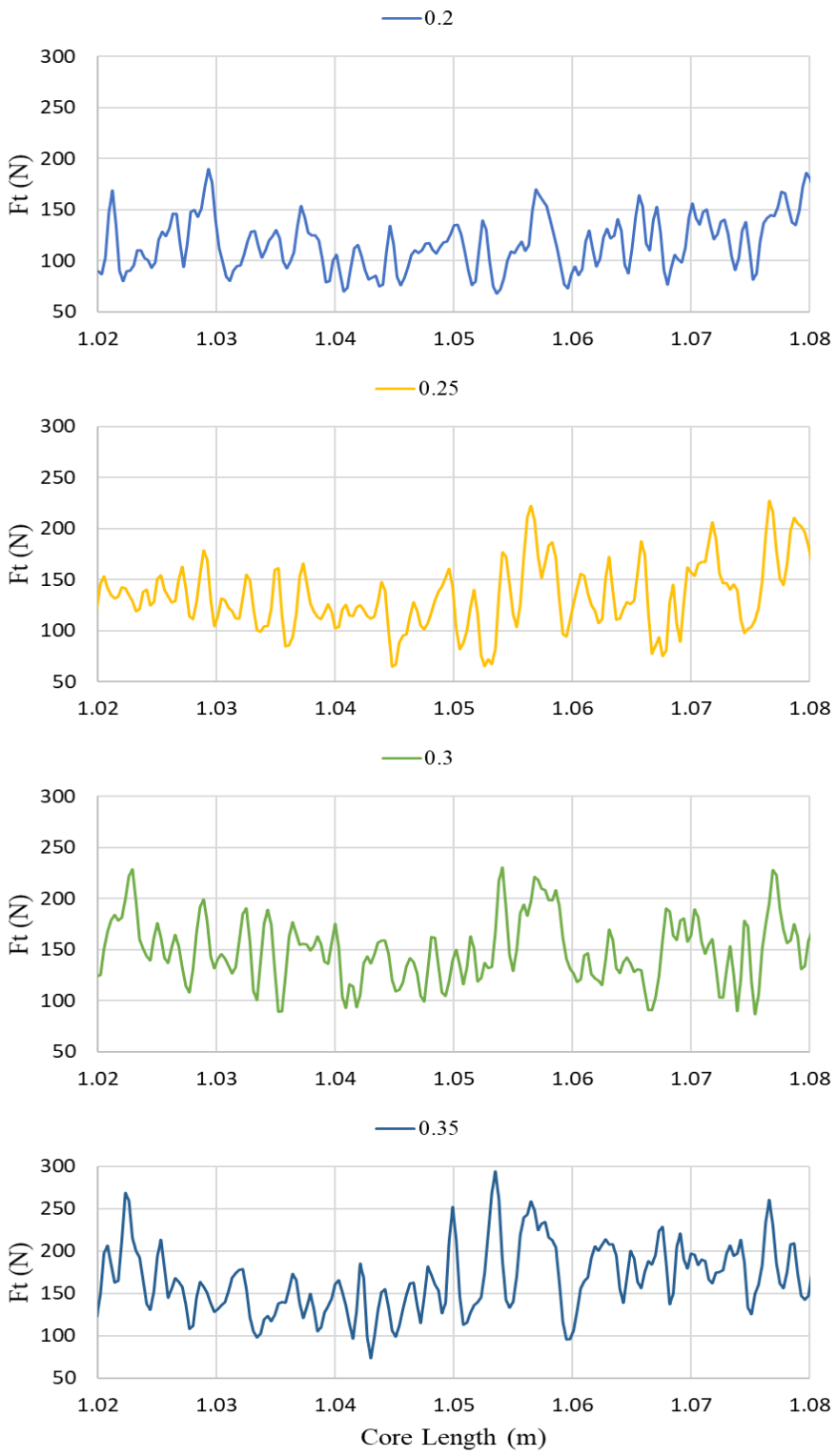

Figure 13: Tangential force signal plotted as a function of core length for each depth of cut to examine the onset of the brittle regime. Saw-tooth like force response becomes more prominent at depth of cut greater than 0.25.

4.3.2 Method 2: Linear Elastic Fracture Mechanics Inflection Point Analysis

Richard et al. (1998) explain the critical transition depth through the relationship of cutting force with the depth of cut, provided that the cutter width is constant. They explain that the failure regime is ductile when the cutting force is directly proportional to the depth of cut. Whereas, brittle regime prevails when the relationship is proportional to the square root of depth of cut. Therefore, a critical transition depth can be determined by detecting this change in a plot of cutting force versus depth of cut as shown in Fig. 14. Past the critical depth of cut, the theory of linear elastic fracture mechanics (LEFM) follows and can be used to determine the fracture properties but not the strength (He and Xu 2015).

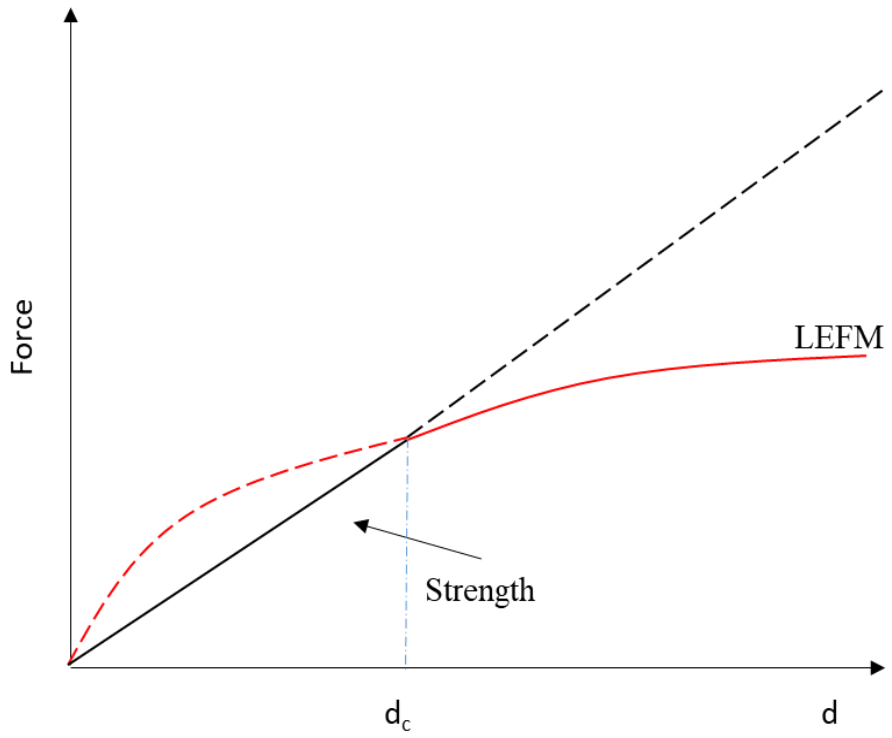

Figure 14: Schematic diagram of the transition from linear to non-linear behavior of the force with depth of cut. The ductile mode of failure dominates when the depth of cut is proportional to the force response. The proportionality no longer holds after the critical transition depth.

Mean forces were computed from the three scratches for each DOC and then plotted as per the methodology explained above to determine d_c. The plot of mean forces versus depth of

cut is shown in Fig. 15, where the inflection point is used to point out the critical depth of cut. Using this method, d_c is rather difficult to decipher, but it seems to be in the range of 0.25 mm to 0.3 mm.

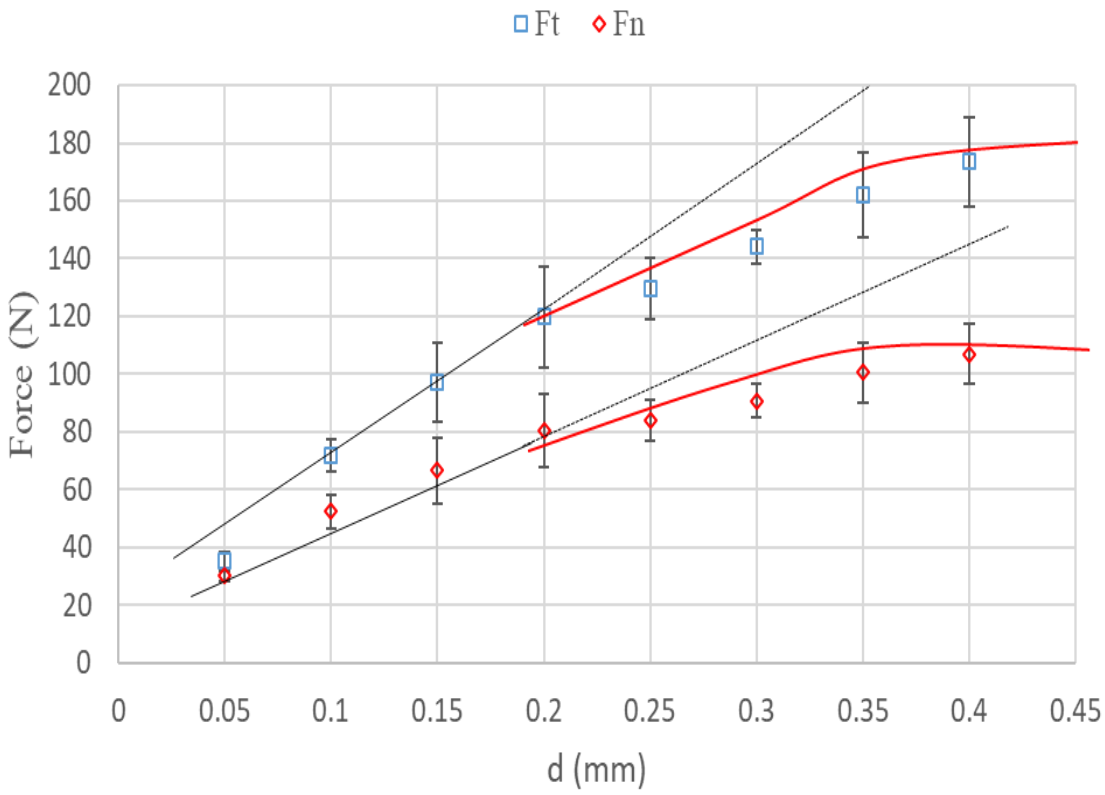

Figure 15: Plot of mean normal and tangential forces with the depth of cut. The error bars denote the standard deviation.

4.3.3 Method 3: The Size Effect Law

Bažant has illustrated that failure regime for a quasi-brittle material, transforms from plastic yielding to fracture failure (Bažant 1984, 2000). A simple size effect law (SEL) follows the way loading capacity governs this transformation valid over a largely varying range of sizes. He expressed the SEL in terms of a nominal stress value, σ_N, which is the maximum load divided by a typical cross sectional area. The SEL is expressed as follows:

$$\boldsymbol{\sigma_N = \frac{C\sigma_Y}{\sqrt{1 + D/D_o}}} \quad \textbf{(3)}$$

Where; σ_Y is the yielding strength, C is a dimensionless constant linked to specimen geometry/shape and loading configuration, D is the size of the structure, and D_o is the transitional size marking the transition of failure mode.

The existence of two failure modes as a function of cutting depth in scratch tests suggests that the depth of cutting can be viewed as a measure of transitional size. Lin and Zhou (2014; 2013) took on this idea and employed the depth of cut as a measure of size. By using cutting data from Nicodeme (1997) and Richard et al. (1998) they showed that Bazant's simple size effect law can explain the scratch data well. As a result, the simple size effect law can bridge the gap between strength and linear elastic fracture mechanics theories using the empirical function as introduced in Eqn. 3 with some modifications for the scratch test. D_o is replaced by d_c, the critical transition depth of cut and D is replaced by d, the depth of cut. The critical transition depth is the intersection of the strength and LEFM asymptotes (He and Xu 2015), as illustrated in Fig. 16 by a schematic of the application of the SEL.

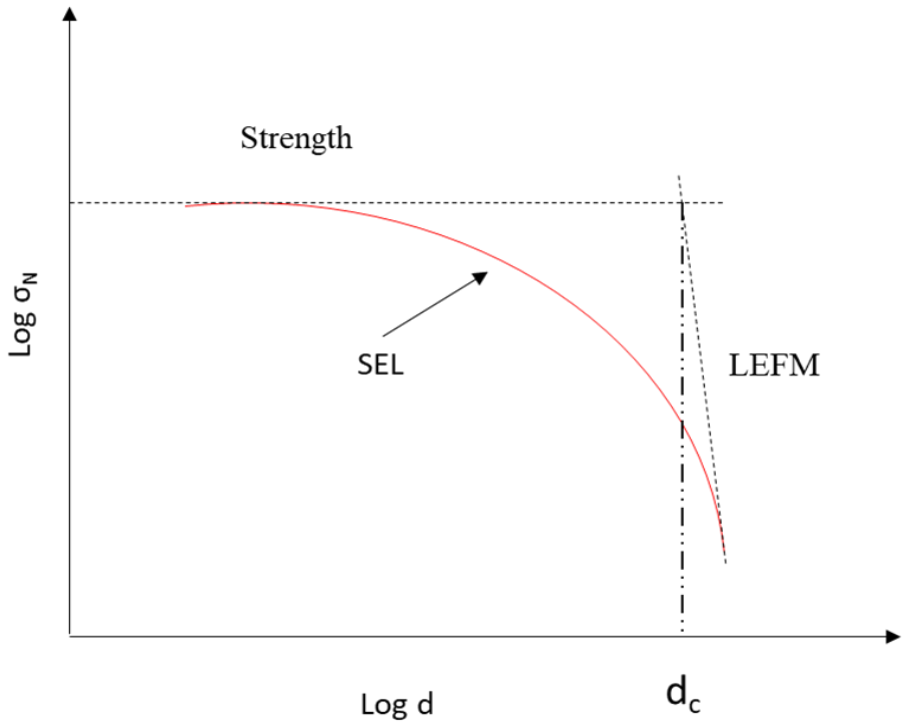

Figure 16: A schematic of Bazant's SEL as applied to rock cutting.

Utilizing the measured forces, the nominal stress was calculated by the following equation:

$$\sigma_N = \frac{F_t}{wd} \tag{4}$$

A log-log plot of the nominal stress calculated from Eqn. 4 and the depth of cut, is shown in Fig. 17. In the same figure, a best fit of Bazant's SEL is shown which gave $C\sigma_Y$ of 70.7 MPa. The d_c, using this method, is found to be 0.29 mm.

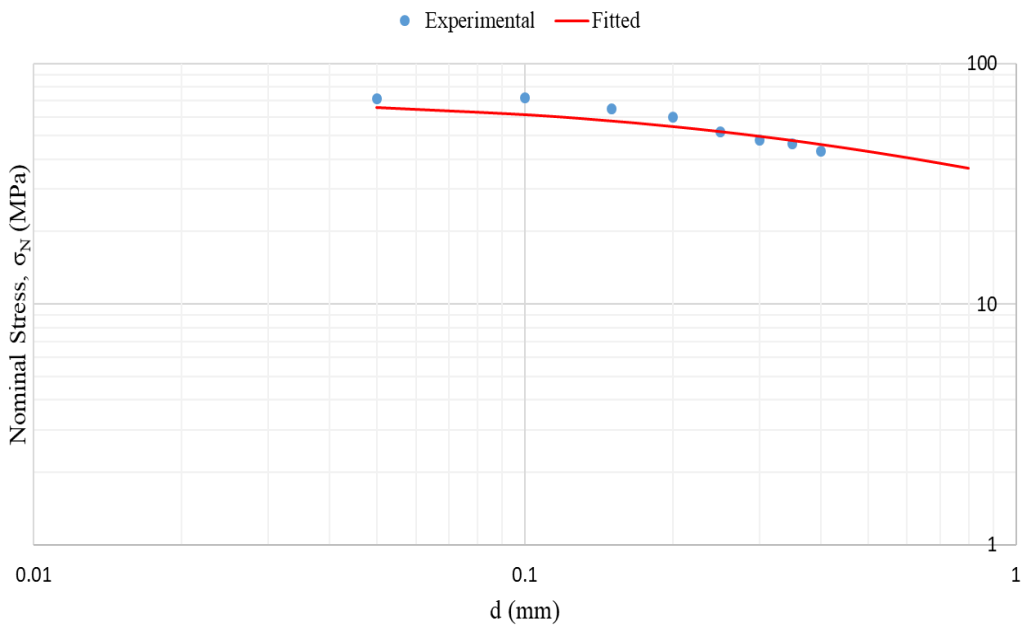

Figure 17: Plot depicting how the nominal stress evolves with the depth of cut. Also shown is the fit achieved using the SEL.

4.3.4 Method 4: Digital Imaging Analysis

All the techniques mentioned above are based on either measured force signals or computing the critical depth using theoretical formulations. To better understand the transformation from one regime to another, however, it is imperative to take aid of visual representations of the scratch powder generated at various depths of cut. In this step, we utilize Helical Micro-CT to scan the residue from each depth at a resolution of one micron.

The scratch residue from each depth of cut was carefully loaded in a slim rubber tube and placed as close as possible to the X-ray source to attain high resolution scans. Figure 18 shows the sample positioned in the *ThermoFisher Heliscan microCT*.

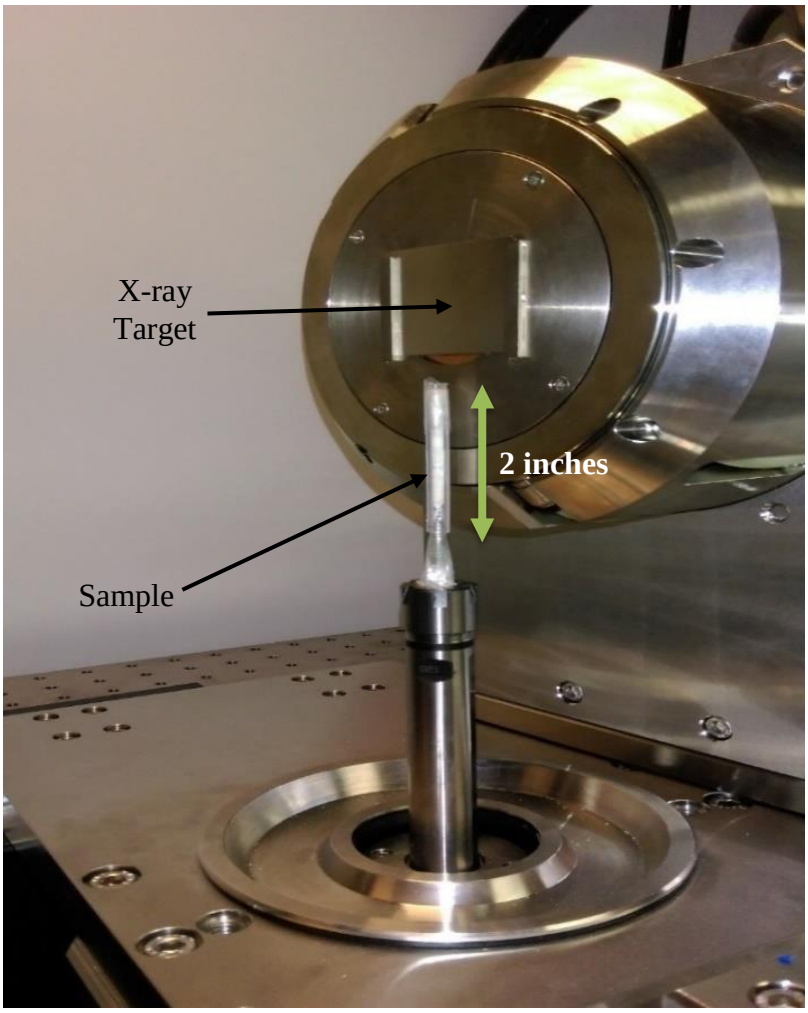

Figure 18: Sample loaded in the *ThermoFisher Heliscan microCT*.

Generally, it is observed that with increasing DOC, the individual grain size is increasing as we expected. Figure 19 provides a montage of scans from 0.05 mm to 0.15 mm DOC. Based on the images, we eliminate these depths from further analysis as they show similar characteristics like size and shape, indicating shear failure process in the ductile regime. Representative grain sizes for each scan is encircled in red

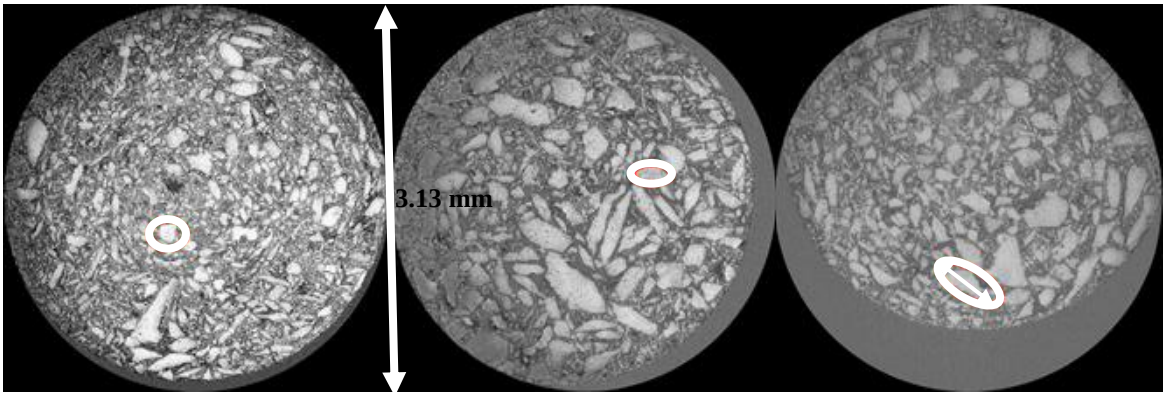

Figure 19: From left to right images of the scans of 0.05, 0.1- and 0.15-mm depths residue. The resolution for each scan is 1 micron.

As we see in the image of the scan for DOC of 0.2 mm (Fig. 20), a distinctive increase in grain size is observed. A representative grain is encircled in white. Based on this alone, however, it cannot be concluded that this increase is accompanied by a regime change.

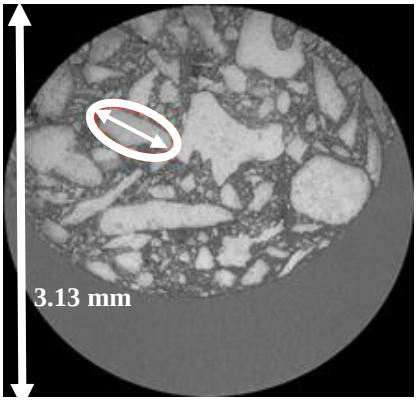

Figure 20: Image of the scan of 0.2 mm depth residue. The scan was performed at a resolution of 1 micron.

Figure 21 shows the scans from DOC of 0.25 mm – 0.35 mm. The white circle in the figure indicates a representative grain for that particular scan. The following qualitative observations can be made:

1. Elongation of the grains as the depth of cut increases.
2. The large grain sizes are representative of formation of chips due to the fracturing process that occurs are greater depths of cut.

3. The change from ductile to brittle regime can be pointed out from 0.25 mm onwards due to the evidence of formation of larger chips, characteristic of brittle mode.

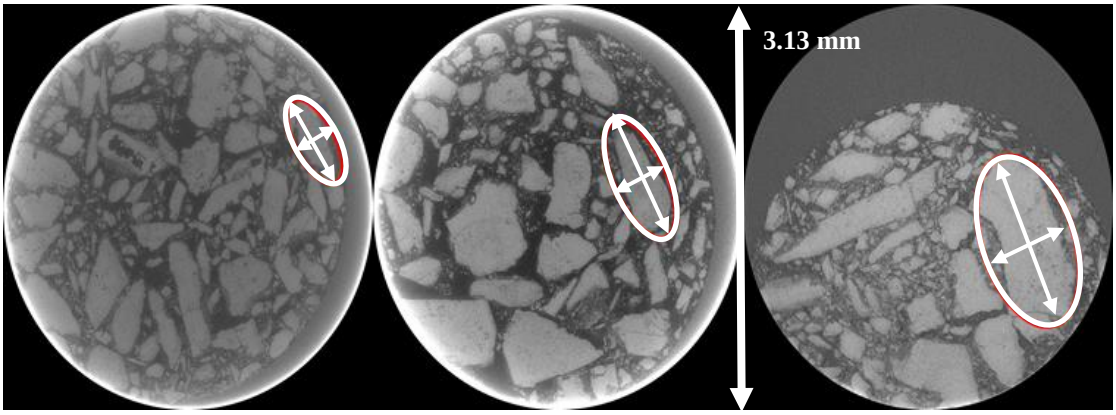

Figure 21 From left to right images of the scans of 0.25, 0.3- and 0.35-mm depths residue. Resolution of each scan is 1 micron.

For each scan, a representative grain was selected and fit to an approximate ellipsoidal shape as shown by the white circles. The length of the major and minor axes of these shapes were calculated and are shown in Table 4. It is observed that the length of the major axis increases abnormally from DOC of 0.3 to 0.35, opposing the steady increase as depicted by the preceding depths of cut. This preliminary analysis of the 2D scans point towards a value of 0.35 mm for the critical depth of cut.

Table 4: The major and minor axes length for encircled representative grains for each depth of cut.

DOC (mm)	Axis	in mm
0.05	Major	0.13
	Minor	0.14
0.10	Major	0.28
	Minor	0.13
0.15	Major	0.36
	Minor	0.17
0.20	Major	0.59
	Minor	0.24
0.25	Major	0.68
	Minor	0.22
0.30	Major	0.84
	Minor	0.28
0.35	Major	1.28
	Minor	0.52

4.4 Conclusion

No method currently can define precisely when the change from ductile to brittle regime takes place. We, therefore, suggest taking guide from digital imaging techniques in order to better understand the morphology of the scratch residue and link it to the failure mode. In this study, it has been shown that micro-CT scanning can help in identifying the point where the chipping action starts. Together with the force signal analysis, critical transition depth can be estimated. The SEL could be accurately applied when we have more data to define a better fit and get an accurate estimation of d_c, the critical depth of cut. Inflection point analysis provides better answers even with scarce data and can be used in conjunction with image analysis to aid the process of determining the critical depth. This is, however, just a preliminary step taken to better qualify the transition from ductile to brittle mode of failure. Looking forward, 3D residue characterization and statistical analysis of the scans are expected to be more helpful in understanding the underlying morphological changes occurring during the regime change.

CHAPTER 5

RESULTS AND DISCUSSION

5.1 Results Interpretation

Before interpreting results, it is imperative to describe the inherent behavior of the different rock types when scratched. This behavior is then kept under consideration during interpretation of the results.

Ideally, we assume that Indiana Limestone is a homogenous rock (Schmidt 1976). During the investigation of the behavior at centimeter scale, however, it was observed that the variation in UCS is of a sizeable degree. Figure 22 shows the ISE log for an Indiana Limestone sample, with the various color depicting the signal intensity, where consistent variation is observed that overshadows the quality of data and the apparent change in values. Importantly, this behavior is consistent throughout all the samples of Indiana Limestone tested in this study. Because of this behavior, resulting impact of fluids or temperature on UCS values should be looked upon with caution.

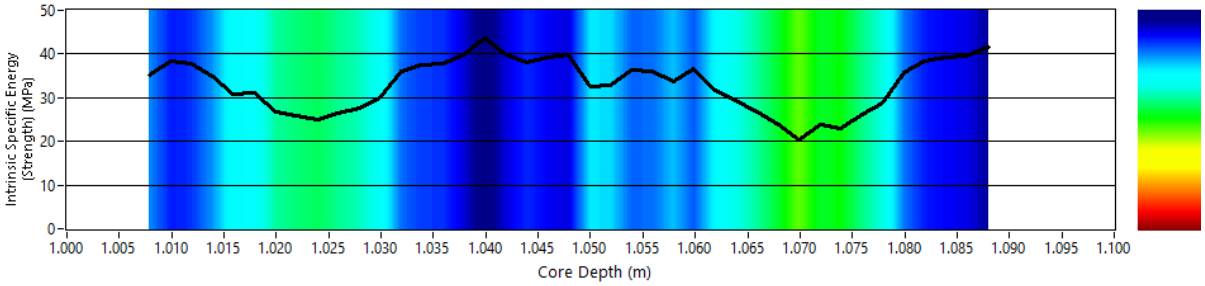

Figure 22: Intrinsic Specific Energy log along the core length for Indiana Limestone, showing consistent variations.

Although Desert Pink Limestone is said to be homogenous in terms of mineralogy (Mohamed and Nasr-El-Din 2013), the same cannot be said concerning its strength. Figure 23 shows the ISE log for a Desert Pink sample, where two distinct zones in terms of the strength response can be observed. The presence of two different zones is also confirmed in the groove photograph below the log showing two distinctive color zones. Consequently, care should be taken during data interpretation pertaining as this behavior might result in erroneous conclusions with regards to the effect of saturation and aging.

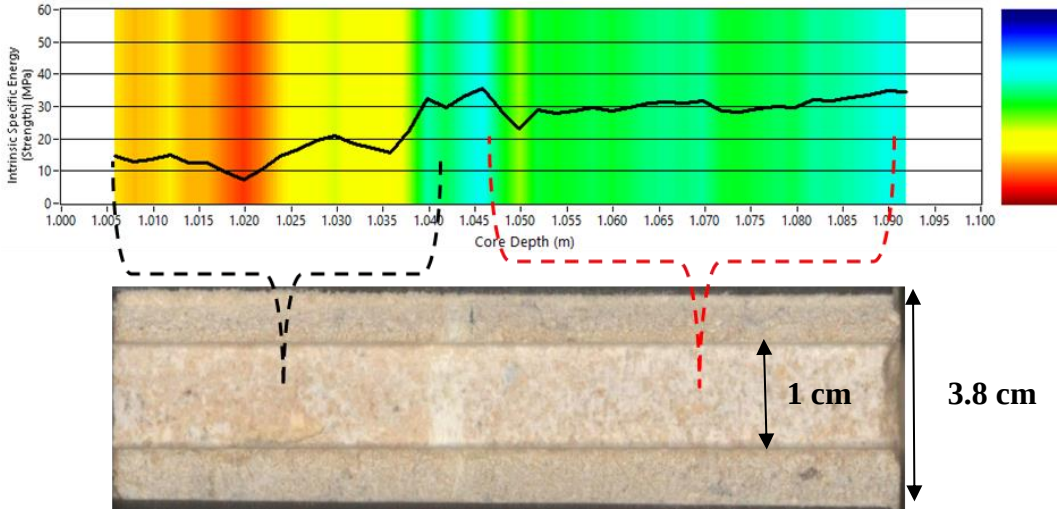

Figure 23: Intrinsic Specific Energy log for Desert Pink Limestone (above) and the groove photograph (below). The presence of two distinct zones of strength is confirmed by distinctive change in color of the groove.

Contrarily, both types of sandstones used in this study display homogenous behavior in terms of the strength as derived from the scratch test. For comparison purposes, a sample UCS log along the core length is provided in Fig. 24 for all the different rock types used. This comparison illustrates the fact that the sandstone rocks show a more uniform behavior in comparison to limestone which show varying strength values at each centimeter. As a result, it is safe to assume that any changes occurring in the sandstone samples would be the result of various external conditions (temperature, liquids etc.) being applied and not the intrinsic rock behavior. The contrary is true for limestone samples as their data

interpretation will be marred by rock intrinsic characteristics, unless a major change in UCS is observed which is beyond the intrinsic variability.

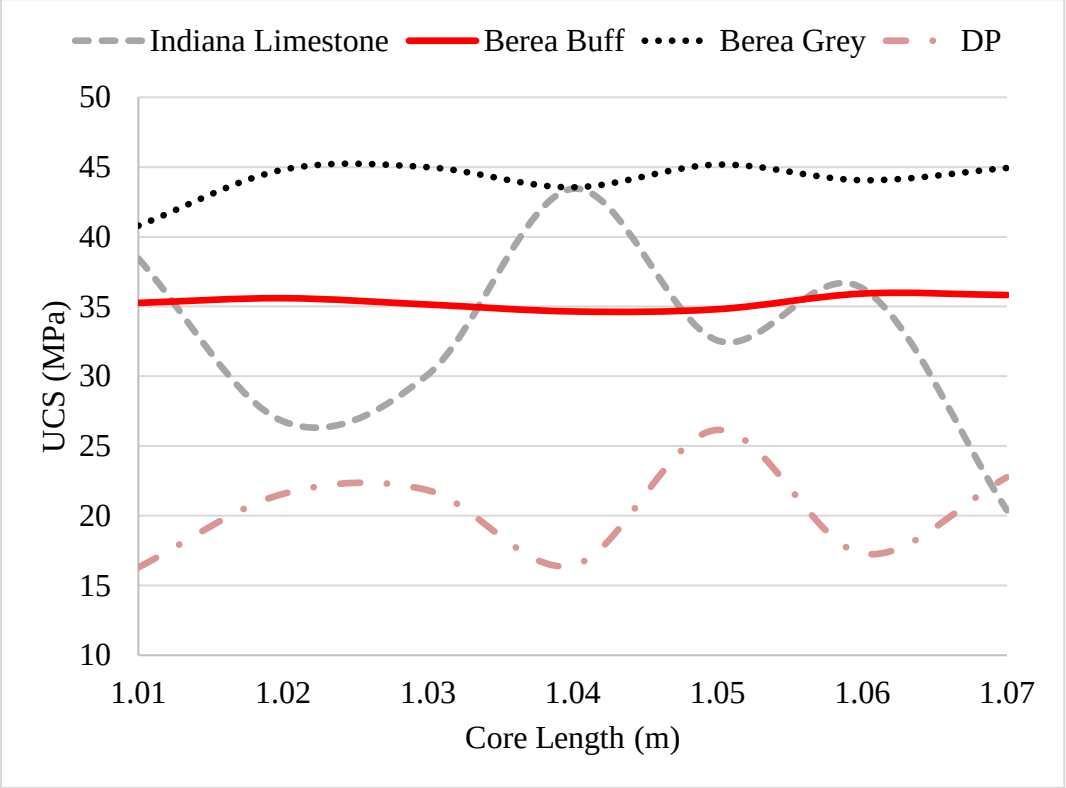

Figure 24: Log of the UCS as a function of core length for the four rock types used in the study, which shows how they vary along the core length.

5.1.1 Samples Saturated in Brine

CO_2 sequestration in deep saline aquifers has been studied in depth as a potential solution to lower the carbon foot print (Silva et al. 2015; Bruant et al. 2002; Rosenbauer and Thomas 2010). Al-Ameri et. al (2014) reported that the geomechanical properties of CO_2 stored rocks deteriorate with time. Therefore, it is essential to quantify the actual in situ strength values before the sequestration process is initiated to evaluate integrity of the formation of interest. High salinity brine similar to those found in deep aquifers (Rathnaweera et al. 2014) is used to study the impact on UCS in comparison to tests at dry conditions.

A total of five samples were tested during this phase. These include; two Indiana Limestone's (X and Y), one Desert Pink Limestone (DP3), one each of Berea Buff (BB1) and Berea Grey (BG1) Sandstone.

The tested carbonate samples do not appear to show any appreciable change in UCS, as the trend shown by the kernel diagram is close to the baseline behavior. Both, Indiana Limestone and Desert Pink show minimal to no change.

Figures 25 and 26 show results for Indiana Limestone X and Y respectively. Trends towards weakening were observed. This, however, is inconclusive because of the heterogeneous nature as discussed earlier.

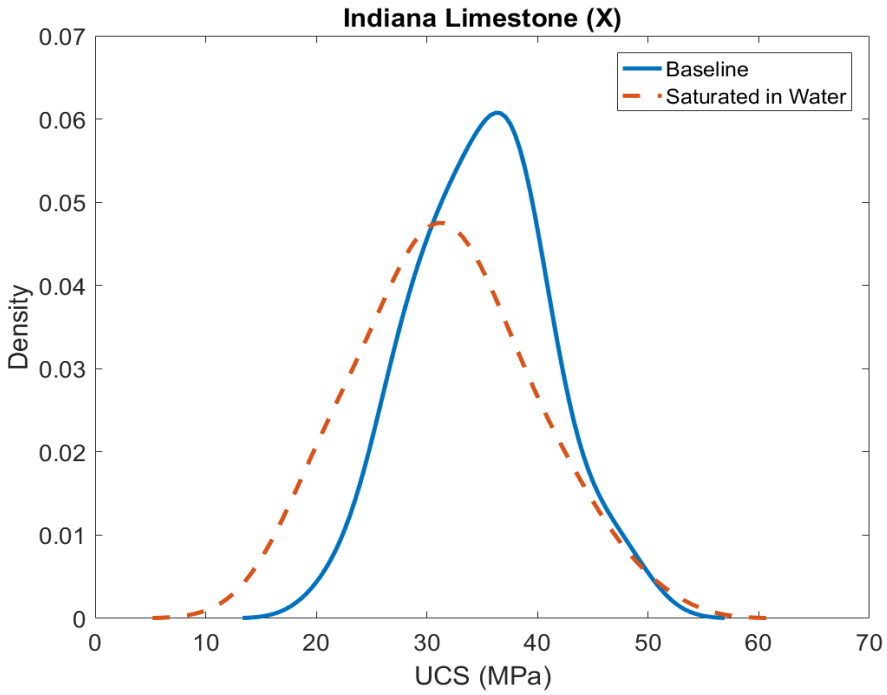

Figure 25: Kernel diagram showing the trend for Indiana Limestone sample X after saturation in brine as compared to the baseline. The trend shown after saturation in brine is similar to baseline case.

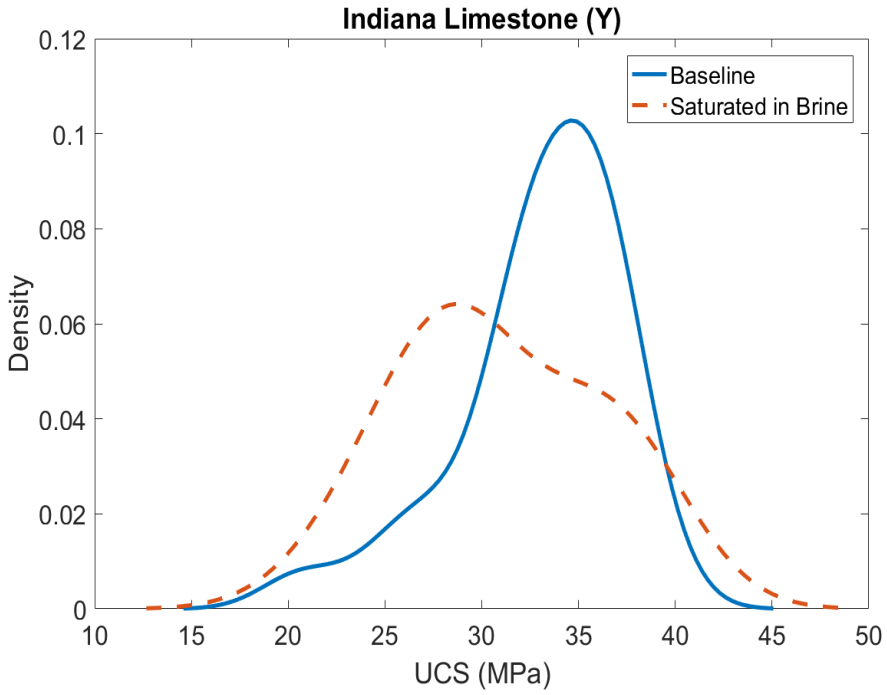

Figure 26: Kernel diagram showing the trend for Indiana Limestone sample Y after saturation in brine as compared to the baseline. The trend shown after saturation in brine is similar to baseline case.

Figure 27 shows the result of a test carried out on Desert Pink Limestone (DP3). Overall, it can be concluded that no significant change has occurred in the strength of DP3 following brine saturation. Occurrence of a bi-modal behavior, however, is observed. This behavior can potentially be explained by the random occurrence of cementing material along scratch length that tends to show a higher strength. Figure 28 shows a clear presence of two strength zones in the sample. Also, color difference as shown in the groove photograph coincides with occurrence of the differing zones.

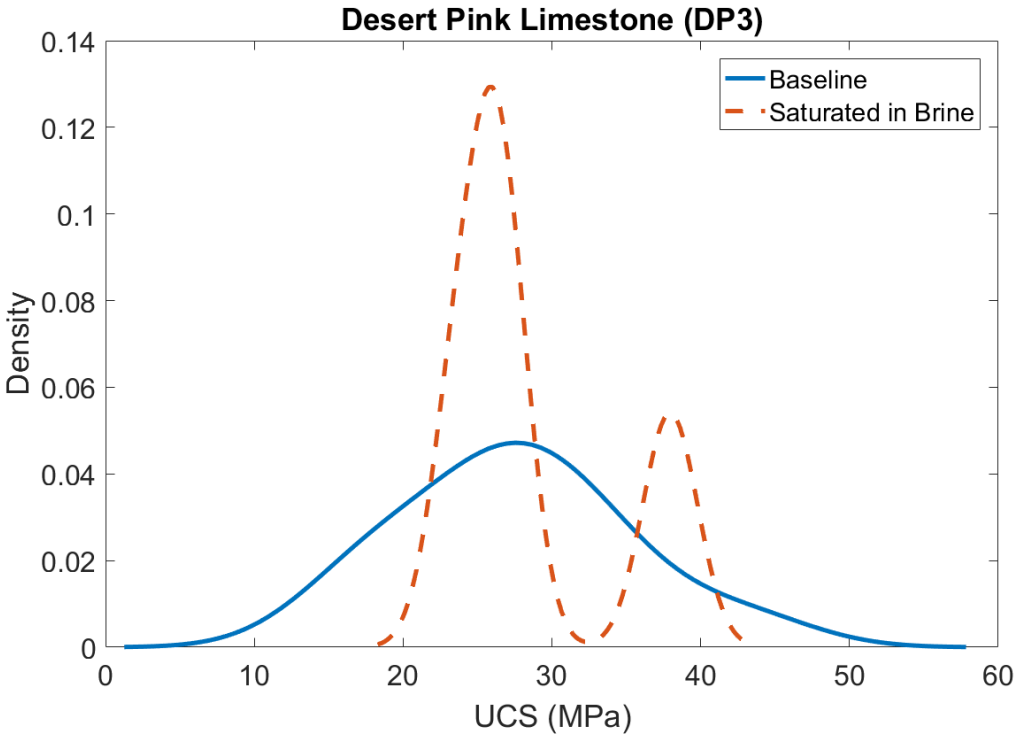

Figure 27: Kernel diagram showing the trend for Desert Pink Limestone sample DP3 that produces a bi-modal behavior after saturation in brine as compared to the baseline.

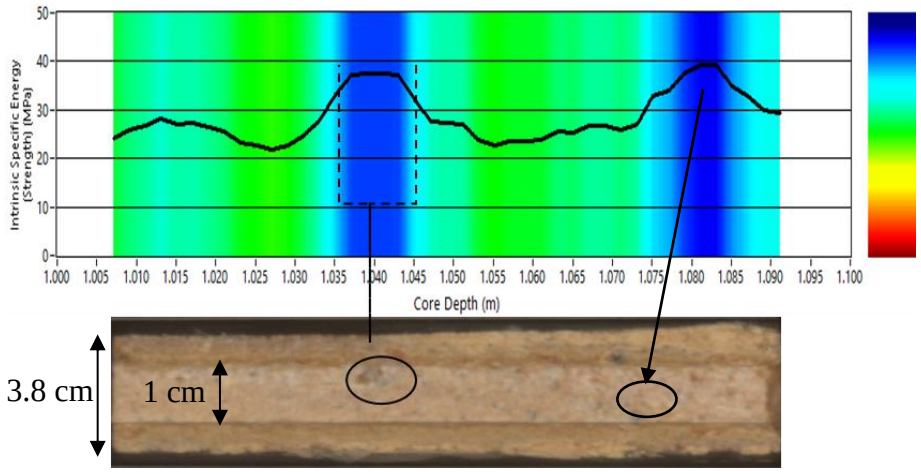

Figure 28: Evidence of cementing material causing spikes in the response as depicted in the ISE log.

Contrary to carbonates, tests on sandstone samples displayed a certain degree of increase in the strength with densities shifting towards the right as shown in Figs. 29 and 30 for Berea Buff (BB1) and Berea Gray (BG1) samples respectively. The weakening in UCS is distinctive in Berea Buff sandstone.

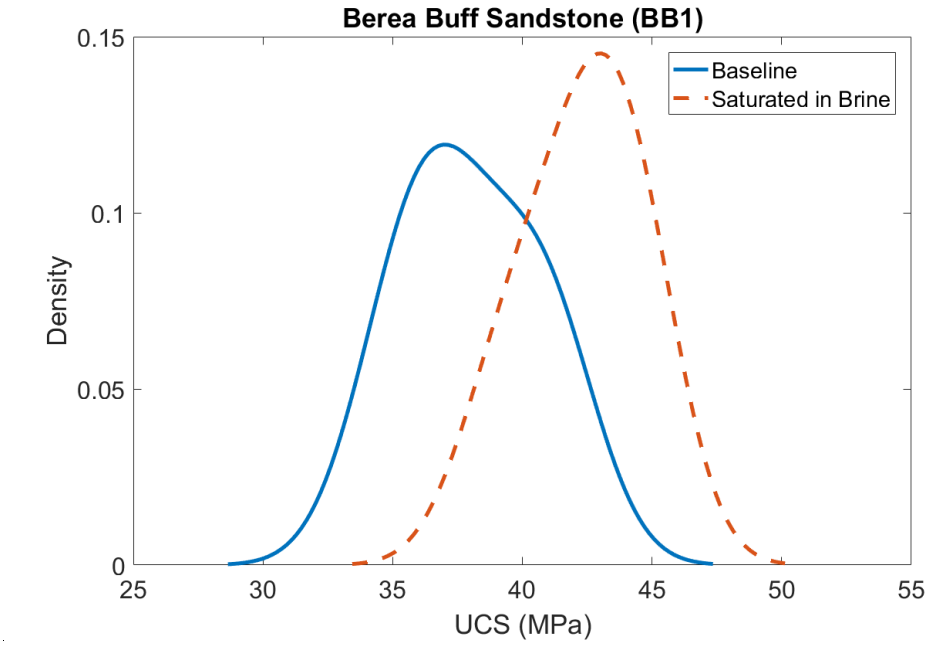

Figure 29: Kernel diagram showing the trend for Berea Buff Sandstone sample BB1 after saturation in brine as compared to the baseline. The shift towards the right of the plot indicates strengthening due to brine saturation.

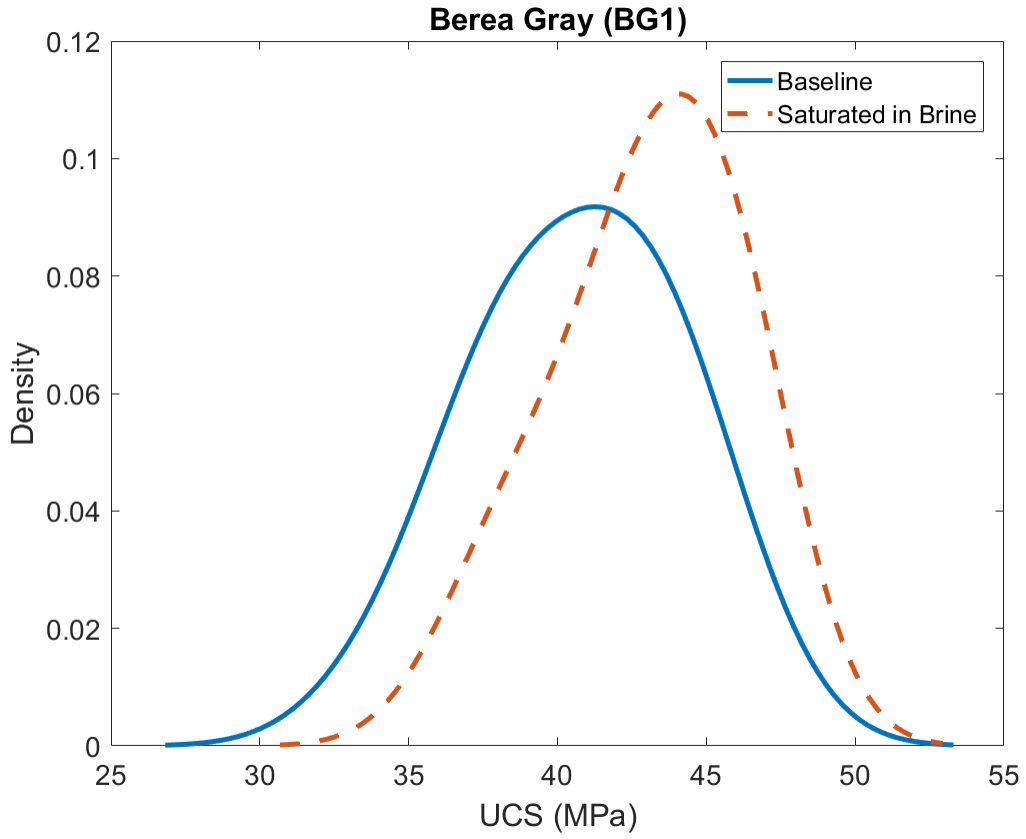

Figure 30: Kernel diagram showing the trend for Berea Grey Sandstone sample BG1 after saturation in brine as compared to the baseline. Strengthening behavior shown by the shift in the plot towards the right.

The effect of high salinity brines on the geomechanical characteristics of sandstones is not completely understood. Several studies, however, documented a formation damage mechanism due to high salinity. Bishop (1997) reported a high degree of pore throat bridging and plugging in the matrix attributed to flocculation of clays covering the pore surface due to the invasion of high salinity filtrate from the drilling mud. Figure 31 shows SEM analysis of the sample Bishop used in his analysis. The first image shows the native state before invasion where the pore throats are clearly visible with finely coated quartz grains. The second image shows the SEM image after invasion illustrating plugging of the pore structure by clusters of Kaolinite.

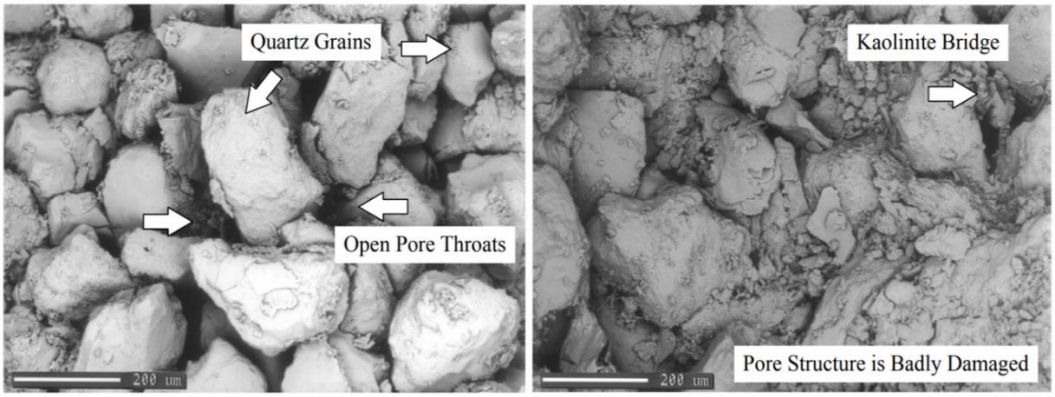

Figure 31: Native state with open pore throats (left). State after invasion of salt saturated filtrate resulting in bridging of pore throats (right) (Bishop 1997).

Shukla et al. (2013) reported an increase in UCS of rock samples with increasing brine salinity. Rathnaweera et al. (2014) investigated the impact of brine concentration on UCS of sandstone samples using conventional UCS test. They showed that UCS increased by about 4% to 10% for a 20% to 30% NaCl concentration respectively. Post-saturation SEM analysis suggested that the increment is due to salt crystal growth in pore spaces. The growth is significant for 20% and 30% brine concentrations as shown in Fig. 32. In our particular case a 20% NaCl concentration resulted in an approximate increase of 4% - 13% for Berea Grey and Berea Buff sandstones respectively.

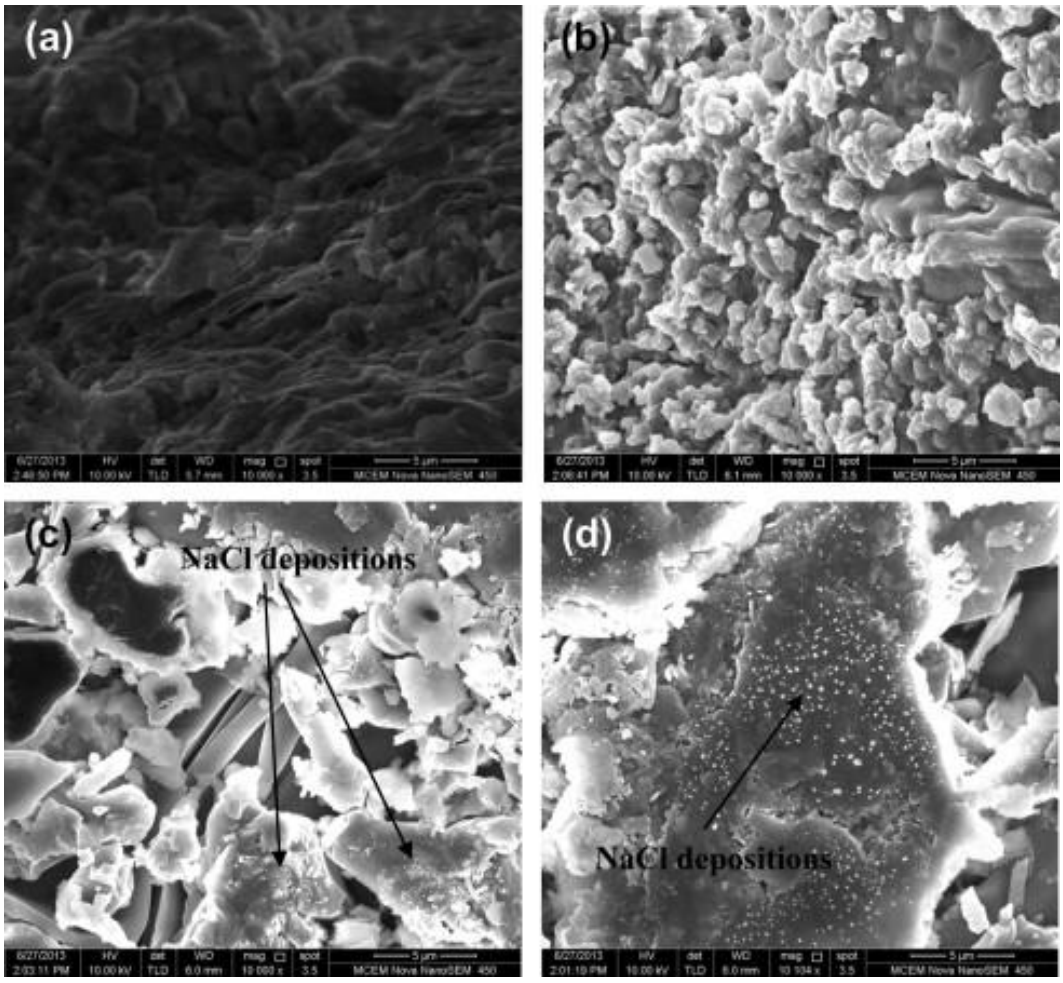

Figure 32: Results from SEM analysis (a) water-saturated sample, (b) 10% NaCl brine, (c) 20%NaCl brine and (d) 30% NaCl brine (Rathnaweera et al. 2014).

Literature suggests that the strengthening behavior as experienced by sandstone samples can be attributed to two main physico-chemical effects (Bishop 1997; Rathnaweera et al. 2014):

1. Crystallization of the salt from the brine in the pore spaces likely leads to a strength enhancement due to reduction of voids.
2. Bridging of pore throats due to flocculation of clay particles lead to a more consolidated rock mass.

Figure 33 summarizes the percentage changes in UCS for the different rock types relative to the baseline UCS due to brine saturation. Two different trends for limestone and sandstone can be observed. A decrease of up to 12% in UCS was measured for limestone. This could be considered as an effect of water-weakening from the brine, neglecting variable behavior of these rock types. For sandstones, brine causes strengthening as discussed earlier. This is also depicted in the quantitative increase in UCS of about 13%.

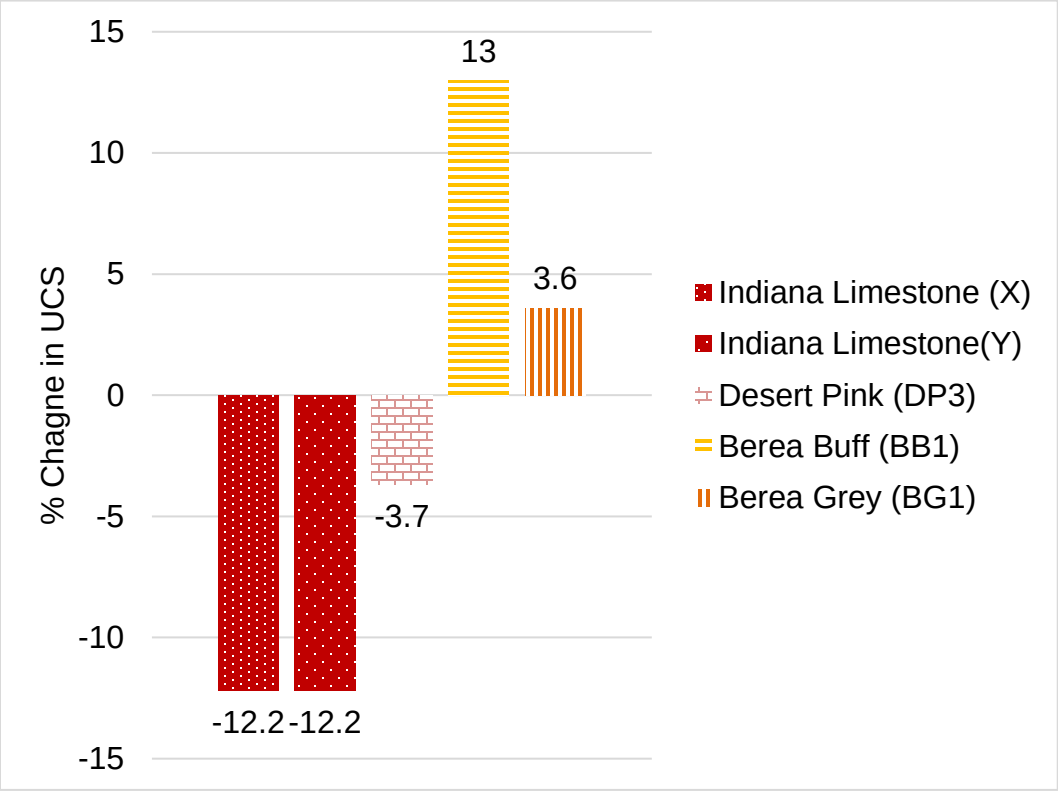

Figure 33: Saturation in Brine. Percentage change in the UCS relative to the baseline UCS. Weakening trend is observed by the limestone samples. Whereas, strengthening is shown by the sandstone samples.

5.1.2 Samples Saturated in Distilled Water

Distilled water is used instead of brine in this phase. This choice is done to isolate the effect of brine strengthening as observed previously.

Four samples are tested in this phase. These include; Indiana Limestone (ILS4), Desert Pink Limestone (DP4), Berea Buff (BB6) and Berea Grey (BG4) sandstone.

A water-weakening trend is observed for both limestone rocks tested. Indiana Limestone (ILS4) shows minimal change as illustrated in Fig. 34. This could be a result of the inherent rock heterogeneity. Hence, definitive conclusion regarding the effect of water cannot be made. Desert Pink Limestone (DP4) displays a significant change in the strength upon water saturation as depicted by the trend in the kernel diagram in Fig. 35. Generally Desert Pink Limestone has greater porosity (29%) than Indiana Limestone (19%) (Freire-Gormaly et al. 2015). This could explain the difference in UCS behavior.

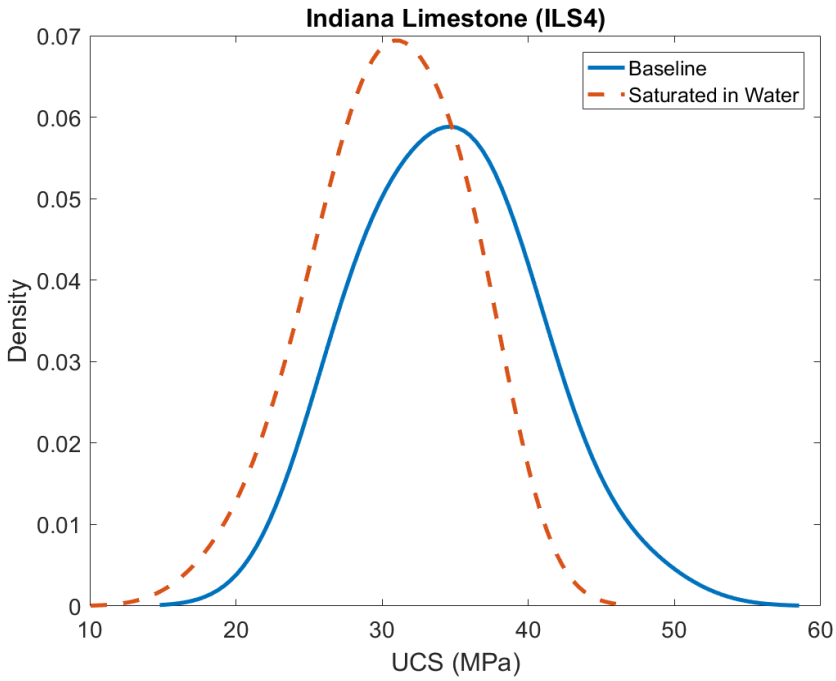

Figure 34: Kernel diagram showing the UCS trend post-water saturation for Indiana Limestone sample ILS4 relative to the baseline. A slight shift towards the left signifies weakening due to distilled water.

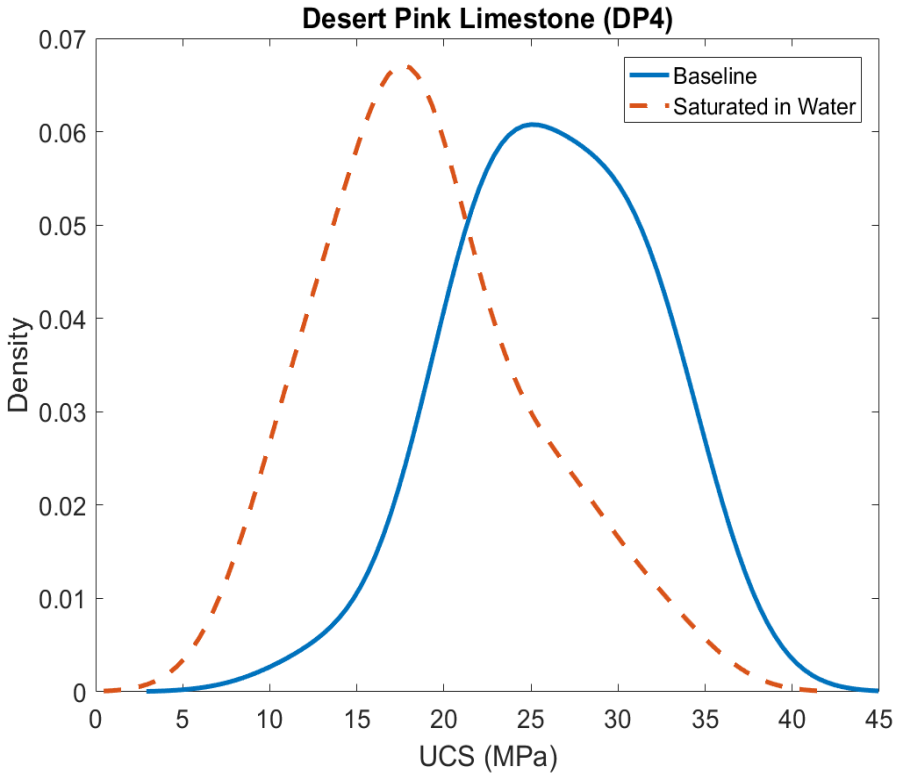

Figure 35: Kernel diagram showing the UCS trend post-water saturation for Desert Pink Limestone sample DP4 relative to the baseline. A larger shift towards the left relative to ILS4 is observed after saturation in distilled water, which is due to a larger porosity in DP4.

A clear weakening in strength was measured for both the sandstone types. This is demonstrated by the shift in the densities towards the left in the kernel diagrams illustrated in Figs. 36 and 37.

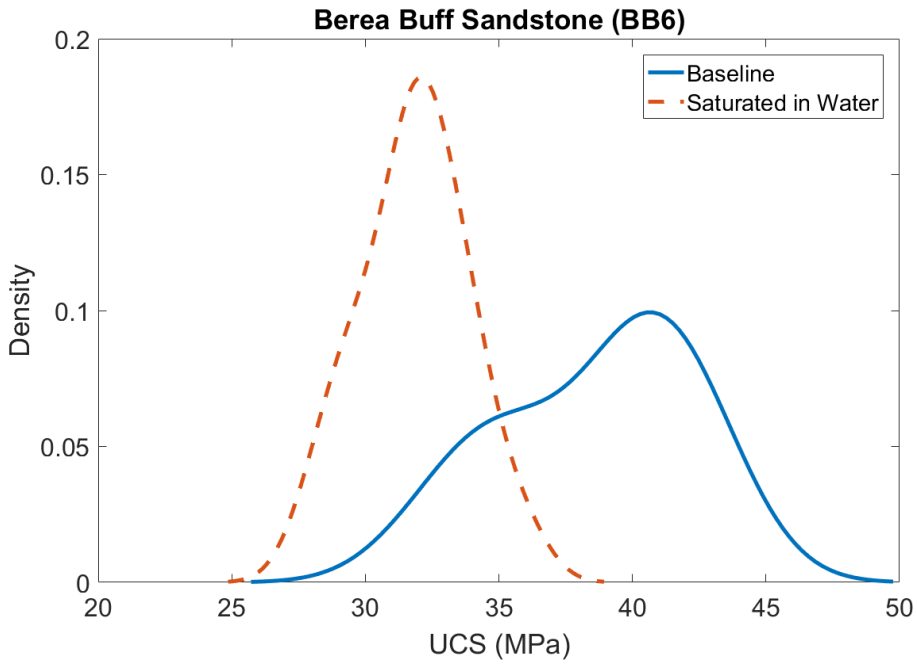

Figure 36: Kernel diagram showing the UCS trend post-water saturation for Berea Buff Sandstone sample BB6 relative to the baseline. The UCS values shift towards the left as indicated by the dashed line, signifying weakening.

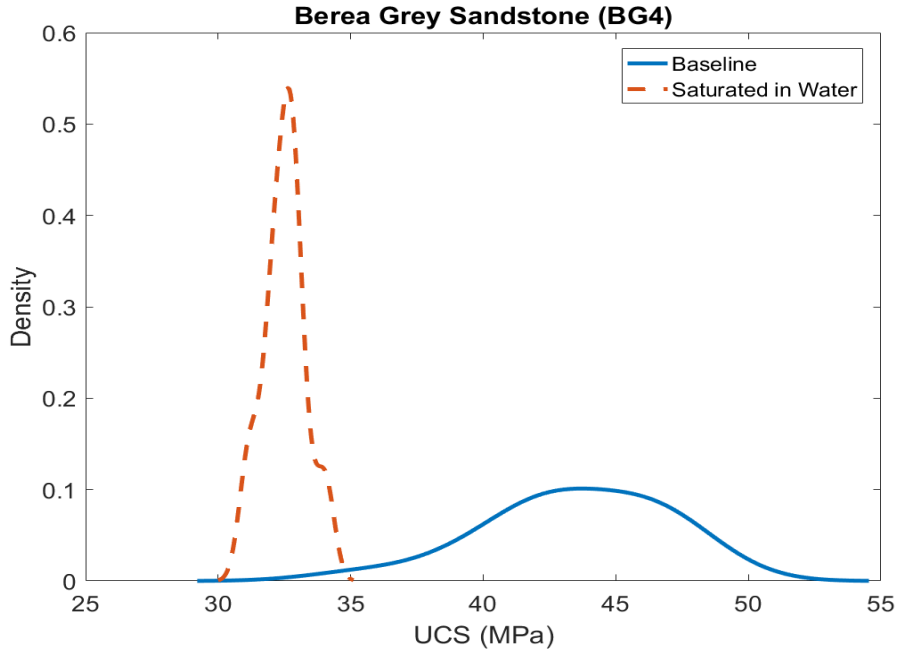

Figure 37: Kernel diagram showing the UCS trend post-water saturation for Berea Grey Sandstone sample BG4 relative to the baseline. The UCS values shift towards the left as indicated by the dashed line, signifying weakening. The shift is larger as compared to BB6, which point towards clay swelling mechanism for the weakening due to greater amount of Illite in BG4.

Figure 38 summarizes the percentage change in UCS observed for all the samples. Overall, limestone samples lost up to approximately 24% of their original UCS. Similar strength reduction was recorded for sandstone samples as well.

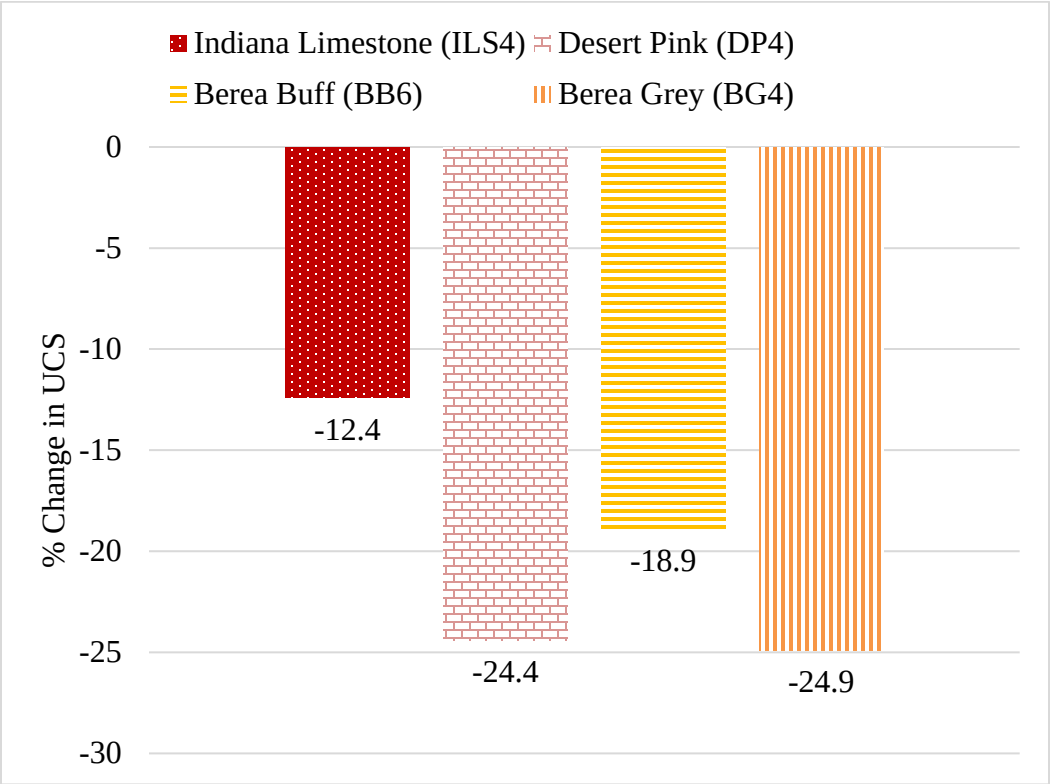

Figure 38: Saturation in Distilled Water. Percentage change in the UCS relative to the baseline UCS for all the samples. Consistent decrease in strength is observed for all the rock samples that were tested.

5.1.3 Samples Saturated in Crude Oil

Crude oil from a Saudi Arabian reservoir was used in this phase. For the carbonates tested, there was minimal to no change in strength as shown by the similar trend to the baseline measurement in the kernel diagrams in Figs. 39 and 40 for Indiana Limestone (ILS2) and Desert Pink Limestone (DP2) respectively.

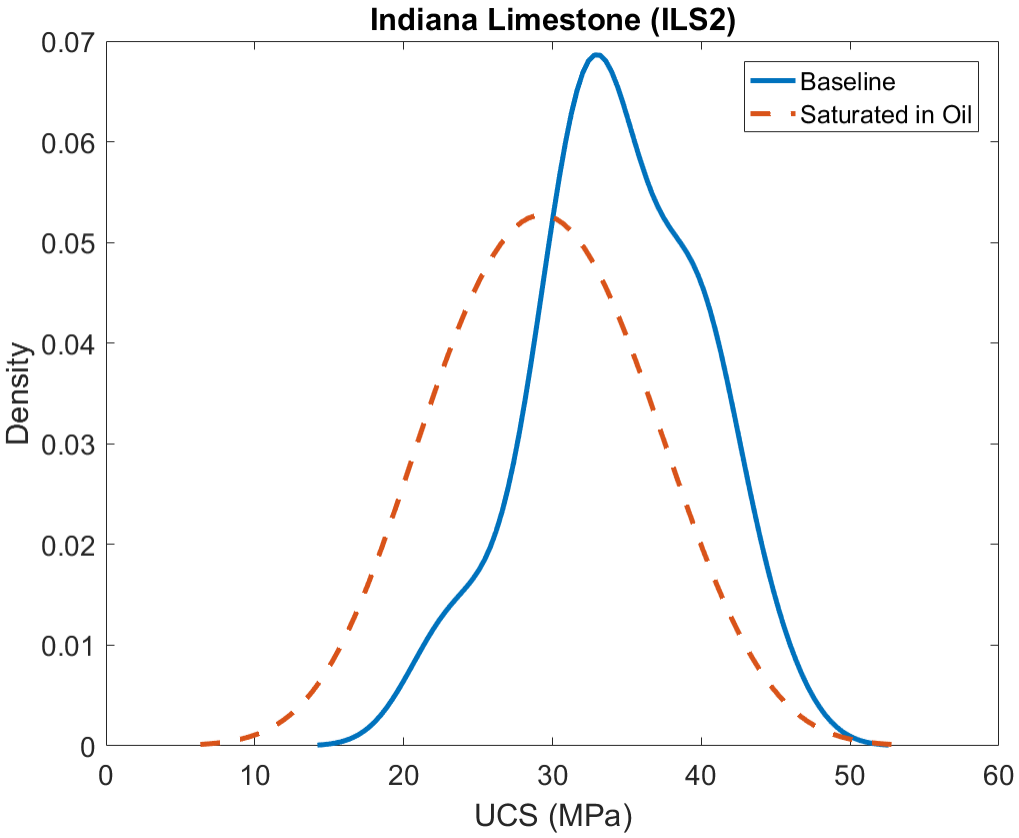

Figure 39: Kernel diagram showing the UCS trend post-oil saturation for Indiana Limestone sample ILS2 relative to the baseline. The kernel diagram after saturation follows similar trend to the baseline UCS, depicting no change in strength.

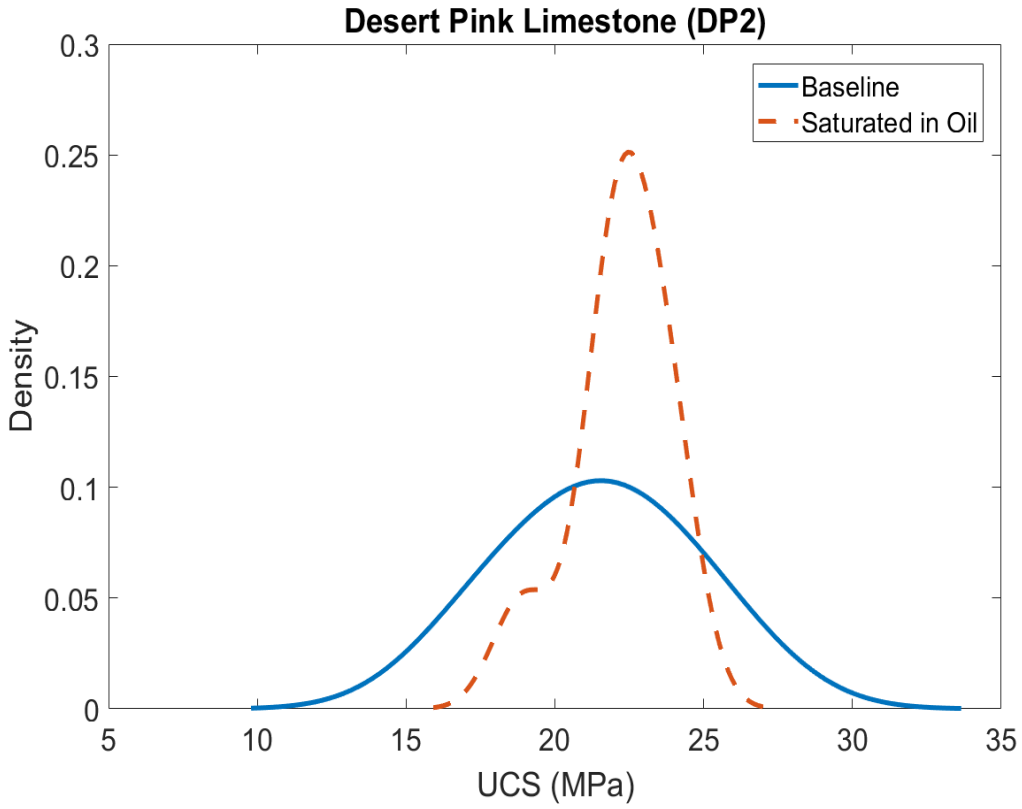

Figure 40: Kernel diagram showing the UCS trend post-oil saturation for Desert Pink Limestone sample DP2 relative to the baseline. The kernel diagram after saturation follows similar trend to the baseline UCS, depicting no change in strength.

Berea Buff Sandstone sample (BB4) tested after oil saturation shows a clear transition from the baseline to a lower strength value as observed in Fig. 41. The kernel diagram for Berea Grey (BG2) in Figure 42, however, does not indicate any considerable change in the UCS value after oil saturation. This insensitivity to oil saturation is probably due to the mineralogical differences between the two sandstone types. Moreover, Berea Grey Sandstone is affected by water saturation not oil and contains certain clay swelling minerals like Illite (Shehata and Nasr-El-Din 2014; Mahmoud and Al-Hashim 2018). This points towards clay swelling as the weakening mechanism.

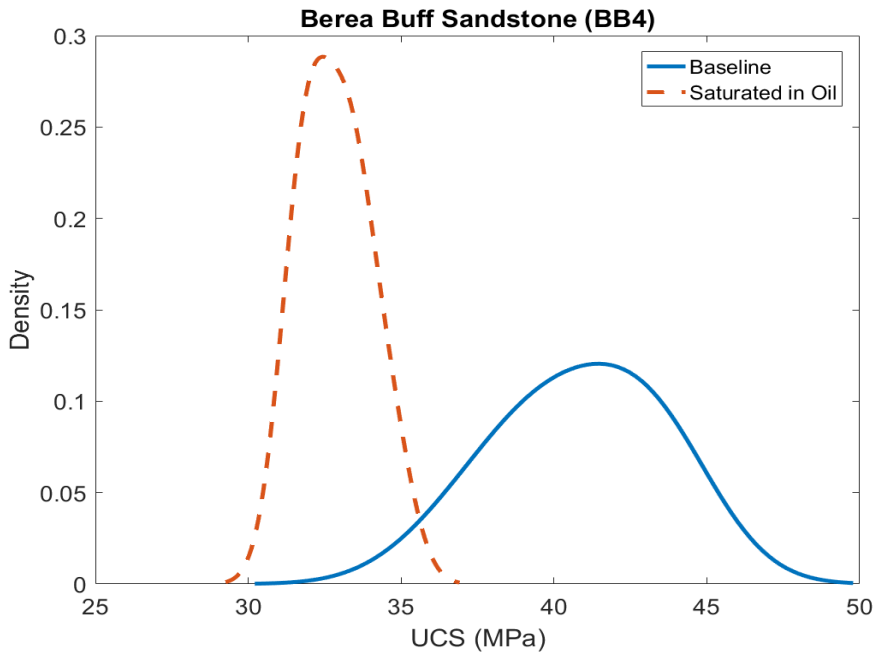

Figure 41: Kernel diagram showing the UCS trend post-oil saturation for Berea Buff Sandstone sample BB4 relative to the baseline. A clear transition from the baseline UCS value to a lower value is observed after sample is saturated in oil.

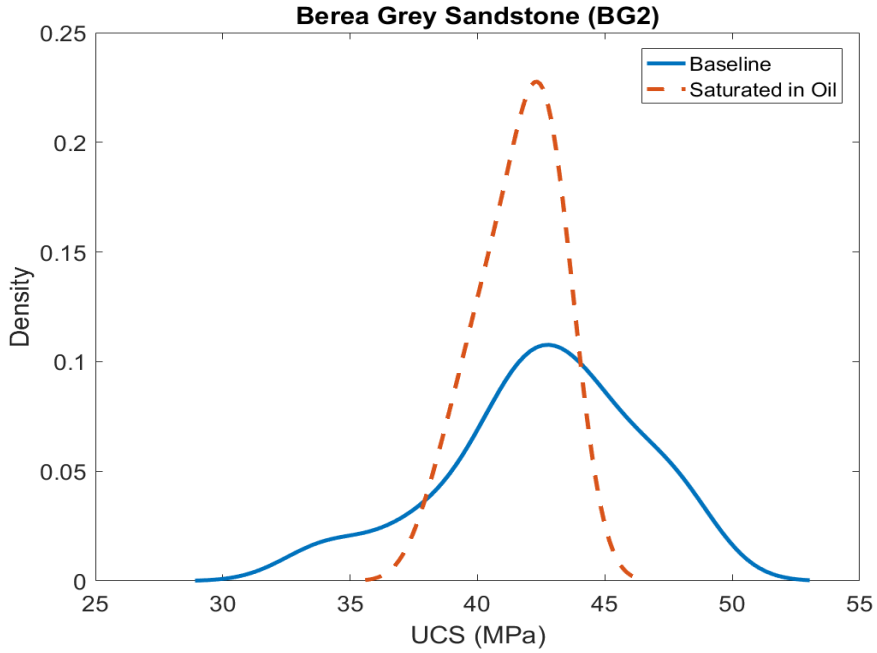

Figure 42: Kernel diagram showing the UCS trend post-oil saturation for Berea Grey Sandstone sample BG2 relative to the baseline. The trend after oil saturation does not show any considerable change.

Percentage change in the UCS values post-oil saturation is shown in Fig. 43. There is a slight weakening effect shown by Indiana Limestone (ILS2), which is not conclusive due to intrinsic rock strength variability. The increase in Desert Pink Limestone (DP2) is misleading due to the presence of multiple strength zones and can be neglected based on overall trend. The Berea Buff Sandstone sample (BB4) experienced about 20% decrease in the UCS.

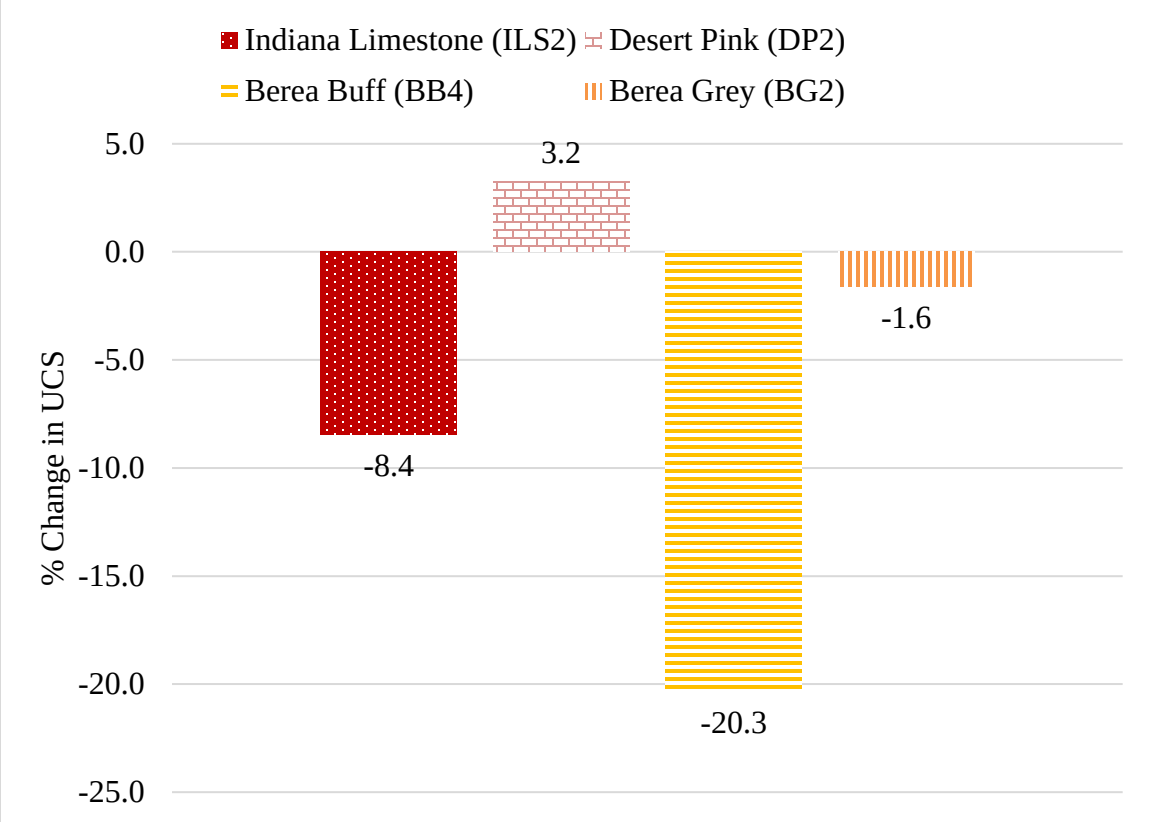

Figure 43: Saturation in Crude Oil. Percentage change in the UCS relative to the baseline UCS for all the samples.

5.1.4 Samples Aged in Brine

This step involves introducing both temperature (150^{o}C) and fluid to the core samples. The same 20% NaCl concentration brine prepared for the saturation phase was used. Due to the size restriction of the cell used, only three samples could be accommodated in this phase of the experiments. Consequently, only Berea Buff sandstone type was tested along with the two limestones.

Observations regarding the tested limestones is as follows:

- Indiana Limestone showed no apparent change in strength values as displayed by Fig. 44 and keeping in mind the fluctuating trends as discussed earlier.
- Desert Pink Limestone illustrated a slight decrease in strength as depicted by the shift to the left in the kernel diagram in Fig. 45. The reduction in strength is not conclusive due to the heterogeneity of the specimen.

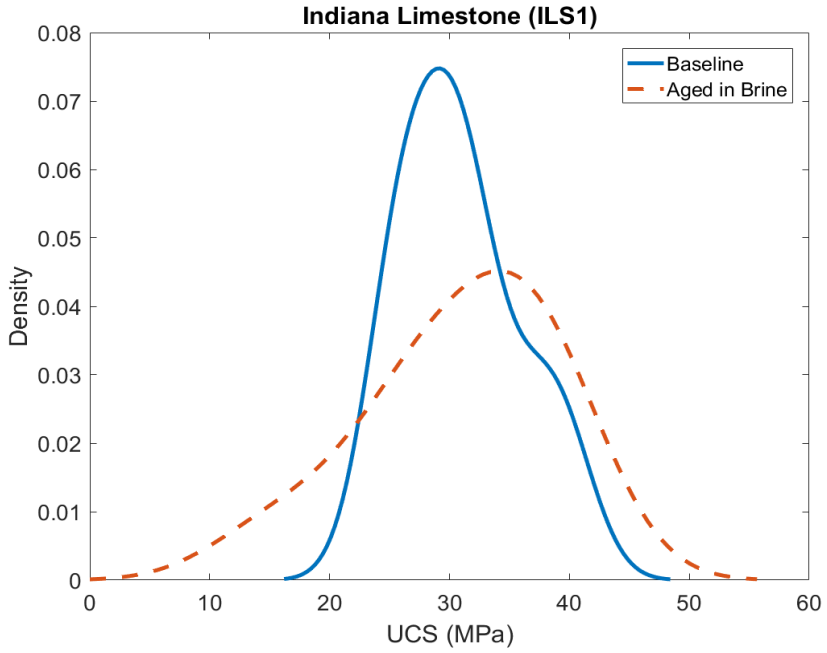

Figure 44: Kernel diagram showing the UCS trend relative to the baseline after aging Indiana Limestone sample ILS1 in brine. No apparent change in UCS observed.

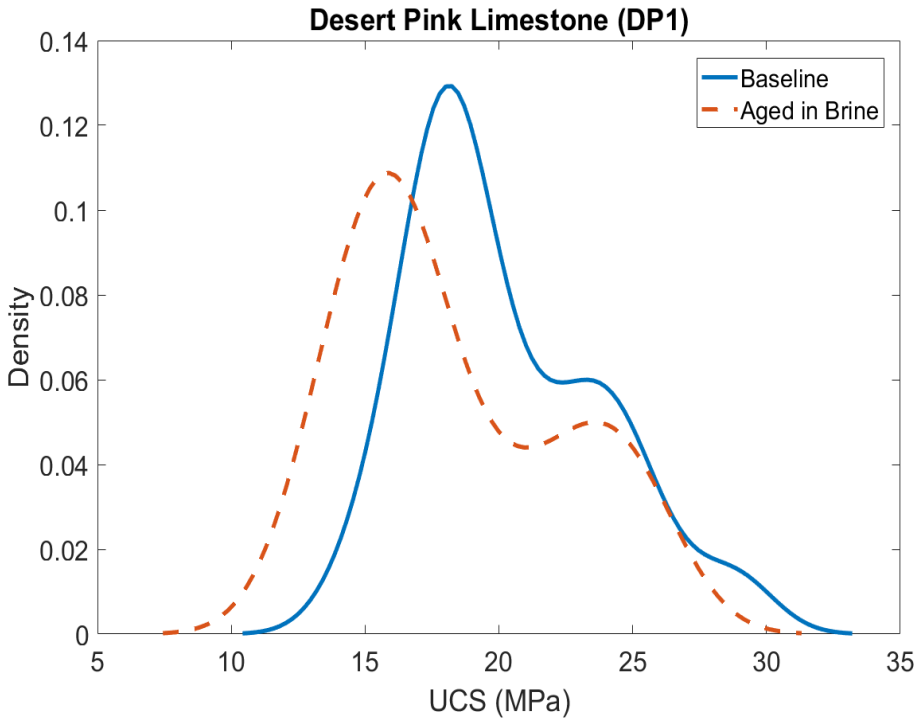

Figure 45: Kernel diagram showing the UCS trend relative to the baseline after aging Desert Pink Limestone sample DP1 in brine. No significant change measured as shown by the similar trend of the aged sample to the baseline.

Berea Buff (BB3) seems to exhibit retention in strength after aging in brine. As observed in Fig. 46, there is an apparent reduction in strength as shown by the trend moving towards the left of the plot. The trend, however, shows that higher strength values are also measured after the aging. Conclusion for this sample is not possible using the available results.

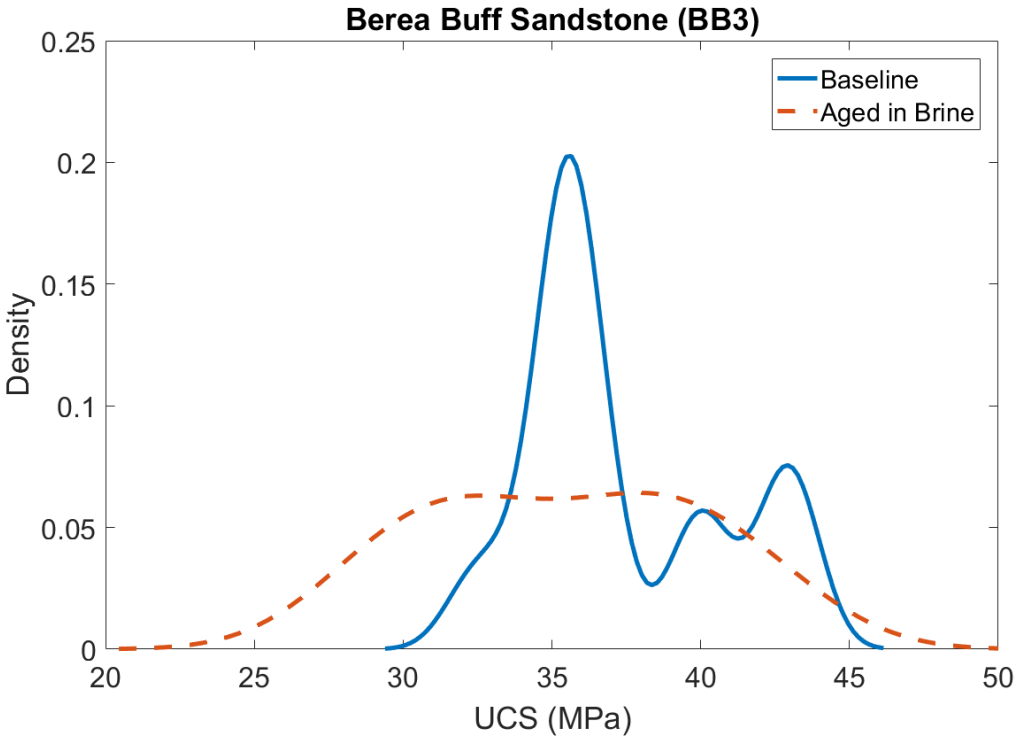

Figure 46: Kernel diagram showing the UCS trend relative to baseline after aging Berea Buff Sandstone sample BB3 in brine. Flatter kernel diagram after aging is reported.

A quantitative assessment using percentage change in medians is produced in Fig. 47. It is to be noted, however, that the qualitative evidence provided above is more powerful in describing the changes. Quantitative assessment might be misleading here due to the heterogeneous behavior of the rock samples.

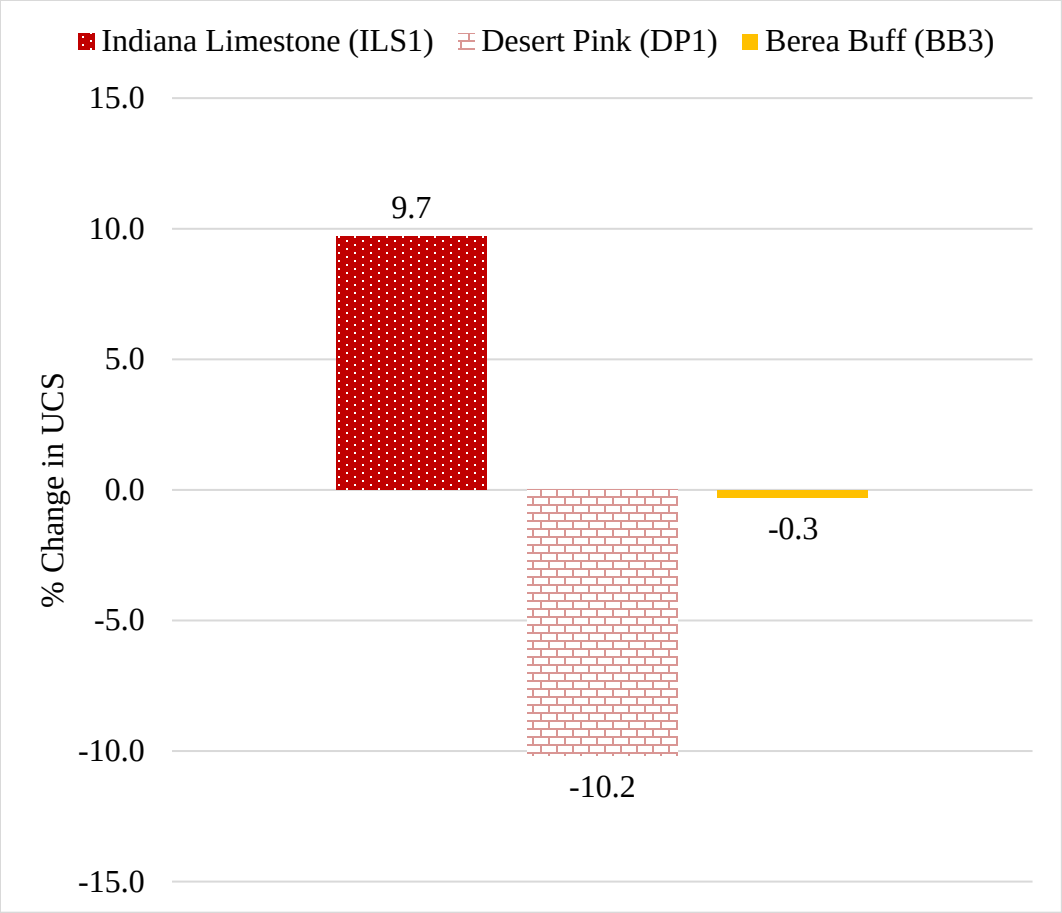

Figure 47: Aging in Brine. Percentage change in the UCS relative to the baseline UCS.

5.1.5 Samples Aged in Distilled Water

For this experimental series, samples were aged at 150°C in combination with distilled water.

The inherent variability in rock strength for Indiana Limestone again lead to inconclusive results as no appreciable change in UCS is observed in the kernel diagram presented in Fig. 48.

In order to better understand the results of Desert Pink Limestone (DP6), it is imperative to consult the ISE log. The kernel diagrams for Desert Pink Limestone (DP6) presented in Fig. 49 depicts a slight affinity towards strengthening. This trend can be better understood by observing the ISE log in Fig. 50. Non-fluctuating behavior is recorded by the post-aged ISE log. This supports the observation that the change is due to the aging process and not because of specimen heterogeneity.

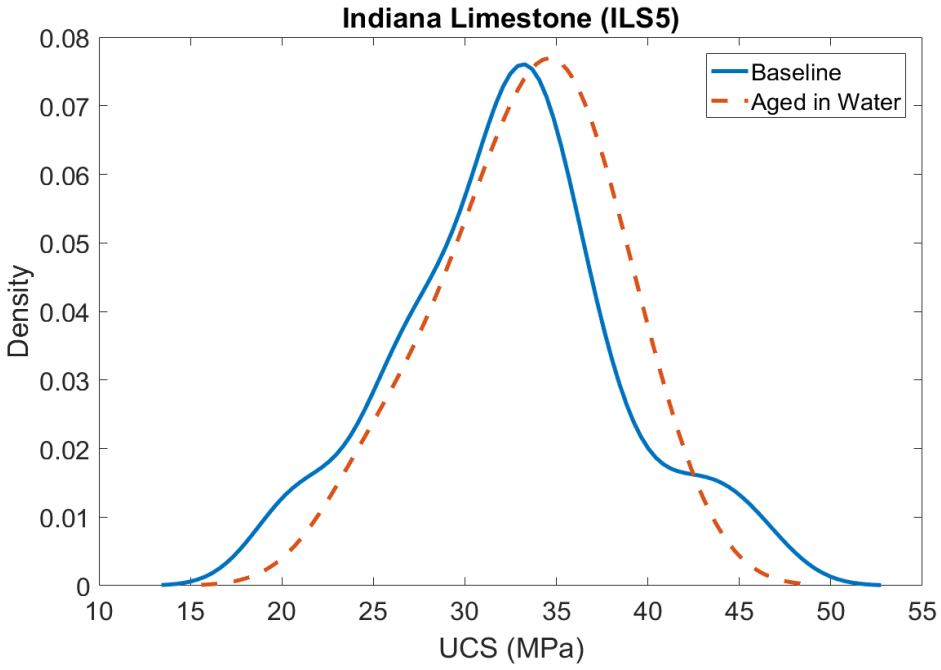

Figure 48: Kernel diagram showing the UCS trend relative to the baseline after aging Indiana Limestone sample ILS5 in distilled water. No appreciable change in UCS is shown by trend for aged sample following the baseline trend.

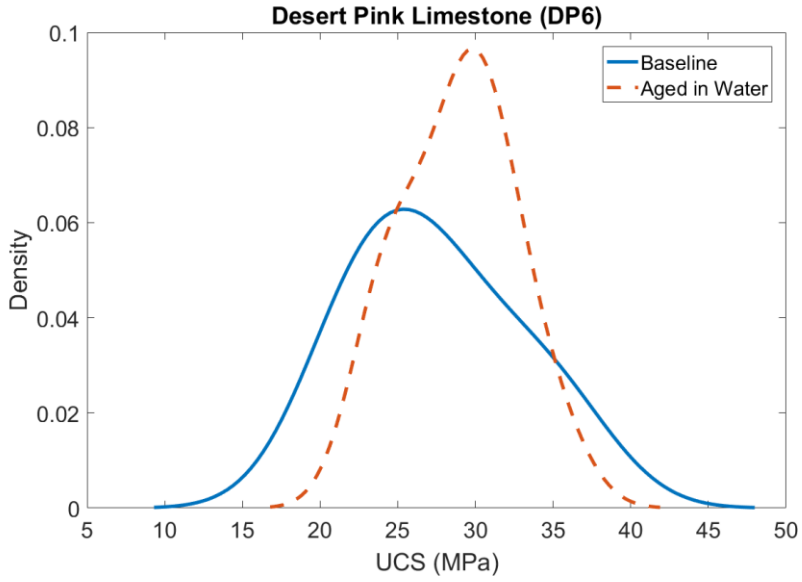

Figure 49: Kernel diagram showing the UCS trend relative to the baseline after aging Desert Pink Limestone sample DP6 in distilled water. A slight increase in UCS is observed after ensuring that this sample is homogenous.

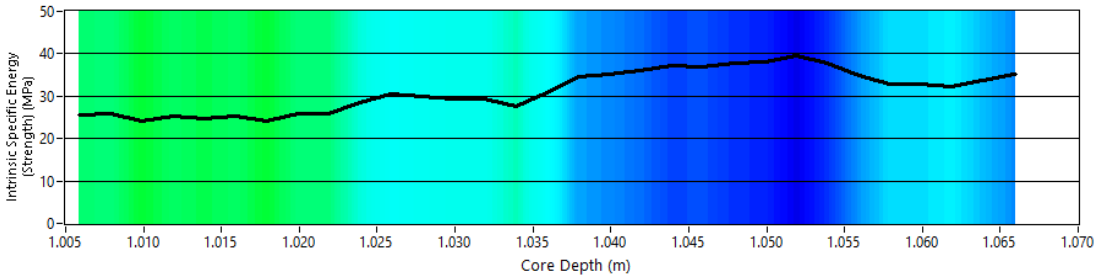

Figure 50 Consistent behavior shown by the ISE log for DP6 that allows for interpretation based on the externally applied aging process.

The sandstone samples tested display a water-weakening impact after being aged in distilled water. Both, Berea Buff (BB7) and Berea Grey (BG3) samples exhibit similar behavior post-saturation. It can be concluded from Figs. 51 and 52 that there are two aspects at play for these rock types:

- First, water causes the strength to deteriorate and hence the shift in the kernel diagrams towards the left.
- Second, temperature opposes the water-weakening effect and thus we see smaller second peaks tending towards higher strength in both samples.

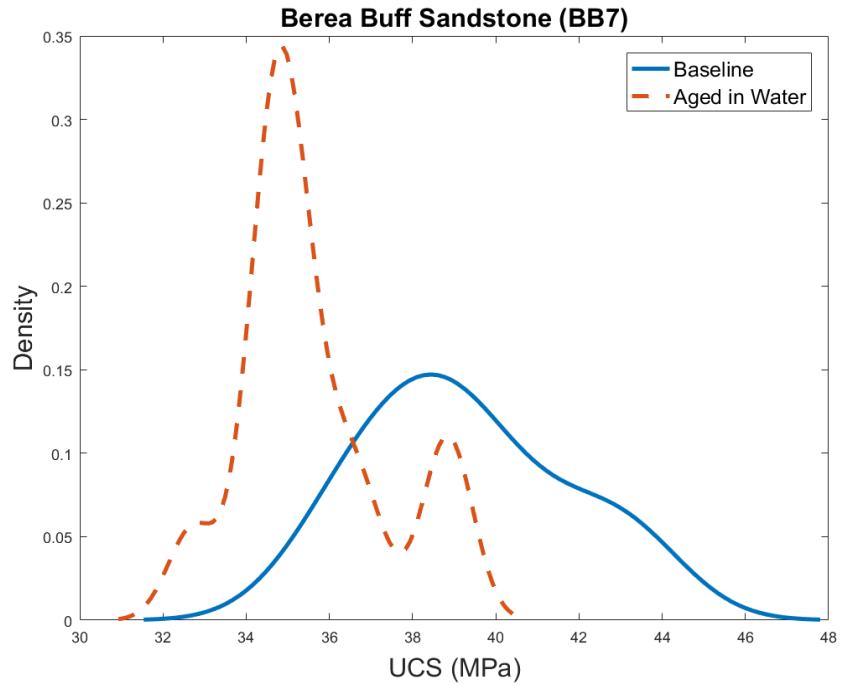

Figure 51: Kernel diagram showing the UCS trend relative to the baseline after aging Berea Buff Sandstone sample BB7 in distilled water. The first peak towards the left signifies the weakening due to water. The second peak towards the right points toward the opposing role of strengthening due to elevated temperature.

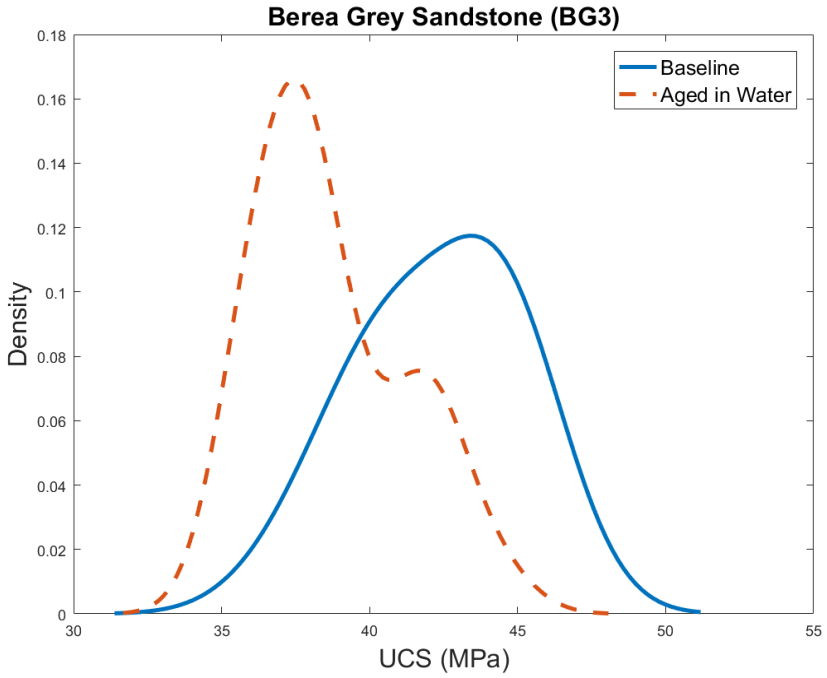

Figure 52: Kernel diagram showing the UCS trend relative to the baseline after aging Berea Grey Sandstone sample BG3 in distilled water. The first peak towards the left signifies the weakening due to water. The second peak towards the right points toward the opposing role of strengthening due to elevated temperature.

To support the claim of strengthening due to temperature, one sandstone and limestone sample each were placed in an oven without any fluid at 150 ^{o}C. Figure 53 displays how the strength for the tested sandstone shows an increasing trend for the UCS when tested after heating the sample continuously for one week. On the contrary, when limestone was heated, minimal change in strength was observed as illustrated in Fig. 54 by the kernel diagram exhibiting no appreciable change in UCS. This analysis leads us to the conclusion that sandstone depicts a higher degree of strengthening at elevated temperatures than limestone and hence supports our observations discussed above. Additionally, limestone tends to establish no appreciable change for the period used in this analysis.

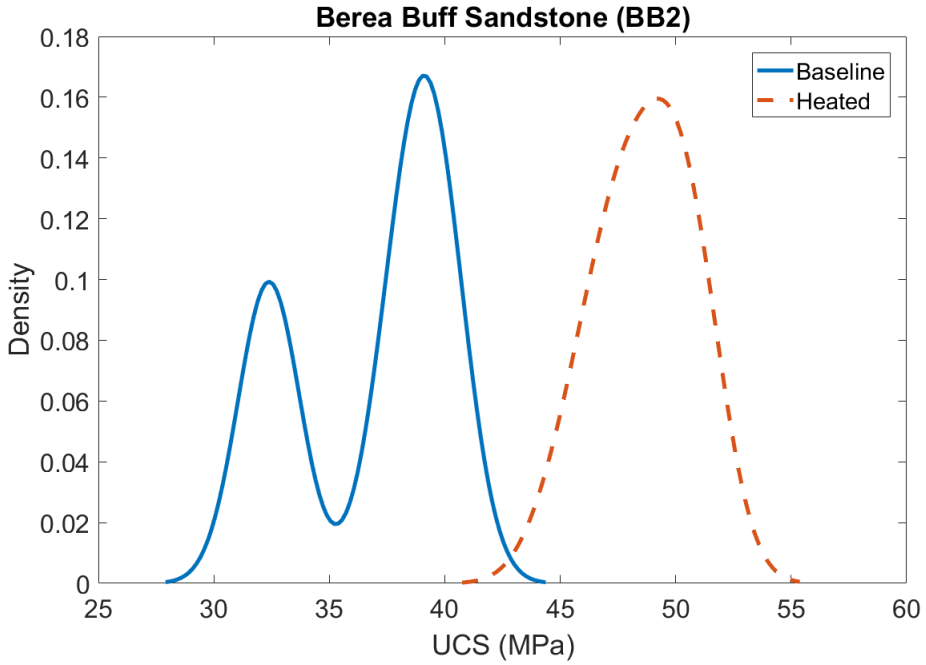

Figure 53: Kernel diagram illustrating strengthening trend for Berea Buff Sandstone sample after heating at 150 ^{o}C for one week.

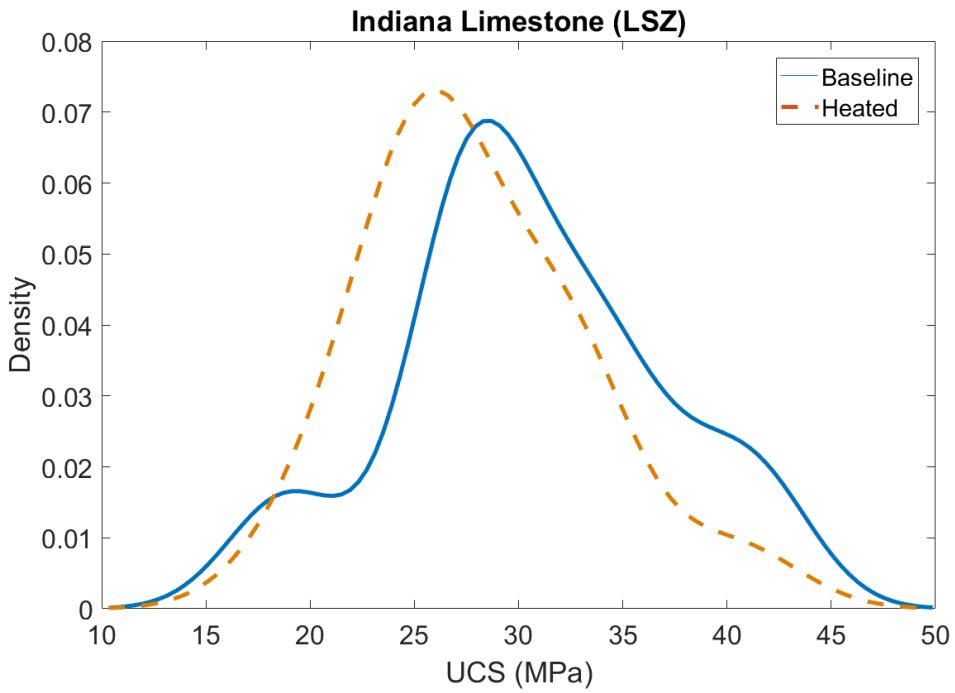

Figure 54: Kernel diagram depicting no appreciable change in trend for Indiana Limestone sample after heating at 150 ºC for one week.

Numerical change in the UCS is reported in Fig. 55. As explained earlier, the change in Indiana limestone sample needs to be looked upon with caution as it might be due to factors other than the aging process. Desert Pink sample (DP6) showed a consistent increase in strength of up to 9%. Both sandstone samples, however, experienced a strength decrement of around 10%.

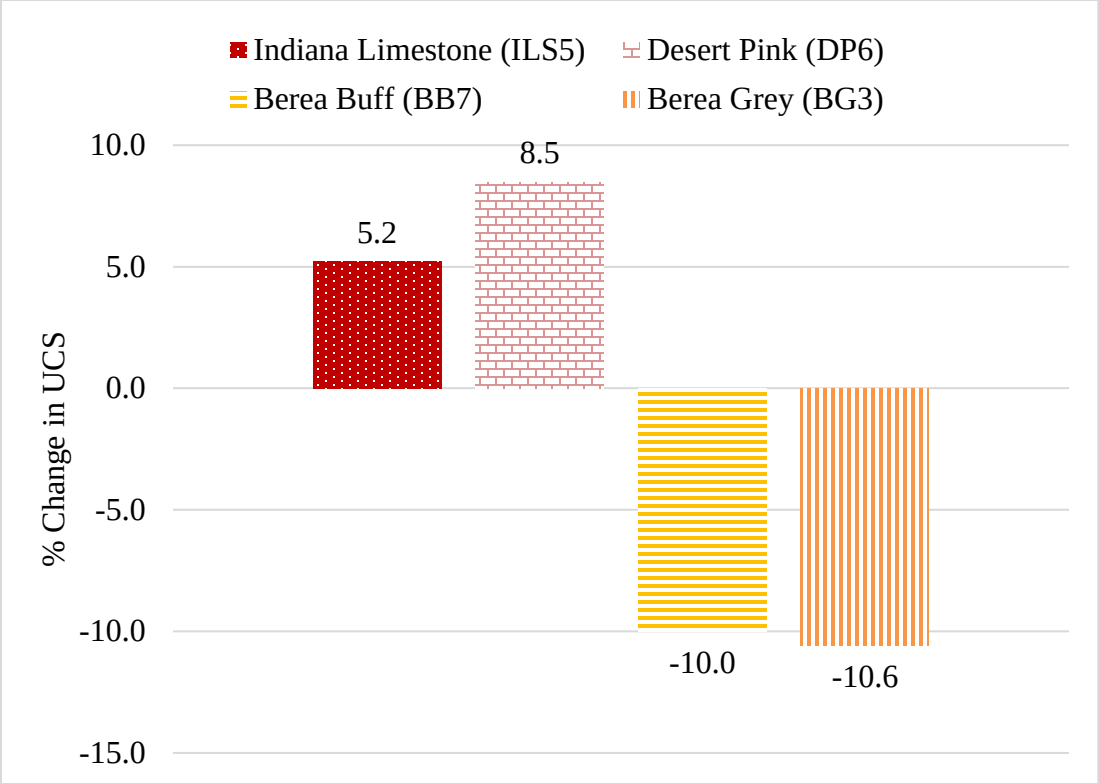

Figure 55: Aging in Distilled Water. Percentage change in the UCS relative to the baseline UCS for all the samples. The results of limestone samples are inconclusive due to their heterogeneous response to the scratch test. A clear decrease of about 11% is observed in the sandstone samples.

5.1.6 Samples Aged in Crude Oil

In this case, the fluid is the same crude oil used in the saturation phase. The fluid was chosen to see the impact of aging samples close to petroleum reservoir conditions.

Indiana Limestone (ILS3) shows no change as indicated by the trend in Fig. 56.

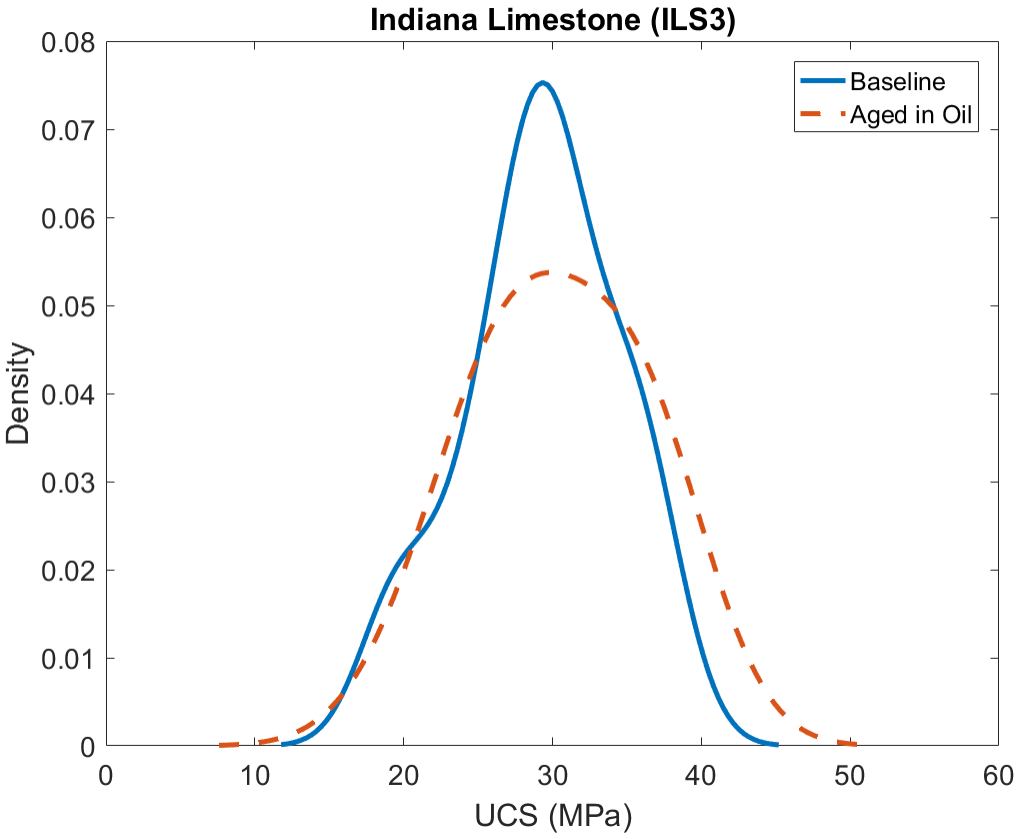

Figure 56: Kernel diagram showing the UCS trend relative to the baseline after aging Indiana Limestone sample ILS3 in crude oil. The trend indicates no change in UCS.

The Desert Pink (DP5) sample displayed an increase in strength upon introduction of heat with crude oil as depicted by the kernel diagram in Fig. 57 which shifts towards the right.

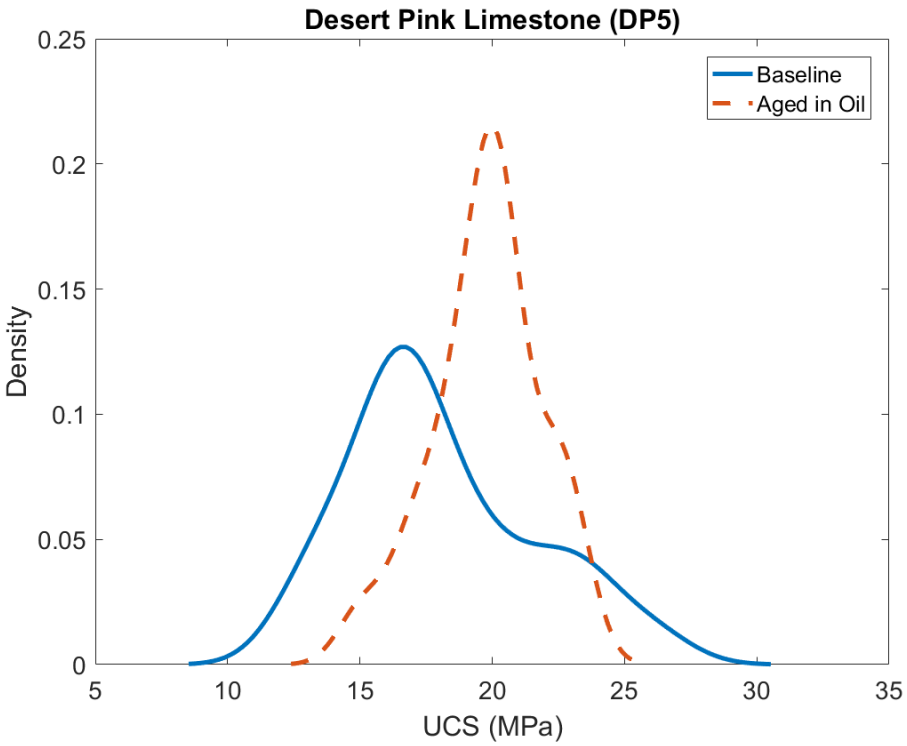

Figure 57: Kernel diagram showing the UCS trend relative to baseline after aging Desert Pink Limestone sample DP5 in crude oil. The kernel diagram for the sample after aging shifts towards the right, indicating strengthening.

Similar observations to those made in the earlier section pertaining to aging in distilled water can be made for the sandstone samples tested in this phase. The Berea Buff (BB5) sample illustrates weakening due to crude oil saturation as shown by the first peak towards the left in the kernel diagram of Fig. 58. The second peak towards the right, however, represents the strengthening impact due to elevated temperature.

The kernel diagram of Berea Grey Sandstone (BG5) in Fig. 59 exhibits a much more pronounced weakening effect that was not observed in the saturation phase. For the aging phase the samples resided in crude oil for a longer time. Hence, this could be an explanation for the change observed in the aging phase. A smaller affinity towards strengthening is observed in the kernel diagram as compared to the Berea Buff sample (BB5).

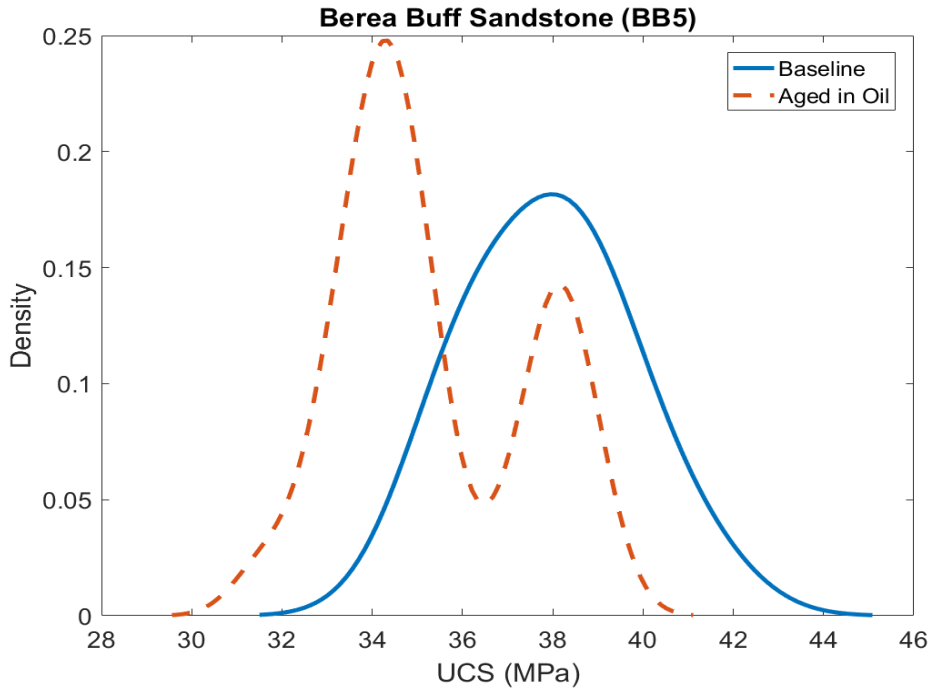

Figure 58: Kernel diagram showing the UCS trend relative to baseline after aging Berea Buff Sandstone sample BB5 in crude oil. The sample illustrates weakening as shown by the first peak towards the left. The second peak towards the right, however, represents the strengthening impact due to elevated temperature.

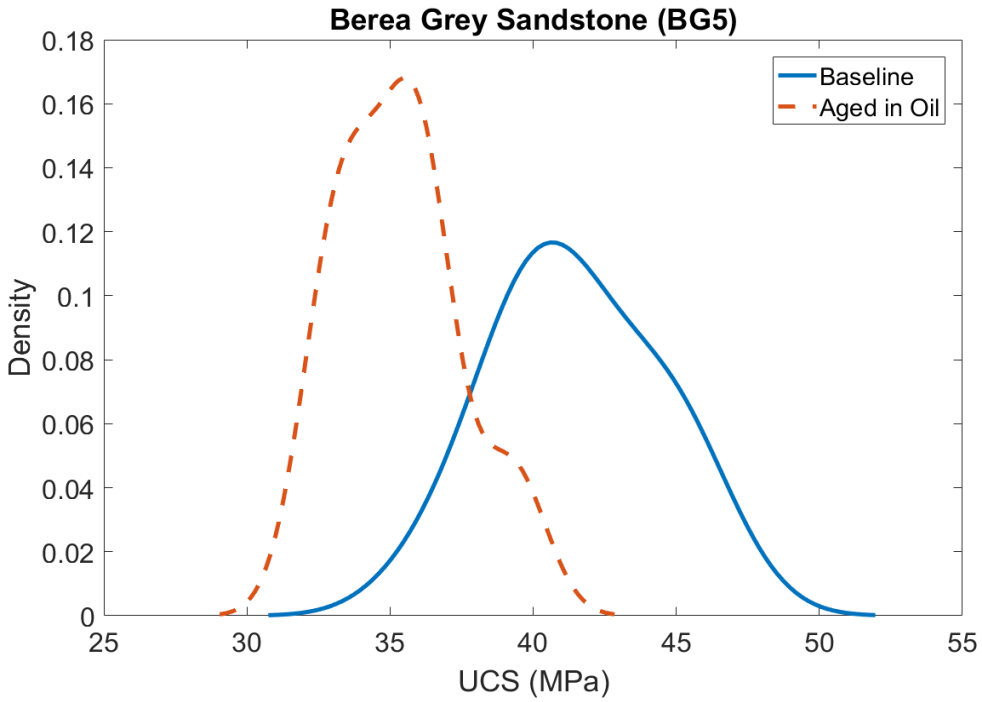

Figure 59: Kernel diagram showing the UCS trend relative to baseline after aging Berea Grey Sandstone sample BG5 in crude oil. Strong weakening is observed by the shift in the diagram towards the left. A smaller affinity towards strengthening is reported as compared to BB5.

Aging in crude oil did not yield an effect on the Indiana Limestone sample with the change in UCS being minimal as illustrated in Fig. 60. Desert Pink Limestone, however, displayed considerable amount of strengthening by up to 17%. Furthermore, both Berea Buff and Berea Grey sandstone depict an overall weakening effect of around 10% and 14% respectively.

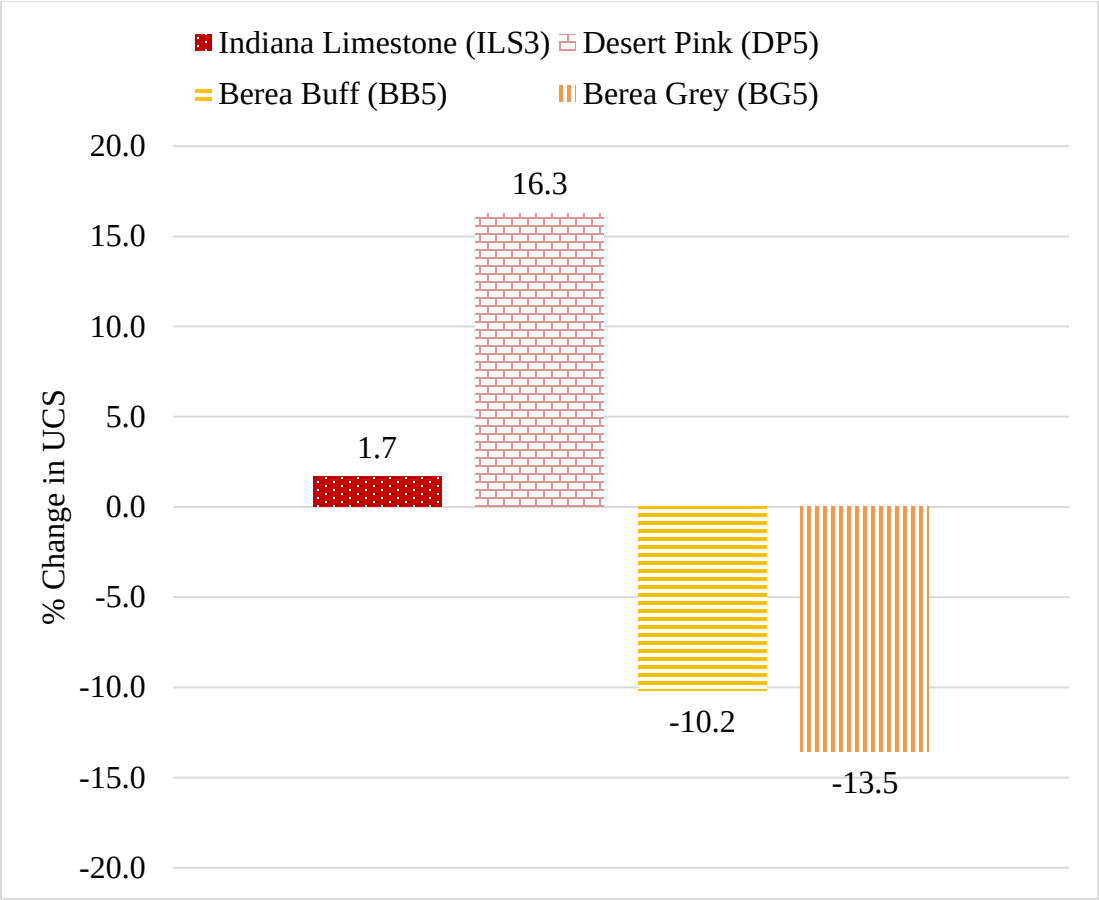

Figure 60: Aging in Crude Oil. Percentage change in the UCS relative to the baseline UCS for all the samples. Desert Pink Limestone shows distinct strengthening. The sandstones, however, show an overall weakening effect.

5.1.7 Effect on Dynamic Poisson's Ratio

The effect on compressional and shear wave velocities due to saturation and aging was investigated in this phase. An ultrasonic device add-on of the Epslog scratch machine was utilized. The schematic for the device is shown in Fig. 61. It is capable of sending and recording both bulk and shear waves. The underlying mechanism is as follows:

1. This device has two probes, a transmitter and a receiver. They are 4 cm apart.
2. The pressure pulses are generated at the transmitter and recorded by the receiver.
3. Time taken for the pulse to travel is recorded.
4. Knowing the distance between the probes, velocity can be calculated.
5. Utilizing the compressional (V_p) and shear (V_s) wave velocities, the dynamic Poisson's ratio (ν_{dyn}) is calculated using Eqn. 5.

$$\nu_{dyn} = \left[\frac{\left(V_p / V_s\right)^2 - 2}{\left\{2\left[\left(V_p / V_s\right)^2 - 1\right]\right\}} \right] \quad \textbf{(5)}$$

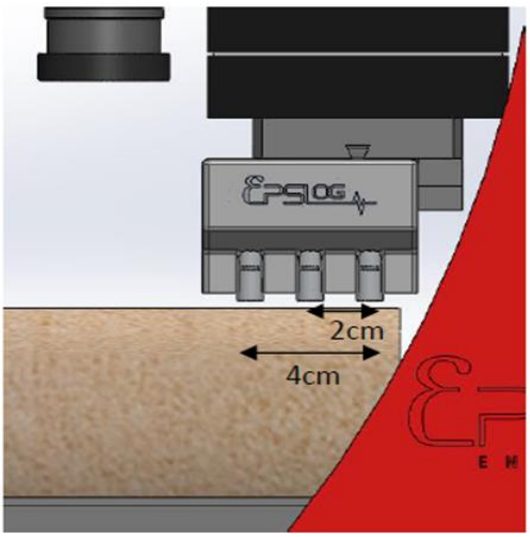

Figure 61: Ultrasonic device add-on for The WOMBAT scratch machine. The transmitter and receiver probes are 4 cm apart and capable of sampling after every 2 cm along the core samples (Epslog, 2018).

The saturation and aging of the limestone samples did not have any appreciable effect on the compressional and shear wave velocities and hence no change in the dynamic Poisson's ratio was observed. For sandstone samples, similar trend was observed for both brine and distilled water. The compressional wave velocity for sandstone samples increased due to increase in bulk density with the inclusion of saturating pore fluids brine and water). The shear wave velocity, however, displayed a slight reduction or no change as they do not travel through fluids. This effect on V_p and V_s causes the velocity ratio (V_p/V_s) to rise, leading to an increase in the calculated dynamic Poisson's ratio. Figure 62 reports the effect on dynamic Poisson's ratio for sandstone samples after being aged and saturated in brine and distilled water. It is observed that aging and saturation in water led to a greater increase in Poisson's ratio as compared to brine. The resulting effect on Poisson's ratio where oil was the saturating fluid has not been reported here as it requires further investigation.

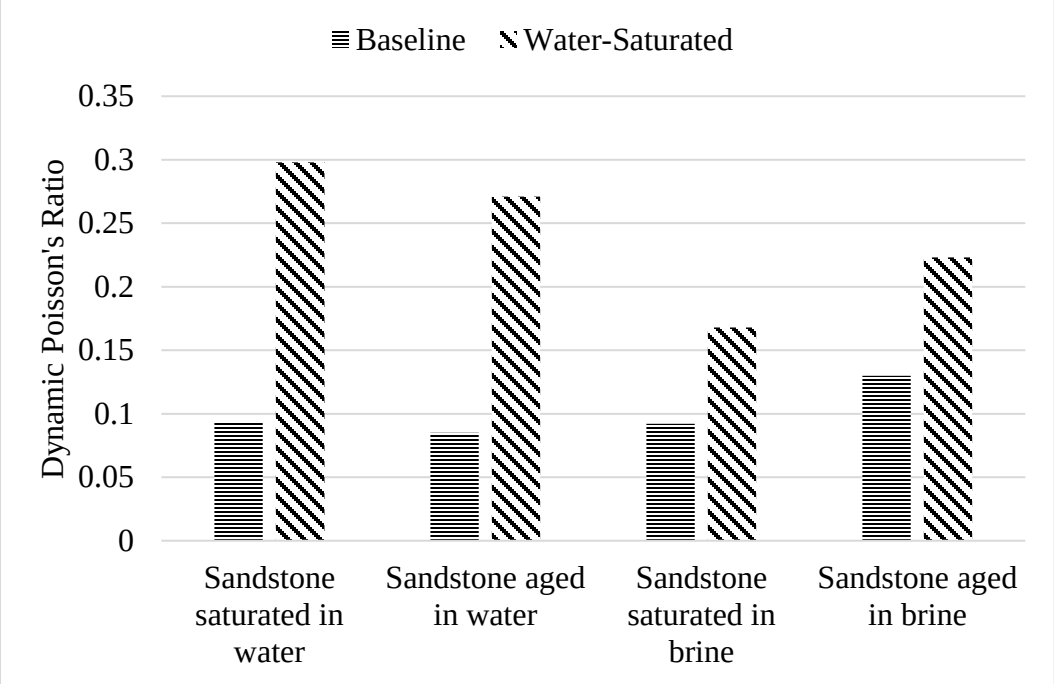

Figure 62: Effect on the dynamic Poisson's ratio due to aging and saturation in brine and distilled water for sandstone samples. The increase is relatively more prominent for the case of water as the saturating pore fluid as compared to brine.

5.2 Discussion

This section summarizes the results obtained for the various saturation and aging protocols. In addition, a comparative study is presented regarding the effect of different fluids and impact of temperature for each rock type. Table 5 in the Appendix summarizes the effect on each rock type due to the various saturation and aging protocols.

5.2.1 Effect of Fluid Saturation

Water-weakening mechanisms have been thoroughly discussed in the literature review section (see Section 2.1.2). Several theories regarding the weakening mechanisms have been proposed including, surface free energy reduction of quartz in the presence of water molecules (Colback and Wiid 1965), lubrication effect reducing friction, chemical and, corrosive weakening (Naghadehi et al. 2010). Notably, there is no universally agreed upon mechanism explaining the water-weakening behavior of rocks (Eeckhout 1976), most likely due to the existence of widely variable rock types/characteristics.

5.2.1.1 Limestone

The limestone samples exhibit either a reduction in strength or no appreciable change in strength upon saturation with brine. In some cases, however, a conclusive statement regarding the results for Indiana Limestone samples is not possible due to the high degree of variability in the strength response. Upon closely observing the experimental results, however, there are certain aspects regarding limestone samples worth discussing. For brine saturated samples, we see that Indiana Limestone depicts a quantitative reduction in strength. This can be associated to the water-weakening mechanism at play. Similarly, a slight decrease in strength is seen for Desert Pink Limestone sample as well.

For limestone samples saturated in distilled water, both Indiana Limestone and Desert Pink Limestone depict water weakening with the latter illustrating a more substantial change. This points to the effect of higher porosity of Desert Pink Limestone samples, as no chemical interaction with the mineral constituents and distilled water is expected. For oil-saturated samples, the experimental results are inconclusive.

Figures 63 and 64 show the relative change for the three saturating fluids for Indiana and Desert Pink Limestone respectively. In terms of percentage change, Indiana Limestone responds similarly to brine and distilled water. The response for crude oil ignoring experimental variations also shows weakening. A distinct water-weakening is reported for Desert Pink Limestone. Moreover, brine and crude oil saturation yielded minimal to no appreciable change in UCS.

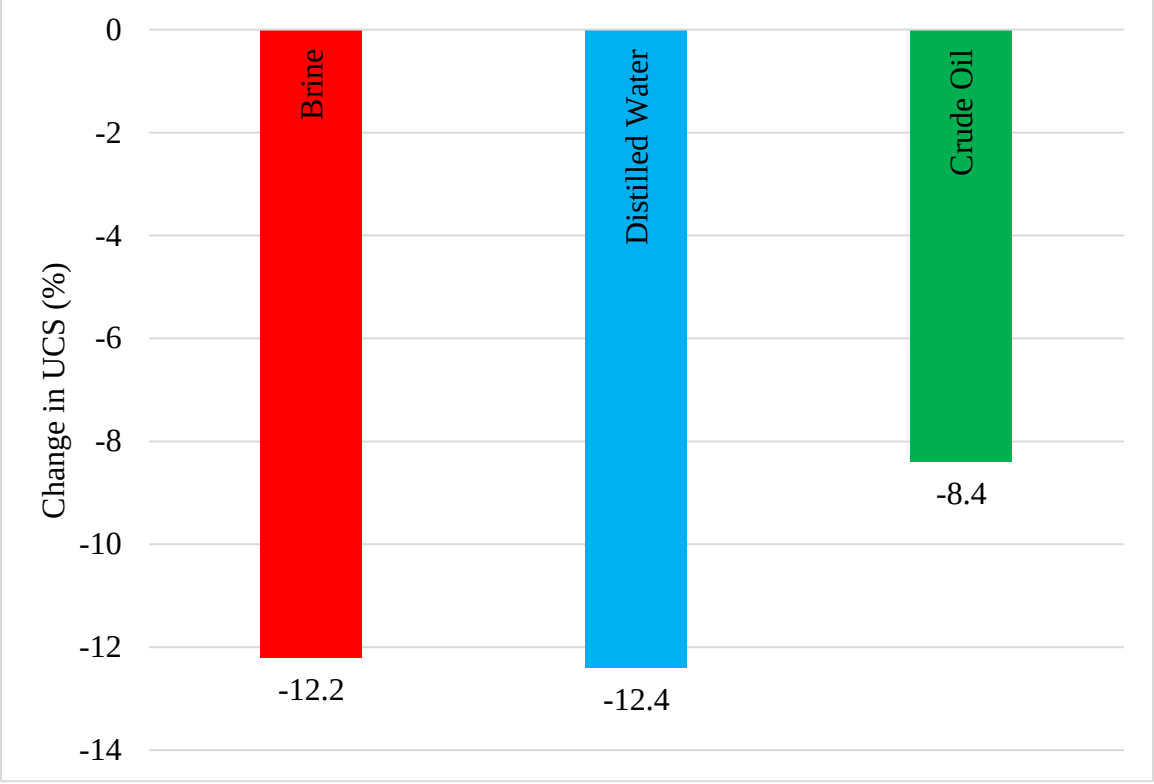

Figure 63: Effect of Fluid Saturation on Indiana Limestone. Percentage change relative to the baseline UCS for saturation of Indiana Limestone samples in brine, distilled water and crude oil.

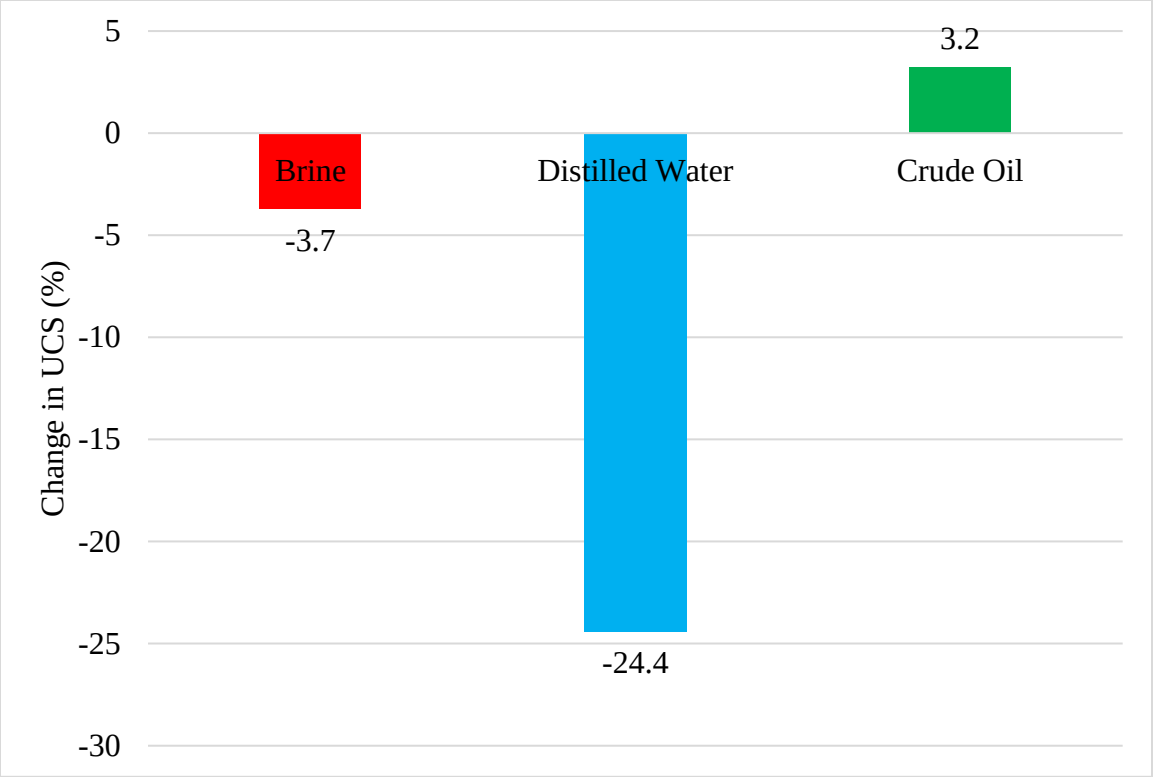

Figure 64: Effect of Fluid Saturation on Desert Pink Limestone. Percentage change relative to the baseline UCS after saturation in brine, distilled water and crude oil.

5.2.1.2 Sandstone

For sandstone samples, the results for brine saturated and water saturated samples are quite distinctive. Samples saturated with brine show strength enhancement. Contrarily, the distilled water saturated samples show a strong water-weakening effect. This experimental observation emphasizes that NaCl crystallization in the pores and flocculation of kaolinite give rise to added friction and hence a strength increase (Bishop 1997; Rathnaweera et al. 2014). The absence of these two physico-chemical processes in the distilled water saturation case, depicts a lack of strengthening effect. It is worthwhile to mention that both sandstone types contain considerable amounts of kaolinite leading to mineral flocculation.

For both types of limestone investigated, the change due to oil saturation was either minimal or inconclusive. On the contrary, Berea Buff Sandstone showed a distinct strength reduction. Berea Grey, however, did not yield any significant change. The fact that Berea

Grey Sandstone is affected by water saturation and not oil saturation, illustrates that clay swelling mechanism might be at work. As this rock type consists of certain clay-swelling minerals like illite. Researchers are yet to fully understand the mechanism of change due to oil saturation. Van Voorhis et al. (1957) reported a reduction in free surface energy in the presence of polar fluids like water but with a lesser effect in non-polar fluids. The free surface energy governs how the liquid interacts with the intergranular forces of the rock. This phenomenon is considered less convincing in the presence of fluids like oil due to the lack of attraction forces between polar surfaces and non-polar molecules. The residual water in the non-polar fluids (Tittmann et al. 1980) or water vapor in the atmosphere is rather suspected to bring about the change in free surface energy, leading to changes in strength (Henao et al. 2017). In addition, the effect of oil saturation is probably dependent on the extent of enhancement in the granular flow to allow for deformation (Thompson 2010). The degree of this effect, however, needs to be further investigated.

Figures 65 and 66 report the relative change for the three saturating fluids on the UCS of Berea Buff and Berea Grey Sandstone respectively. It is evident that brine caused an increase in strength for both types of sandstones. The increase is greater for Berea Buff of 13% as opposed to 3.6% for Berea Grey.

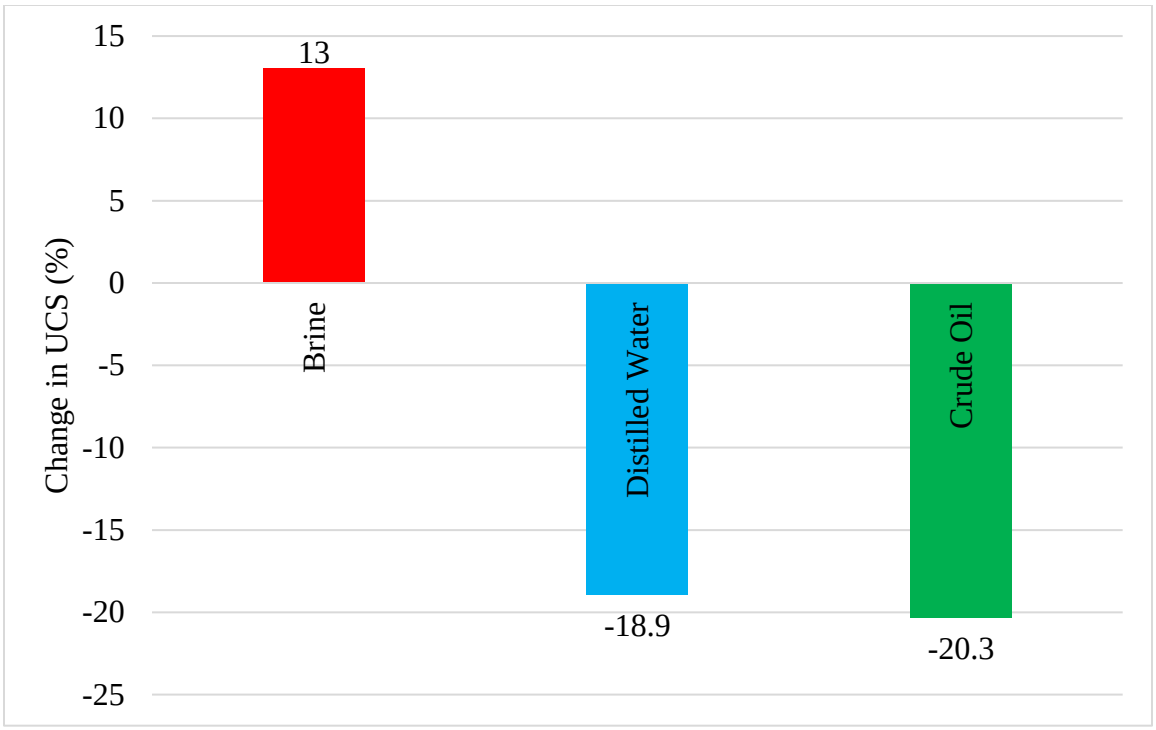

Figure 65: Effect of Fluid Saturation on Berea Buff Sandstone. Percentage change relative to the baseline UCS for brine, distilled water and crude oil.

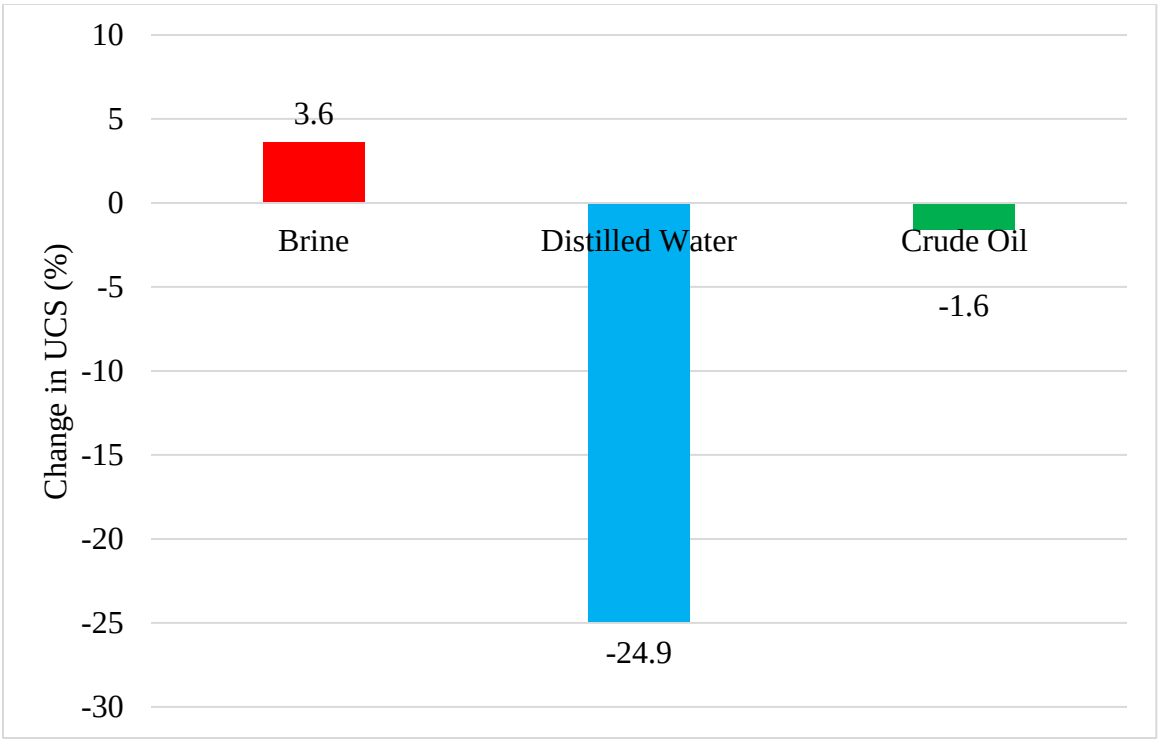

Figure 66: Effect of Fluid Saturation on Berea Grey Sandstone. Percentage change relative to the baseline UCS for brine, distilled water and crude oil.

5.2.2 Effect of Aging

The effect of high temperatures on rock strength has been studied comprehensively. The extent of change in rock mechanical behavior at elevated temperatures reported in the literature, however, is quite variable. This variation is due to a number of factors involved in dictating the change including, mineralogical composition and porosity (Sygała et al. 2013), as well as the strength of mineral constituents and their thermal expansion characteristics (Wan et al. 2009). Most investigations in literature are for very high temperatures and in the absence of any liquids. Conversely, this study focused on the combined effect of liquids and temperature concerning petroleum reservoirs. It is observed that the temperature consolidates the weakening effect as observed in the saturation phase. The overall effect is, however, of a reduction in the UCS.

5.2.2.1 Brine and Distilled Water

Aging in brine yields little to no effect on the strength of all rock types that are investigated. Using distilled water for aging, however, illustrate clear results. All samples indicate various degrees of rock strengthening as compared to the distilled water only case where weakening is observed. This phenomenon is summarized in Fig. 67, which illustrates comparison of the saturated phase versus the aging phase for all the samples. Temperature caused a partial improvement in the strength characteristics. The overall trend, however, is towards weakening as reported by a decrease of about 11% in the UCS for sandstone samples relative to the baseline UCS.

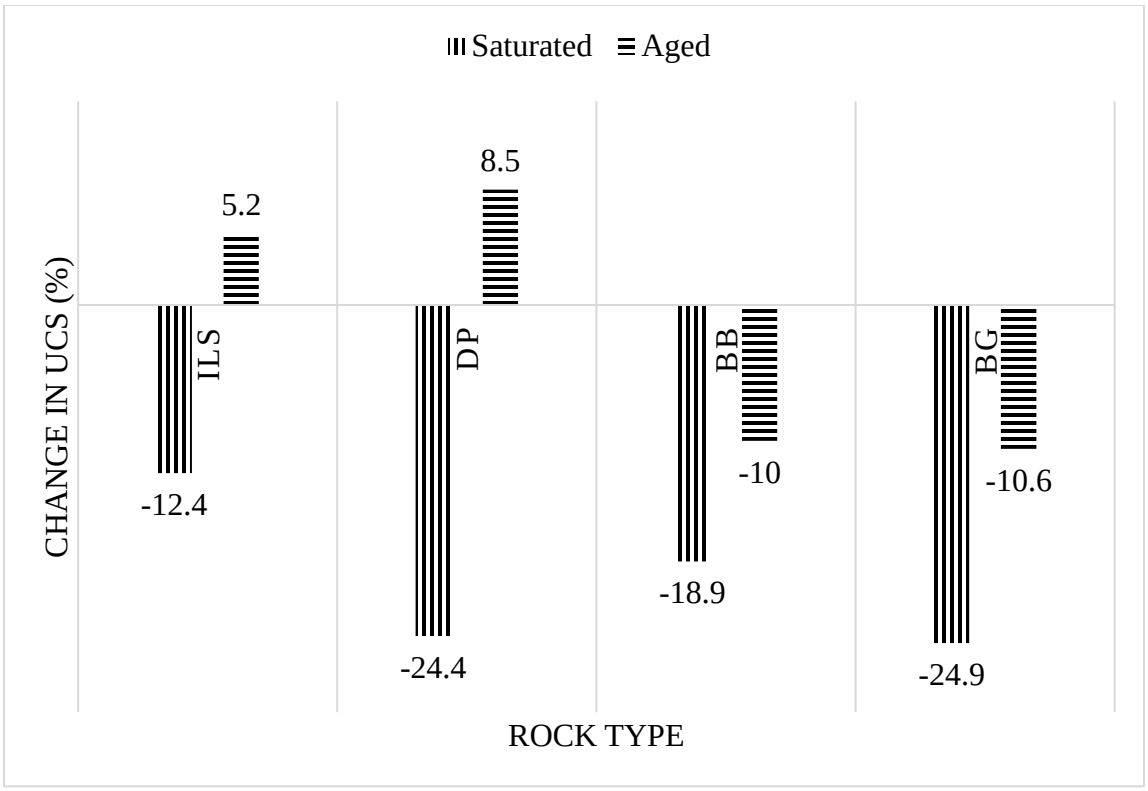

Figure 67: Fluid – Distilled Water. Comparison of percentage change in the UCS between saturated and aged phases in distilled water for all the rock types.

Strengthening is more prominent for sandstone as compared to limestone. The change shown by the latter is more due to inherent rock variations in the strength response as discussed in Section 5.1. Scientific literature reports that the change in limestone strength with temperature is minimal with a tentatively decreasing trend up to very high temperatures of 400-600 ^{o}C (Zhang et al. 2009; Mao et al. 2009). For the sandstone sample saturated in brine, an overall spread in the UCS data was observed giving rise to a flatter kernel diagram. This is attributed to a combination of temperature and brine strengthening, in addition to weakening effect due to chemical reactions which might have occurred between the brine and mineral constituents of the sample at 150 ^{o}C. The effect needs to be further investigated using other sandstone rock types. Rao et al. (2007) reported that the strength of sandstone samples they tested increased with a linear trend up to temperatures

of 250 ^{o}C and subsequently deteriorated. They concluded that the deciding factor for an increase or decrease in strength is related to the degree of drying or microcracking respectively. Lintao et al. (2017) studied the change in rock strength in combination with computed tomography scanning to describe the processes taking place at elevated temperatures. At initial temperatures up to 400 ^{o}C it was observed that evaporation of absorbed water within the pores have a constructive impact on rock strength due to the availability of additional pore space to permit compaction. This is in agreement with the conclusions by Erguler and Ulusay (2009) that thermal evaporation allows the rock to be more compact/denser and resistant to applied forces. Despite the strengthening behavior due to temperature, overall it can be concluded that weakening of the rock has occurred as compared to the UCS measurements made on the samples at ambient conditions.

5.2.2.2 Crude Oil

The combined effect of temperature and crude oil on geomechanical properties has not been considered prior to this study. Figure 68 presents a comparison for saturation and aging stages of the experiments with crude oil. The tested Indiana Limestone sample did not show any effect of aging in crude oil. Desert Pink Limestone, however, experienced an increase in strength. For sandstone samples, we observe that aging in oil has an overall detrimental effect on their UCS. This is similar to the results obtained for samples aged in distilled water. Contrary to the saturation phase, the Berea Grey sandstone sample shows a weakening effect of aging with crude oil with a decrease in UCS of about 14%. The difference in the impact of saturation and aging stages can be linked to physico-chemical reactions occurring at elevated temperatures.

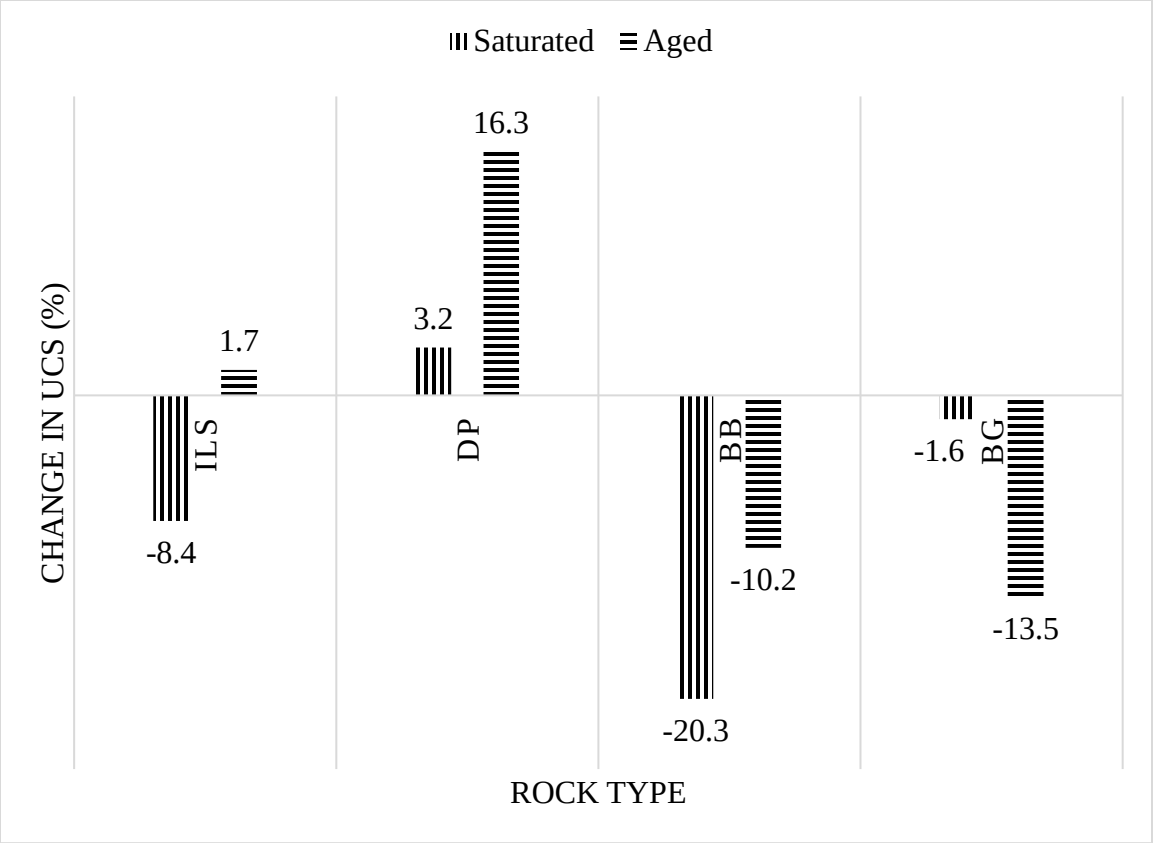

Figure 68: Fluid – Crude Oil. Comparison of percentage change in the UCS between saturated and aged phases in crude oil for all the rock types.

CHAPTER 6

CONCLUSIONS AND RECOMMENDATIONS

6.1 Conclusions

The effects of fluid saturation and temperature on the rock strength are a major research topic across multiple disciplines in the scientific community due to its practical importance in various engineering domains. This work presents an experimental analysis on the effect of brine, distilled water, crude oil and elevated temperature on the strength characteristics of two types of limestone and sandstone rocks. UCS was derived utilizing the scratch test on outcrop samples saturated with various liquids. Furthermore, change in UCS was studied as a function of the combined effect of fluid and temperature (aging) to elucidate changes closer to in situ reservoir conditions. Based on the obtained experimental data, the following conclusions were made:

1. 20% brine concentration causes an increase of about 13% and 4% in the UCS for Berea Buff and Berea Grey sandstones respectively. The limestones tested after brine saturation indicate a weakening trend potentially due to the absence of physico-chemical reactions, with up to a 12% reduction for Indiana Limestone.
2. Distilled water clearly causes reduction in UCS for all the rock types tested in this study. This reduction is highly variable for different sandstones and limestones. The reduction in sandstone varies from 19%-25% for Berea Buff and Berea Grey

Sandstones respectively, whereas, limestones UCS is weakened by 12% for the Indiana Limestone sample and up to 24 % for Desert Pink Limestone.

3. Limestone samples did not show any noticeable change with respect to UCS upon oil saturation. Berea Buff Sandstone sample was weakened by about 20% due to oil. Berea Grey Sandstone, however, showed a minimal weakening impact of about 2%. Since Berea Grey has a greater amount of clay swelling minerals (Mahmoud and Al-Hashim 2018) than Berea Buff (Mohamed and Nasr-El-Din 2013), and the oil had a negligible effect on the sample, clay swelling seems to be the mechanism for water-weakening.
4. Introducing high temperature in combination with about 200000 ppm brine saturation did not yield a change in UCS for all the samples after aging for one week.
5. Aging in distilled water displayed consistent strengthening in all the samples except for Indiana Limestone sample, where the change is inconclusive. This behavior caused the UCS of Desert Pink Limestone to increase by about 9%. An overall weakening trend was observed, however, for both Berea Buff and Berea Grey Sandstones by up to 11%. Comparing this stage to the saturation protocol suggests that the temperature played a significant role in overall reduction of the weakening effect introduced by the liquid.
6. Aging in crude oil showed to have a strengthening effect on the Desert Pink Limestone sample, increasing the UCS by about 17%. Both sandstone types indicate an overall weakening effect. The UCS of Berea Buff Sandstone was decreased by 10% due to aging, as opposed to a decrease of 20% because of oil

saturation. Berea Grey Sandstone unlike the saturation in oil phase, displayed sensitivity to the aging in oil stage with a UCS decrement of about 14%.

7. Experimental evidence suggested that rock strength characteristics are affected in the presence of saturating pore fluids. In addition, it has been observed that varying changes occur in UCS when the rock is aged at elevated temperatures. There is a general weakening trend in the presence of distilled water and crude oil. In brine, however, it is reported that sandstones have a strengthening trend which needs to be further investigated in terms of chemistry of the interaction between brine and rock mineral components.
8. Weakening, as a consequence of saturation and aging of the rock points towards a methodical overestimation of in situ strength if results of testing at ambient conditions are extrapolated.

This study provides practical evidence of change in rock strength characteristics at conditions closer to the reservoir environment. This stresses the importance to develop lab-based experimental platforms to conduct scratch testing at in situ conditions. Furthermore, this effort emphasizes the need to change current protocols in place for carrying out geomechanical tests and develop refined procedures that consider the reservoir conditions. This will allow accurate estimation of rock mechanical parameters and eventually yield improved geomechanical models, requisite for important decision making.

6.2 Best Practices

During this study, we discovered certain best practices that should be adopted when conducting geomechanical analysis utilizing the scratch machine. These are listed below:

1. Conduct geological characterization of the core including XRD, XRF, and SEM analysis. This allows for better analysis of the data from scratch test with regards to differentiating scatter in the strength data due to mineralogical differences and actual rock heterogeneity.
2. Avoid scratching the same groove again as the groove walls may contribute to an added frictional force. Figure 69 shows three cutting profiles as experimented by Dagrain et. al (2001) where they established that the 'U-cut' shape provided the greatest frictional resistance. To demonstrate this effect at work, we tried scratching the same groove again after saturating the sample in water. We recorded post-saturation UCS values to increase by approximately 34%. Upon further investigation and scratching an untested part of the same core, however, showed a decrease in strength. Figure 70 reports these results. Scratching the same groove after the sample has been unloaded requires a high degree of precision, as a minor offset between the groove and the cutter will yield additional forces. It can, therefore, be confirmed that scratching the same groove leads to inaccurate estimate of the UCS due to additional forces not attributed to the rock matter. If the same groove is to be scratched again, it is suggested to remove the sidewalls and perform a slab cut as shown in Fig. 69.

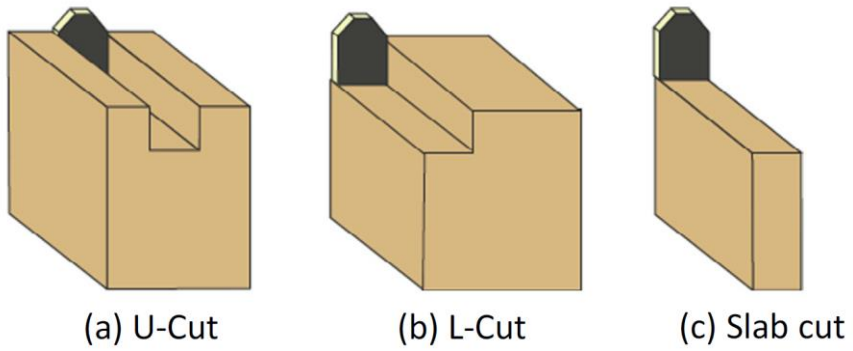

Figure 69: Three cutting profiles as tested by Dagrain et. al. (2001).

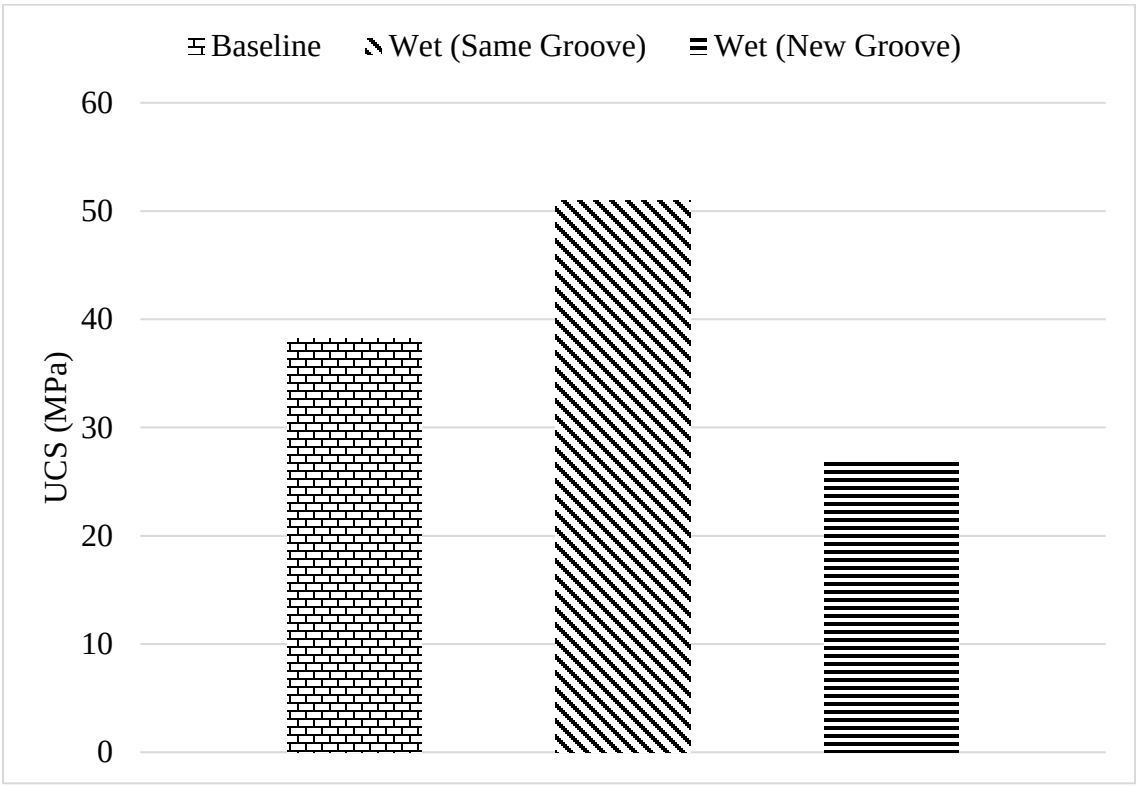

Figure 70: Effect of Groove Walls. UCS for a sample post-water saturation after scratching the same groove and an untested part of the sample showing the effect of additional force contribution due to the groove walls.

3. To better define the strength characteristics of the rock, it is recommended to carry out scratch tests at a minimum of three different locations of the sample. This not only establishes statistical evidence, but also captures any variation in the sample.
4. Ensure proper cleaning of the scratch residue prior to each run. As improper cleaning might result in residue imposing additional forces on the cutter.

5. Each scratch test should be complemented with groove photograph as part of scratch data analysis protocol. This helps in interpreting the data and any variations occurring due to rock intrinsic characteristics such as fractures, vugs, and cementation material.

6.3 Recommendations for Future Work

To supplement and further understand the mechanisms responsible for the change in UCS of the rocks, we suggest the following work to be conducted:

1. Geochemical analysis of the interaction between various fluids with rock mineral constituents: XRD alone is insufficient to understand the underlying mechanism of change due to fluid saturation. It may be possible that minerals lining the pore surface interact with the fluids to cause a change. These minerals are present in smaller amounts that cannot be detected using XRD which quantifies bulk compositions. One possible method is to use the Quantitative Evaluation of Minerals by Scanning Electron Microscopy (QEMSCAN), which allows for a complete chemical analysis and provides high resolution images and mineral maps (Gottlieb et al. 2000). Ayling et al. (2012) demonstrated the ability of QEMSCAN to analyze fluid chemistries and evolution of alterations in geothermal systems on the micron scale. The same concept can be utilized to learn about the spatial distributions of minerals and their probability of interacting with the introduced fluids during the saturation and aging processes.
2. Imaging at high temperatures: To better understand and characterize the processes responsible for change in the UCS at high temperatures, it is imperative to take aid of imaging techniques. There do exist examples of studies where imaging has been used to explain the process at play during deformability of rock matter. Glatz et al. (2018) designed an experimental platform to visualize processes occurring in the rock matter at elevated temperatures and pressures utilizing CT-scan analysis. To

study pore scale mechanisms, however, a specialized setup suitable for micro-CT analysis will be required.

3. Provisions for scratch testing at elevated temperatures should be designed and implemented to study the UCS response of the rocks at in situ temperatures. This design needs to consider a couple of restrictions that currently prevents scratching at elevated temperatures. Firstly, there needs to be a certain area of the core that allows free movement of the cutter from one end to the other. Secondly, as the sample is at elevated temperature, it needs to be held tightly during the test to prevent relative motion. Finally, temperature rating of the platform at which the sample is positioned and held in place needs to be taken into account.
4. Investigation of intrinsic energy and force response due to variable curvature: Currently scratch tests are conducted on a level surface of the core sample. To implement a tool suitable to scratch in situ, however, will require models that can translate scratch data on variable curvatures representative of typical borehole surfaces.
5. Exploring the force response through signal processing and analysis: Investigating the force signals for various depths of cut can allow understanding the onset of the brittle mode of failure. An example of such analysis would be to investigate the frequency of the generated force signals.

References

Aadnøy, Bernt, and Reza Looyeh. 2011. *Petroleum Rock Mechanics*. Elsevier. https://doi.org/10.1016/C2009-0-64677-8.

Adachi, Jose I, Emmanuel Detournay, and Andrew Drescher. 1996. "Determination of Rock Strength Parameters from Cutting Tests." *Proc. NARMS*, 1517–23.

Ahmadi Sheshde, E., and A. Cheshomi. 2015. "New Method for Estimating Unconfined Compressive Strength (UCS) Using Small Rock Samples." *Journal of Petroleum Science and Engineering* 133 (September): 367–75. https://doi.org/10.1016/j.petrol.2015.06.022.

Al-Ameri, Wahbi Abdulqader, Abdulazeez Abdulraheem, Mohamed Ahmednasreldin Mahmoud, Osman Mahmoud Abdullatif, and Abdulrauf Abdulrasheed Adebayo. 2014. "Effect of CO2 Sequestration Period on the Mechanical Properties of Carbonate Aquifers." In *Abu Dhabi International Petroleum Exhibition and Conference*. Society of Petroleum Engineers. https://doi.org/10.2118/171702-MS.

Almenara, JR, and E Detournay. 1992. "Cutting Experiments in Sandstones with Blunt PDC Cutters." In *Rock Characterization: ISRM Symposium, Eurock'92, Chester, UK, 14--17 September 1992*, 215–20. Thomas Telford Publishing.

Anwar, H.Z., H. Shimada, M. Ichinose, and K. Matsui. 1998. "Deterioration of Mechanical Properties of Coal Measure Rocks due to Water." In *Mine Planning and Equipment Selection*, edited by Raj K. Singhal, 257–61. CRC Press.

API, Exploration and Production Department. 1998. *API Recommended Practice 40*. *Recommended Practices for Core Analysis*. Second. American Petroleum Institute.

Ashena, R., G. Thonhauser, A. Ghalambor, V. Rasouli, and R. Manasipov. 2018. "Determination of Maximum Allowable Safe Core Retrieval Rates." In *SPE International Conference and Exhibition on Formation Damage Control*. Society of Petroleum Engineers. https://doi.org/10.2118/189480-MS.

Ashena, Rahman, and Gerhard Thonhauser. 2018. "Mechanical Core Damage Investigation and Mitigation." In *Coring Methods and Systems*, 123–33. Cham: Springer International Publishing. https://doi.org/10.1007/978-3-319-77733-7_8.

ASTM. 1995. "Standard Test Method for Unconfined Compressive Strength of Intact Rock Core Specimens." In *Annual Book of ASTM Standards*, edited by AMERICAN SOCIETY FOR TESTING AND MATERIALS. AMERICAN SOCIETY FOR TESTING AND MATERIALS.

Aubert, J. E., P. Maillard, J. C. Morel, and M. Al Rafii. 2016. "Towards a Simple Compressive Strength Test for Earth Bricks?" *Materials and Structures* 49 (5): 1641–54. https://doi.org/10.1617/s11527-015-0601-y.

Aydin, A., and A. Basu. 2005. "The Schmidt Hammer in Rock Material Characterization." *Engineering Geology* 81 (1): 1–14. https://doi.org/10.1016/j.enggeo.2005.06.006.

Ayling, Bridget, Peter Rose, Susan Petty, Ezra Zemach, and Peter Drakos. 2012. "QEMSCAN (Quantitative Evaluation of Minerals by Scanning Electron Microscopy): Capability and Application to Fracture Characterization in Geothermal Systems." In *PROCEEDINGS, Thirty-Seventh Workshop on Geothermal Reservoir Engineering*. Stanford: Stanford University.

https://pangea.stanford.edu/ERE/pdf/IGAstandard/SGW/2012/Ayling.pdf.
Badri, Mohammed, and Reza Taherian. 2013. “Geomechanical Logging Tool (US 2013/0269931 A1).”
Barla, G., and N. Innaurato. 1973. “Indirect Tensile Testing of Anisotropic Rocks.” *Rock Mechanics Felsmechanik Mecanique Des Roches* 5 (4): 215–30. https://doi.org/10.1007/BF01301795.
Barton, Timothy, S. Bhatt, G. Molinda, and C. Mark. 2008. “Effects of Specimen Age on the Uniaxial Compressive Strength and Moisture Content of Weak Coal Measure Rocks.” *27 Th International Conference on Ground Control in Mining*, 332–37.
Bauer, Robert A. 1984. “The Relationship Of Uniaxial Compressive Strength To Point-Load And Moisture Content Indices Of Highly Anisotropic Sediments Of The Illinois Basin.” In *The 25th U.S. Symposium on Rock Mechanics (USRMS)*. American Rock Mechanics Association. https://doi.org/ARMA-84-0398.
Bauer, Robert A. 1980. “The Loss of Natural Moisture Content and Its Effect on the Mechanical Properties of Some Pennsylvanian Shales from the Illinois Basin.” In *1st Conf. on Ground Control Problems in the Illinois Basin*, 89–94.
Bažant, Zdeněk P. 1984. “Size Effect in Blunt Fracture: Concrete, Rock, Metal.” *Journal of Engineering Mechanics* 110 (4): 518–35. https://doi.org/10.1061/(ASCE)0733-9399(1984)110:4(518).
———. 2000. “Size Effect.” *International Journal of Solids and Structures* 37 (1–2): 69–80. https://doi.org/10.1016/S0020-7683(99)00077-3.
Belani, Ashkok, and Steve Orr. 2008. “A Systematic Approach to Hostile Environments.” *Journal of Petroleum Technology* 60 (7): 34–39. https://doi.org/10.2118/0708-0034-JPT.
Bell, F.G. 1978. “The Physical and Mechanical Properties of the Fell Sandstones, Northumberland, England.” *Engineering Geology* 12 (January): 1–29. https://doi.org/10.1016/0013-7952(78)90002-9.
Berckhemer, H., A. Rauen, H. Winter, H. Kern, A. Kontny, M. Lienert, G. Nover, et al. 1997. “Petrophysical Properties of the 9-Km-Deep Crustal Section at KTB.” *Journal of Geophysical Research: Solid Earth* 102 (B8): 18337–61. https://doi.org/10.1029/96JB03396.
Bishop, Simon R. 1997. “The Experimental Investigation of Formation Damage Due to the Induced Flocculation of Clays Within a Sandstone Pore Structure by a High Salinity Brine.” In *SPE European Formation Damage Conference*. Society of Petroleum Engineers. https://doi.org/10.2118/38156-MS.
Broch, E., and J.A. Franklin. 1972. “The Point-Load Strength Test.” *International Journal of Rock Mechanics and Mining Sciences & Geomechanics Abstracts* 9 (6): 669–76. https://doi.org/10.1016/0148-9062(72)90030-7.
Brown, Edwin Thomas. 1981. *Rock Characterization Testing and Monitoring*. Pergamon Press.
Bruant, Robert G., Jr. Jr., Michael A. Celia, Andrew J. Guswa, and Catherine A. Peters. 2002. “Peer Reviewed: Safe Storage of CO2 in Deep Saline Aquifiers.” *Environmental Science & Technology* 36 (11): 240A–245A. https://doi.org/10.1021/es0223325.
Burchette, Trevor P. 2012. “Carbonate Rocks and Petroleum Reservoirs: A Geological Perspective from the Industry.” *Geological Society, London, Special Publications* 370

(1): 17–37. https://doi.org/10.1144/SP370.14.
Burshtein, L. S. 1969. “Effect of Moisture on the Strength and Deformability of Sandstone.” *Soviet Mining Science* 5 (5): 573–76. https://doi.org/10.1007/BF02501278.
Cargill, J S, and A Shakoor. 1990. “Evaluation of Empirical Methods for Measuring the Uniaxial Compressive Strength of Rock.” *International Journal of Rock Mechanics and Mining Sciences & Geomechanics Abstracts* 27 (6): 495–503. https://doi.org/10.1016/0148-9062(90)91001-N.
Carles, P., and P. Lapointe. 2005. “Water-Weakening of Carbonates under Stress: New Insights into Pore-Volume Compressibility Measurements.” *Petrophysics* 46 (5).
Chang, Chandong, Mark D. Zoback, and Abbas Khaksar. 2006. “Empirical Relations between Rock Strength and Physical Properties in Sedimentary Rocks.” *Journal of Petroleum Science and Engineering* 51 (3–4): 223–37. https://doi.org/10.1016/j.petrol.2006.01.003.
Chen, Szu-Ying, Yair Kaufman, Kai Kristiansen, Dongjin Seo, Alex M. Schrader, Mohammed B. Alotaibi, Howard A. Dobbs, et al. 2017. “Effects of Salinity on Oil Recovery (the ‘Dilution Effect’): Experimental and Theoretical Studies of Crude Oil/Brine/Carbonate Surface Restructuring and Associated Physicochemical Interactions.” *Energy & Fuels* 31 (9): 8925–41. https://doi.org/10.1021/acs.energyfuels.7b00869.
Chen, Yen Chi. 2017. “A Tutorial on Kernel Density Estimation and Recent Advances.” *Biostatistics & Epidemiology* 1 (1): 161–87. https://doi.org/10.1080/24709360.2017.1396742.
Cho, Jung-Woo, Hanna Kim, Seokwon Jeon, and Ki-Bok Min. 2012. “Deformation and Strength Anisotropy of Asan Gneiss, Boryeong Shale, and Yeoncheon Schist.” *International Journal of Rock Mechanics and Mining Sciences* 50 (February): 158–69. https://doi.org/10.1016/j.ijrmms.2011.12.004.
Churcher, P.L., P.R. French, J.C. Shaw, and L.L. Schramm. 1991. “Rock Properties of Berea Sandstone, Baker Dolomite, and Indiana Limestone.” In *SPE International Symposium on Oilfield Chemistry*. Society of Petroleum Engineers. https://doi.org/10.2118/21044-MS.
Closmann, P.J., and W.B. Bradley. 1979. “The Effect of Temperature on Tensile and Compressive Strengths and Young Modulus of Oil Shale.” *Society of Petroleum Engineers Journal* 19 (5): 301–12. https://doi.org/10.2118/6734-PA.
Colback, PSB, and B L Wiid. 1965. “The Influence of Moisture Content on The Compressive Strength of Rocks.” *Geophysics*, 65–83.
Dagrain, Fabrice, Emmanuel Detourna, and Thomas Richard. 2001. “Influence of Cutter Geometry in Rock Cutting.” In *DC Rocks 2001, The 38th US Symposium on Rock Mechanics (USRMS)*. American Rock Mechanics Association.
Dagrain, Fabrice, T Richard, and Edmond Poyol. 2004. “Strength Logging of Geomaterials from Scratch Tests.” In *EUROCK 2004 & 53rd Geomechanics Colloquium*.
Dagrain, F, E Poyol, and T Richard. 2004. “Strength Logging of Geomaterials from Scratch Tests.” In *EUROCK 2004 and 53rd Geomechanics Colloquium*.
Darlington, William J., Pathegama G. Ranjith, and S. K. Choi. 2011. “The Effect of Specimen Size on Strength and Other Properties in Laboratory Testing of Rock and Rock-Like Cementitious Brittle Materials.” *Rock Mechanics and Rock Engineering*

44 (5): 513–29. https://doi.org/10.1007/s00603-011-0161-6.
Deere, Don Uel, and RP Miller. 1966. “Engineering Classification and Index Properties for Intact Rock.”
Demarco, Manuela Morales, Eberhard Jahns, Jörg Rüdrich, Pedro Oyhantcabal, and Siegfried Siegesmund. 2007. “The Impact of Partial Water Saturation on Rock Strength: An Experimental Study on Sandstone [Der Einfluss Einer Partiellen Wassersättigung Auf Die Mechanischen Gesteinseigenschaften: Eine Fallstudie an Sandsteinen].” *Zeitschrift Der Deutschen Gesellschaft Für Geowissenschaften* 158 (4): 869–82. https://doi.org/10.1127/1860-1804/2007/0158-0869.
Deng, HF, JL Li, Min Zhu, KW Wang, LH Wang, and Ch-J Deng. 2012. “Experimental Research on Strength Deterioration Rules of Sandstone under ‘saturation--Air Dry’circulation Function.” *Chinese Journal of Rock and Soil Mechanics* 11: 3306–13.
Detournay, E., and P. Defourny. 1992. “A Phenomenological Model for the Drilling Action of Drag Bits.” *International Journal of Rock Mechanics and Mining Sciences & Geomechanics Abstracts* 29 (1): 13–23. https://doi.org/10.1016/0148-9062(92)91041-3.
Detournay, Emmanuel, Andrew Drescher, Paul Defournay, and Dominique Fourmaintraux. 1995. “Assessment of Rock Strength Properties from Cutting Tests: Preliminary Experimental Evidence.” In *Proc. of the Colloquium Mundanum on Chalk and Shales, Brussels*, 13–1.
Detournay, Emmanuel, Andrew Drescher, and David A Hultman. 1997. Portable rock strength evaluation device, issued 1997.
Dey, T., and P. Halleck. 1981. “Some Aspects of Size-Effect in Rock Failure.” *Geophysical Research Letters* 8 (7): 691–94. https://doi.org/10.1029/GL008i007p00691.
Dube, A. K, and B. Singh. 1972. “Effect of Humidity on Tensile Strength of Sandstone.” *Journal of Mines, Metals & Fuels* 20 (1): 8–10. http://cimfr.csircentral.net/1238/.
Duclos, R., and J. Paquet. 1991. “High-Temperature Behaviour of Basalts—role of Temperature and Strain Rate on Compressive Strength and KIc Toughness of Partially Glassy Basalts at Atmospheric Pressure.” *International Journal of Rock Mechanics and Mining Sciences & Geomechanics Abstracts* 28 (1): 71–76. https://doi.org/10.1016/0148-9062(91)93234-W.
Dyke, C. G., and L. Dobereiner. 1991. “Evaluating the Strength and Deformability of Sandstones.” *Quarterly Journal of Engineering Geology and Hydrogeology* 24 (1): 123–34. https://doi.org/10.1144/GSL.QJEG.1991.024.01.13.
Eeckhout, Edward M. Van. 1976. “The Mechanisms of Strength Reduction due to Moisture in Coal Mine Shales.” *International Journal of Rock Mechanics and Mining Sciences & Geomechanics Abstracts* 13 (2): 61–67. https://doi.org/10.1016/0148-9062(76)90705-1.
Eeckhout, Edward M. Van, and Syd S. Peng. 1975. “The Effect of Humidity on the Compliances of Coal Mine Shales.” *International Journal of Rock Mechanics and Mining Sciences & Geomechanics Abstracts* 12 (11): 335–40. https://doi.org/10.1016/0148-9062(75)90166-7.
Eliebid, Mohammed, Mohamed Mahmoud, Reyad Shawabkeh, Salaheldin Elkatatny, and Ibnelwaleed A. Hussein. 2018. “Effect of CO 2 Adsorption on Enhanced Natural Gas Recovery and Sequestration in Carbonate Reservoirs.” *Journal of Natural Gas*

Science and Engineering 55 (July): 575–84. https://doi.org/10.1016/j.jngse.2017.04.019.
Epslog, S A. n.d. “Epslog S.a. 76” 32 (0): 1–3.
Erguler, Z.A., and R. Ulusay. 2009. “Water-Induced Variations in Mechanical Properties of Clay-Bearing Rocks.” *International Journal of Rock Mechanics and Mining Sciences* 46 (2): 355–70. https://doi.org/10.1016/j.ijrmms.2008.07.002.
Farmer, IW, and Z Rakowski. 1991. “Main Lecture: Rock Testing—Deficiencies and Selection.” In *Proceedings of the International Conference on Geomechanics*, 3–7.
Fener, M., S. Kahraman, A. Bilgil, and O. Gunaydin. 2005. “A Comparative Evaluation of Indirect Methods to Estimate the Compressive Strength of Rocks.” *Rock Mechanics and Rock Engineering* 38 (4): 329–43. https://doi.org/10.1007/s00603-005-0061-8.
Ferreira, Francisco Henriques, Victor Manuel, Domingues Menezes, and Michael Strugale. 2014. “UCS Estimation through Uniaxial Compressive Test , Scratch Test and Based Log Empirical Correlation,” no. 1998.
Freire-Gormaly, Marina, Jonathan S. Ellis, Aimy Bazylak, and Heather L. MacLean. 2015. “Comparing Thresholding Techniques for Quantifying the Dual Porosity of Indiana Limestone and Pink Dolomite.” *Microporous and Mesoporous Materials* 207 (May): 84–89. https://doi.org/10.1016/j.micromeso.2015.01.002.
Gajic, Violeta, Vesna Matovic, Nebojsa Vasic, and Danica Sreckovic-Batocanin. 2011. “Petrophysical and Mechanical Properties of the Struganik Limestone (Vardar Zone, Western Serbia).” *Geoloski Anali Balkanskog Poluostrva*, no. 72: 87–100. https://doi.org/10.2298/GABP1172087G.
Gatens, J.M., C.W. Harrison, D.E. Lancaster, and F.K. Guidry. 1990. “In-Situ Stress Tests and Acoustic Logs Determine Mechanical Propertries and Stress Profiles in the Devonian Shales.” *SPE Formation Evaluation* 5 (3): 248–54. https://doi.org/10.2118/18523-PA.
Germay, Christophe, and Thomas Richard. 2014. “The Scratch Test: A High Resolution Log of Rock Strength with Application to Geomechanic and Petrophysic.” *SPWLA 55th Annual Logging Symposium* 50: 1–13. http://www.earthdoc.org/publication/publicationdetails/?publication=75009.
Ghazvinian, A., and M.R. Hadei. 2012. “Effect of Discontinuity Orientation and Confinement on the Strength of Jointed Anisotropic Rocks.” *International Journal of Rock Mechanics and Mining Sciences* 55 (October): 117–24. https://doi.org/10.1016/j.ijrmms.2012.06.008.
Gholami, R., and V. Rasouli. 2014. “Mechanical and Elastic Properties of Transversely Isotropic Slate.” *Rock Mechanics and Rock Engineering* 47 (5): 1763–73. https://doi.org/10.1007/s00603-013-0488-2.
Glatz, Guenther, Alexandre Lapene, Louis M. Castanier, and Anthony R. Kovscek. 2018. “An Experimental Platform for Triaxial High-Pressure/high-Temperature Testing of Rocks Using Computed Tomography.” *Review of Scientific Instruments* 89 (4): 45101. https://doi.org/10.1063/1.5030204.
Gottlieb, P., G. Wilkie, D. Sutherland, E. Ho-Tun, S. Suthers, K. Perera, B. Jenkins, S. Spencer, A. Butcher, and J. Rayner. 2000. “Using Quantitative Electron Microscopy for Process Mineralogy Applications.” *JOM* 52 (4): 24–25. https://doi.org/10.1007/s11837-000-0126-9.
Graue, Arne, Bjørn Gerry Viksund, Terje Eilertsen, and Robert Moe. 1999. “Systematic

Wettability Alteration by Aging Sandstone and Carbonate Rock in Crude Oil." *Journal of Petroleum Science and Engineering* 24 (2–4): 85–97. https://doi.org/10.1016/S0920-4105(99)00033-9.

Gunsallus, K.L., and F.H. Kulhawy. 1984. "A Comparative Evaluation of Rock Strength Measures." *International Journal of Rock Mechanics and Mining Sciences & Geomechanics Abstracts* 21 (5): 233–48. https://doi.org/10.1016/0148-9062(84)92680-9.

Hack, Robert, and Marco Huisman. 2002. "Estimating the Intact Rock Strength of a Rock Mass by Simple Means." In *9th Congress of the International Association for Engineering Geology and the Environment*, edited by J. L. van Rooy and C. A. Jermy, 1971–77. Section Engineering Geology, Centre for Technical Geosciences, International Institute for Aerospace Survey and Earth Sciences (ITC).

Hadizadeh, J., and R.D. Law. 1991. "Water-Weakening of Sandstone and Quartzite Deformed at Various Stress and Strain Rates." *International Journal of Rock Mechanics and Mining Sciences & Geomechanics Abstracts* 28 (5): 431–39. https://doi.org/10.1016/0148-9062(91)90081-V.

Hale, P. A., and Abdul Shakoor. 2003. "A Laboratory Investigation of the Effects of Cyclic Heating and Cooling, Wetting and Drying, and Freezing and Thawing on the Compressive Strength of Selected Sandstones." *Environmental and Engineering Geoscience* 9 (2): 117–30. https://doi.org/10.2113/9.2.117.

Hawkes, I., and M. Mellor. 1970. "Uniaxial Testing in Rock Mechanics Laboratories." *Engineering Geology* 4 (3): 179–285. https://doi.org/10.1016/0013-7952(70)90034-7.

Hawkins, A. B., and B. J. McConnell. 1992. "Sensitivity of Sandstone Strength and Deformability to Changes in Moisture Content." *Quarterly Journal of Engineering Geology and Hydrogeology* 25 (2): 115–30. https://doi.org/10.1144/GSL.QJEG.1992.025.02.05.

He, Xianqun, and Chaoshui Xu. 2015. "Determining Strength and Fracture Toughness of Rock from Scratch Tests." In *ISRM Regional Symposium - EUROCK 2015*. International Society for Rock Mechanics.

He, Xianqun, Chaoshui Xu, Kang Peng, and Gun Huang. 2017. "Simultaneous Identification of Rock Strength and Fracture Properties Via Scratch Test." *Rock Mechanics and Rock Engineering* 50 (8): 2227–34. https://doi.org/10.1007/s00603-017-1224-0.

Henao, T., C. Sondergeld, and C. Rai. 2017. "The Effect of Saturating Fluids on Tensile and Compressive Strength of Quarzitic Sandstones." In *51st U.S. Rock Mechanics/Geomechanics Symposium*. American Rock Mechanics Association.

Hettema, M.H.H., T.H. Hanssen, and B.L. Jones. 2002. "Minimizing Coring-Induced Damage in Consolidated Rock." In *SPE/ISRM Rock Mechanics Conference*. Society of Petroleum Engineers. https://doi.org/10.2118/78156-MS.

Hill, R., B. Storakers, and A. B. Zdunek. 1989. "A Theoretical Study of the Brinell Hardness Test." *Proceedings of the Royal Society A: Mathematical, Physical and Engineering Sciences* 423 (1865): 301–30. https://doi.org/10.1098/rspa.1989.0056.

Hjelmeland, O.S., and L.E. Larrondo. 1986. "Experimental Investigation of the Effects of Temperature, Pressure, and Crude Oil Composition on Interfacial Properties." *SPE Reservoir Engineering* 1 (4): 321–28. https://doi.org/10.2118/12124-PA.

Hoeg, K., M. Gutierrez, and L. E. Oino. 2000. “The Effect of Fluid Content on the Mechanical Behaviour of Fractures in Chalk.” *Rock Mechanics and Rock Engineering* 33 (2): 93–117. https://doi.org/10.1007/s006030050037.

Holt, Rune M. 2001. “Petrophysics under Stress.” In *6th Nordic Symposium on Petrophysics*. NTNU, Trondheim, Norway.

Holt, Rune M., Marco Brignoli, Erling Fjaer, Tor Erling Unander, and Cor J. Kenter. 1994. “Core Damage Effects on Compaction Behaviour.” In *Rock Mechanics in Petroleum Engineering*. Society of Petroleum Engineers. https://doi.org/10.2118/28027-MS.

Homand, S., and J. F. Shao. 2000. “Mechanical Behaviour of a Porous Chalk and Effect of Saturating Fluid.” *Mechanics of Cohesive-Frictional Materials* 5 (7): 583–606. https://doi.org/10.1002/1099-1484(200010)5:7<583::AID-CFM110>3.0.CO;2-J.

Huang, Sheng, Kaiwen Xia, Fei Yan, and Xiating Feng. 2010. “An Experimental Study of the Rate Dependence of Tensile Strength Softening of Longyou Sandstone.” *Rock Mechanics and Rock Engineering* 43 (6): 677–83. https://doi.org/10.1007/s00603-010-0083-8.

Hucka, V. 1965. “A Rapid Method of Determining the Strength of Rocks in Situ.” *International Journal of Rock Mechanics and Mining Sciences & Geomechanics Abstracts* 2 (2): 127–34. https://doi.org/10.1016/0148-9062(65)90009-4.

Jadhunandan, P.P., and N.R. Morrow. 1995. “Effect of Wettability on Waterflood Recovery for Crude-Oil/Brine/Rock Systems.” *SPE Reservoir Engineering* 10 (1): 40–46. https://doi.org/10.2118/22597-PA.

Jahed Armaghani, Danial, Mohd For Mohd Amin, Saffet Yagiz, Roohollah Shirani Faradonbeh, and Rini Asnida Abdullah. 2016. “Prediction of the Uniaxial Compressive Strength of Sandstone Using Various Modeling Techniques.” *International Journal of Rock Mechanics and Mining Sciences* 85 (May): 174–86. https://doi.org/10.1016/j.ijrmms.2016.03.018.

Jenq-Neng Hwang, Shyh-Rong Lay, and A. Lippman. 1994. “Nonparametric Multivariate Density Estimation: A Comparative Study.” *IEEE Transactions on Signal Processing* 42 (10): 2795–2810. https://doi.org/10.1109/78.324744.

Jiang, Quan, Jie Cui, Xiating Feng, and Yujing Jiang. 2014. “Application of Computerized Tomographic Scanning to the Study of Water-Induced Weakening of Mudstone.” *Bulletin of Engineering Geology and the Environment* 73 (4): 1293–1301. https://doi.org/10.1007/s10064-014-0597-5.

Jumikis, Alfreds R. 1966. “Some Engineering Aspects of Brunswick Shale.” In *1st ISRM Congress*. International Society for Rock Mechanics and Rock Engineering.

Jung, Woo-Jin, Yuji Ogata, Yuji Wada, Masahiro Seto, Kunihisa Katsuyama, and Terushige Okawa. 2001. “Effects of Water Saturation and Strain Rate on the Tensile Strength of Rocks under Dynamic Load.” *Doboku Gakkai Ronbunshu* 673: 53–59.

Kahraman, S. 2001. “Evaluation of Simple Methods for Assessing the Uniaxial Compressive Strength of Rock.” *International Journal of Rock Mechanics and Mining Sciences* 38 (7): 981–94. https://doi.org/10.1016/S1365-1609(01)00039-9.

Kalantari, Sajjad, Hamid Hashemolhosseini, and Alireza Baghbanan. 2018. “Estimating Rock Strength Parameters Using Drilling Data.” *International Journal of Rock Mechanics and Mining Sciences* 104 (April): 45–52. https://doi.org/10.1016/j.ijrmms.2018.02.013.

Karakul, Hasan, and Resat Ulusay. 2013. “Empirical Correlations for Predicting Strength

Properties of Rocks from P-Wave Velocity Under Different Degrees of Saturation." *Rock Mechanics and Rock Engineering* 46 (5): 981–99. https://doi.org/10.1007/s00603-012-0353-8.

Khaksar, A., P Taylor, and Z Fang. 2009a. "Rock Strength from Core and Logs, Where We Stand and Ways to Go." *... EAGE Conference and ...*, no. June: 8–11. https://doi.org/10.2118/121972-MS.

Khaksar, A., Philip Geoffrey Taylor, Zhi Fang, Toby John Kayes, Abraham Salazar, and Khalil Rahman. 2009. "Rock Strength from Core and Logs, Where We Stand and Ways to Go." In *EUROPEC/EAGE Conference and Exhibition*. Society of Petroleum Engineers. https://doi.org/10.2118/121972-MS.

Khaksar, A, F Gui, P G Taylor, A Younessi, K Rahman, Baker Hughes, T Richard, and Epslog Sa. 2014. "Enhanced Rock Strength Modelling , Combining Triaxial Compressive Tests , Non-Destructive Index Testing and Well Logs."

Khaksar, A, P Taylor, and Z Fang. 2009b. "Rock Strength from Core and Logs, Where We Stand and Ways to Go." *... EAGE Conference and ...*, no. June: 8–11. https://doi.org/10.2118/121972-MS.

Lan, Hengxing, C. Derek Martin, and Bo Hu. 2010. "Effect of Heterogeneity of Brittle Rock on Micromechanical Extensile Behavior during Compression Loading." *Journal of Geophysical Research* 115 (B1): B01202. https://doi.org/10.1029/2009JB006496.

Lashkaripour, G.R., and R. Ajalloeian. 2000. "The Effect Of Water Content On The Mechanical Behaviour Of Fine-Grained Sedimentary Rocks." In *ISRM International Symposium*. International Society for Rock Mechanics and Rock Engineering.

Laubscher, D.H. 1990. "A Geomechanics Classification System for the Rating of Rock Mass in Mine Design." *Journal of the Southern African Institute of Mining and Metallurgy* 90 (10): 257–73.

Lin, Jeen-Shang, and Yaneng Zhou. 2013. "Can Scratch Tests Give Fracture Toughness?" *Engineering Fracture Mechanics* 109 (September): 161–68. https://doi.org/10.1016/j.engfracmech.2013.06.002.

Lin, M. L., F. S. Jeng, L. S. Tsai, and T. H. Huang. 2005. "Wetting Weakening of Tertiary Sandstones—microscopic Mechanism." *Environmental Geology* 48 (2): 265–75. https://doi.org/10.1007/s00254-005-1318-y.

Lintao, Yang, Alec M. Marshall, Dariusz Wanatowski, Rod Stace, and Thushan Ekneligoda. 2017. "Effect of High Temperatures on Sandstone – a Computed Tomography Scan Study." *International Journal of Physical Modelling in Geotechnics* 17 (2): 75–90. https://doi.org/10.1680/jphmg.15.00031.

Lisabeth, Harrison P., and Wenlu Zhu. 2015. "Effect of Temperature and Pore Fluid on the Strength of Porous Limestone." *Journal of Geophysical Research: Solid Earth* 120 (9): 6191–6208. https://doi.org/10.1002/2015JB012152.

Liu, Guangsheng, Li Li, Mike Yao, David Landry, Farid Malek, Xiaocong Yang, and Lijie Guo. 2017. "An Investigation of the Uniaxial Compressive Strength of a Cemented Hydraulic Backfill Made of Alluvial Sand." *Minerals* 7 (1): 4. https://doi.org/10.3390/min7010004.

Liu, Zaobao, Jianfu Shao, Weiya Xu, and Qier Wu. 2015. "Indirect Estimation of Unconfined Compressive Strength of Carbonate Rocks Using Extreme Learning Machine." *Acta Geotechnica* 10 (5): 651–63. https://doi.org/10.1007/s11440-014-

0316-1.
M. Hassan, Amjed, and Hasan S. Al-Hashim. 2016. “Cost Effective Chelating Agent EOR Fluid System for Carbonate Reservoirs.” In *SPE Kingdom of Saudi Arabia Annual Technical Symposium and Exhibition*. Society of Petroleum Engineers. https://doi.org/10.2118/182788-MS.
Mahmoud, Ahmed Abdulhamid, and Hasan Al-Hashim. 2018. “Insight into the Mechanism for Oil Recovery Using EDTA Chelating Agent Solutions from Clayey Sandstone Rocks.” *Journal of Petroleum Science and Engineering* 161 (February): 625–35. https://doi.org/10.1016/j.petrol.2017.11.046.
Mann, R. L., and I. Fatt. 1960. “EFFECT OF PORE FLUIDS ON THE ELASTIC PROPERTIES OF SANDSTONE.” *GEOPHYSICS* 25 (2): 433–44. https://doi.org/10.1190/1.1438713.
Mao, Xian-biao, Lian-ying ZHANG, Tian-zhen LI, and Hai-shun LIU. 2009. “Properties of Failure Mode and Thermal Damage for Limestone at High Temperature.” *Mining Science and Technology (China)* 19 (3): 290–94. https://doi.org/10.1016/S1674-5264(09)60054-5.
Marinos, Paul, and Evert Hoek. 2001. “Estimating the Geotechnical Properties of Heterogeneous Rock Masses such as Flysch.” *Bulletin of Engineering Geology and the Environment* 60 (2): 85–92. https://doi.org/10.1007/s100640000090.
McPhee, C., J Reed, and Izaskun Zubizarreta. 2015. *Core Analysis: A Best Practice Guide*. Elsevier.
Mishra. 2016. “Kernel Density Estimators.” CVonline: The Evolving, Distributed, Non-Proprietary, On-Line Compendium of Computer Vision. 2016. http://homepages.inf.ed.ac.uk/rbf/CVonline/LOCAL_COPIES/AV0405/MISHRA/kde.html.
Mishra, Brijes, and Priyesh Verma. 2015. “Uniaxial and Triaxial Single and Multistage Creep Tests on Coal-Measure Shale Rocks.” *International Journal of Coal Geology* 137 (January): 55–65. https://doi.org/10.1016/j.coal.2014.11.005.
Mohamad, Edy Tonnizam, Danial Jahed Armaghani, Ehsan Momeni, and Seyed Vahid Alavi Nezhad Khalil Abad. 2015. “Prediction of the Unconfined Compressive Strength of Soft Rocks: A PSO-Based ANN Approach.” *Bulletin of Engineering Geology and the Environment* 74 (3): 745–57. https://doi.org/10.1007/s10064-014-0638-0.
Mohamed, Ibrahim, and Hisham A. Nasr-El-Din. 2013. “Fluid/Rock Interactions During CO2 Sequestration in Deep Saline Carbonate Aquifers: Laboratory and Modeling Studies.” *SPE Journal* 18 (3): 468–85. https://doi.org/10.2118/151142-PA.
Naeimipour, A., J. Rostami, I. S. Buyuksagis, and O. Frough. 2018. “Estimation of Rock Strength Using Scratch Test by a Miniature Disc Cutter on Rock Cores or inside Boreholes.” *International Journal of Rock Mechanics and Mining Sciences* 107 (July 2017): 9–18. https://doi.org/10.1016/j.ijrmms.2018.03.020.
Naghadehi, M. Zare, R. KhaloKakaie, and S. R. Torabi. 2010. “The Influence of Moisture on Sandstone Properties in Iran.” *Proceedings of the Institution of Civil Engineers - Geotechnical Engineering* 163 (2): 91–99. https://doi.org/10.1680/geng.2010.163.2.91.
Nicodeme, P. 1997. “Transition between Ductile and Brittle Mode in Rock Cutting.” *Rapport de Stage d’Option Scientifique, Ecole Polytechnique*.

Noufal, Abdelwahab, Christophe Germay, Tanguy Lhomme, Gehad Hegazy, and Thomas Richard. 2015. “Enhanced Core Analysis Workflow for the Geomechanical Characterization of Reservoirs in a Giant Offshore Field , Abu Dhabi.” *Abu Dhabi International Petroleum Exhibition and Conference*.

Nova, R. 1980. “The Failure of Transversely Isotropic Rocks in Triaxial Compression.” *International Journal of Rock Mechanics and Mining Sciences & Geomechanics Abstracts* 17 (6): 325–32. https://doi.org/10.1016/0148-9062(80)90515-X.

Nova, R., and A. Zaninetti. 1990. “An Investigation into the Tensile Behaviour of a Schistose Rock.” *International Journal of Rock Mechanics and Mining Sciences & Geomechanics Abstracts* 27 (4): 231–42. https://doi.org/10.1016/0148-9062(90)90526-8.

Ojo, O., and N. Brook. 1990. “The Effect of Moisture on Some Mechanical Properties of Rock.” *Mining Science and Technology* 10 (2): 145–56. https://doi.org/10.1016/0167-9031(90)90158-O.

Parate, NS. 1973. “Influence of Water on the Strength of Limestone.” *Transactions of the Society of Mining, AIME* 254: 127–31.

Pells, Philip J.N. 1993. “Uniaxial Strength Testing.” In *Rock Testing and Site Characterization*, 67–85. Elsevier. https://doi.org/10.1016/B978-0-08-042066-0.50010-0.

Price, N. J. 1960. “The Compressive Strength of Coal Measure Rocks.” *Colliery Engineering 37* 437: 283–92.

Rajabzadeh, M. A., Z. Moosavinasab, and G. Rakhshandehroo. 2012. “Effects of Rock Classes and Porosity on the Relation between Uniaxial Compressive Strength and Some Rock Properties for Carbonate Rocks.” *Rock Mechanics and Rock Engineering* 45 (1): 113–22. https://doi.org/10.1007/s00603-011-0169-y.

Ramos da Silva, Mikaël, Christian Schroeder, and Jean-Claude Verbrugge. 2008. “Unsaturated Rock Mechanics Applied to a Low-Porosity Shale.” *Engineering Geology* 97 (1–2): 42–52. https://doi.org/10.1016/j.enggeo.2007.12.003.

Ranjith, P. G., Daniel R. Viete, Bai Jie Chen, and M. Samintha A. Perera. 2012. “Transformation Plasticity and the Effect of Temperature on the Mechanical Behaviour of Hawkesbury Sandstone at Atmospheric Pressure.” *Engineering Geology* 151 (November): 120–27. https://doi.org/10.1016/j.enggeo.2012.09.007.

Rao, Dandina N. 1999. “Wettability Effects in Thermal Recovery Operations.” *SPE Reservoir Evaluation & Engineering* 2 (5): 420–30. https://doi.org/10.2118/57897-PA.

Rao, Qiu-hua, Zhi Wang, Hai-feng Xie, and Qiang Xie. 2007. “Experimental Study of Mechanical Properties of Sandstone at High Temperature.” *Journal of Central South University of Technology* 14 (S1): 478–83. https://doi.org/10.1007/s11771-007-0311-x.

Rathnaweera, T.D., P.G. Ranjith, and M.S.A. Perera. 2014. “Salinity-Dependent Strength and Stress–strain Characteristics of Reservoir Rocks in Deep Saline Aquifers: An Experimental Study.” *Fuel* 122 (April): 1–11. https://doi.org/10.1016/j.fuel.2013.11.033.

Reddish, D.J., and Ergül Yasar. 1996. “A New Portable Rock Strength Index Test Based on Specific Energy of Drilling.” *International Journal of Rock Mechanics and Mining Sciences & Geomechanics Abstracts* 33 (5): 543–48. https://doi.org/10.1016/0148-

9062(95)00083-6.
Reviron, N., T. Reuschlé, and J.-D. Bernard. 2009. “The Brittle Deformation Regime of Water-Saturated Siliceous Sandstones.” *Geophysical Journal International* 178 (3): 1766–78. https://doi.org/10.1111/j.1365-246X.2009.04236.x.
Richard, T., E. Detournay, A. Drescher, P. Nicodeme, and D. Fourmaintraux. 1998. “The Scratch Test As A Means To Measure Strength of Sedimentary Rocks.” In *SPE/ISRM Rock Mechanics in Petroleum Engineering*. Society of Petroleum Engineers. https://doi.org/10.2118/47196-MS.
Richard, Thomas, Fabrice Dagrain, Edmond Poyol, and Emmanuel Detournay. 2012. “Rock Strength Determination from Scratch Tests.” *Engineering Geology* 147–148 (October): 91–100. https://doi.org/10.1016/j.enggeo.2012.07.011.
Risnes, R., M.V. Madland, M. Hole, and N.K. Kwabiah. 2005. “Water Weakening of Chalk— Mechanical Effects of Water–glycol Mixtures.” *Journal of Petroleum Science and Engineering* 48 (1–2): 21–36. https://doi.org/10.1016/j.petrol.2005.04.004.
Roegiers, Jean-Claude. 1993. “The Use of Rock Mechanics in Petroleum Engineering: General Overview.” In *Surface and Underground Project Case Histories*, 605–16. Elsevier. https://doi.org/10.1016/B978-0-08-042068-4.50032-6.
Roehl, P.O., and P.W. Choquette. 1985. *Carbonate Petroleum Reservoirs*. Edited by Perry O. Roehl and Philip W. Choquette. Casebooks in Earth Sciences. New York, NY, NY: Springer New York. https://doi.org/10.1007/978-1-4612-5040-1.
Rosen, Richard, Bill Mickelson, Jason Fry, George Hill, Bob Knabe, and Munir Sharf-Aldin. 2007. “Recent Experience with Unconsolidated Core Analysis.” In *International Symposium of the Society of Core Analysts*.
Rosenbauer, R.J., and B. Thomas. 2010. “Carbon Dioxide (CO2) Sequestration in Deep Saline Aquifers and Formations.” In *Developments and Innovation in Carbon Dioxide (CO2) Capture and Storage Technology*, 57–103. Elsevier. https://doi.org/10.1533/9781845699581.1.57.
Santarelli, F.J., and M.B. Dusseault. 1991. “Core Quality Control In Petroleum Engineering.” In *The 32nd U.S. Symposium on Rock Mechanics (USRMS)*. American Rock Mechanics Association.
Schei, G, E Fjaer, E Detournay, C J Kenter, G F Fuh, and F Zausa. 2000. “The Scratch Test: An Attractive Technique for Determining Strength and Elastic Properties of Sedimentary Rocks.” *SPE Annual Technical Conference and Exhibition*, no. SPE 63255: 1–7. https://doi.org/10.2118/63255-MS.
Schmidt, Richard A. 1976. “Fracture-Toughness Testing of Limestone.” *Experimental Mechanics* 16 (5): 161–67. https://doi.org/10.1007/BF02327993.
Schön, Jürgen H. 2015. “Pore Space Properties.” In , 21–84. https://doi.org/10.1016/B978-0-08-100404-3.00002-0.
Schroeder, C. 1995. “LE ‘PORE COLLAPSE’: ASPECT PARTICULIER DE L’INTERACTION FLUIDE-SQUELETTE DANS LES CRAIES?” *Institut Francais Des Sciences et Technologies Des Transports, de l’Aménagement et Des Réseaux (IFSTTAR)*, 53–60.
Shakoor, A., and E. H. Barefield. 2009. “Relationship between Unconfined Compressive Strength and Degree of Saturation for Selected Sandstones.” *Environmental and Engineering Geoscience* 15 (1): 29–40. https://doi.org/10.2113/gseegeosci.15.1.29.

Shehata, Ahmed Mahmoud, and Hisham A. Nasr-El-Din. 2014. “Role of Sandstone Mineral Compositions and Rock Quality on the Performance of Low-Salinity Waterflooding.” In *International Petroleum Technology Conference*. International Petroleum Technology Conference. https://doi.org/10.2523/IPTC-18176-MS.

Shukla, Richa, P. G. Ranjith, S. K. Choi, A. Haque, Mohan Yellishetty, and Li Hong. 2013. “Mechanical Behaviour of Reservoir Rock Under Brine Saturation.” *Rock Mechanics and Rock Engineering* 46 (1): 83–93. https://doi.org/10.1007/s00603-012-0246-x.

Silva, G.P.D. De, P.G. Ranjith, and M.S.A. Perera. 2015. “Geochemical Aspects of CO2 Sequestration in Deep Saline Aquifers: A Review.” *Fuel* 155 (September): 128–43. https://doi.org/10.1016/j.fuel.2015.03.045.

Silva, V.R.S De, P.G. Ranjith, M.S.A. Perera, and B Wu. 2017. “Evaluation of Acoustic and Mechanical Properties of Sedimentary Rock under Different Saturation Conditions .” In *51st US Rock Mechanics / Geomechanics Symposium*. American Rock Mechanics Association.

Spain, David R., Raja Naidu, William Dawson, German D. Merletti, Rajeev Kumar, and Dai Yu Guo. 2015. “Integrated Workflow for Selecting Hydraulic Fracture Initiation Points in the Khazzan Giant Tight Gas Field, Sultanate of Oman.” In *Abu Dhabi International Petroleum Exhibition and Conference*. Society of Petroleum Engineers. https://doi.org/10.2118/177939-MS.

Suarez-Rivera, Roberto, Gary Ostroff, KaiSoon Tan, Bill Begnaud, Wesley Martin, and Tony Bermudez. 2003. “Continuous Rock Strength Measurements On Core And Neural Network Modeling Result In Significant Improvements In Log-Based Rock Strength Predictions Used To Optimize Completion Design and Improve Prediction of Sanding Potential and Wellbore Stability.” *SPE Annual Technical Conference and Exhibition*, no. SPE 84558: 1–9. https://doi.org/10.2118/84558-MS.

Sygała, Anna, Mirosława Bukowska, and Tomasz Janoszek. 2013. “High Temperature Versus Geomechanical Parameters of Selected Rocks – The Present State of Research.” *Journal of Sustainable Mining* 12 (4): 45–51. https://doi.org/10.7424/jsm130407.

Sylte, J.E., L.K. Thomas, D.W. Rhett, D.D. Bruning, and N.B. Nagel. 1999. “Water Induced Compaction in the Ekofisk Field.” In *SPE Annual Technical Conference and Exhibition*. Society of Petroleum Engineers. https://doi.org/10.2118/56426-MS.

Tariq, Zeeshan, S. M. Elkatatny, M. A. Mahmoud, A. Abdulraheem, A. Z. Abdelwahab, and M. Woldeamanuel. 2017. “Development of New Correlation of Unconfined Compressive Strength for Carbonate Reservoir Using Artificial Intelligence Techniques.” In *51st U.S. Rock Mechanics/Geomechanics Symposium*. American Rock Mechanics Association.

Thompson, Joshua Caine. 2010. “CHEMO-MECHANICAL EFFECTS ON ROCK STRENGTH, YOUNG’S MODULUS AND POISSON’S RATIO.” The University of Utah.

Tittmann, B. R., V. A. Clark, J. M. Richardson, and T. W. Spencer. 1980. “Possible Mechanism for Seismic Attenuation in Rocks Containing Small Amounts of Volatiles.” *Journal of Geophysical Research* 85 (B10): 5199. https://doi.org/10.1029/JB085iB10p05199.

Török, Á., and B. Vásárhelyi. 2010. “The Influence of Fabric and Water Content on Selected Rock Mechanical Parameters of Travertine, Examples from Hungary.”

Engineering Geology 115 (3–4): 237–45. https://doi.org/10.1016/j.enggeo.2010.01.005.

Tsiambaos, G, and N Sabatakakis. 2004. "Considerations on Strength of Intact Sedimentary Rocks." *Engineering Geology* 72 (3–4): 261–73. https://doi.org/10.1016/j.enggeo.2003.10.001.

Tsur-Lavie, Y., and S. A. Denekamp. 1982. "Comparison of Size Effect for Different Types of Strength Tests." *Rock Mechanics* 15 (4): 243–54. https://doi.org/10.1007/BF01240592.

Turki, W.H. 1991. "Drilling and Production of Khuff Gas Wells, Saudi Arabia." In *SPE/IADC Drilling Conference*. Society of Petroleum Engineers. https://doi.org/10.2118/21975-MS.

Ulusay, Reşat. 2015. *The ISRM Suggested Methods for Rock Characterization, Testing and Monitoring: 2007-2014*. Edited by Reşat Ulusay. Cham: Springer International Publishing. https://doi.org/10.1007/978-3-319-07713-0.

Varela, R. A., D. Marchal, A. M. Perez Mazas, J. Porras Lagarrigue, F. Sattler, G. Cavazzoli, and E. Lagarrigue. 2016. "Integrated Geomechanical Characterization for Vaca Muerta Fm.: Shale Oil Well Integration from Logs, Core, and Pressures for Fracture Optimization." In *50th U.S. Rock Mechanics/Geomechanics Symposium*. American Rock Mechanics Association.

Vasarhelyi, B. 2005. "Statistical Analysis of the Influence of Water Content on the Strength of the Miocene Limestone." *Rock Mechanics and Rock Engineering* 38 (1): 69–76. https://doi.org/10.1007/s00603-004-0034-3.

Vásárhelyi, B., and P. Ván. 2006. "Influence of Water Content on the Strength of Rock." *Engineering Geology* 84 (1–2): 70–74. https://doi.org/10.1016/j.enggeo.2005.11.011.

Verstrynge, E., R. Adriaens, J. Elsen, and K. Van Balen. 2014. "Multi-Scale Analysis on the Influence of Moisture on the Mechanical Behavior of Ferruginous Sandstone." *Construction and Building Materials* 54 (March): 78–90. https://doi.org/10.1016/j.conbuildmat.2013.12.024.

Vlis, AC. 1970. "Rock Classification by a Simple Hardness Test." *International Society of Rock Mechanics, Proceedings* 1 (1–19).

Vutukuri, V.S. 1974. "The Effect of Liquids on the Tensile Strength of Limestone." *International Journal of Rock Mechanics and Mining Sciences & Geomechanics Abstracts* 11 (1): 27–29. https://doi.org/10.1016/0148-9062(74)92202-5.

Wan, Zhi-jun, Yang-sheng Zhao, Yuan Zhang, and Chong Wang. 2009. "Research Status Quo and Prospection of Mechanical Characteristics of Rock under High Temperature and High Pressure." *Procedia Earth and Planetary Science* 1 (1): 565–70. https://doi.org/10.1016/j.proeps.2009.09.090.

Wang, W., and A. Gupta. 1995. "Investigation of the Effect of Temperature and Pressure on Wettability Using Modified Pendant Drop Method." In *SPE Annual Technical Conference and Exhibition*. Society of Petroleum Engineers. https://doi.org/10.2118/30544-MS.

White, Jon M., and Marian Mazurkiewicz. 1989. "Effect of Moisture Content on Mechanical Properties of Nemo Coal, Moberly, Missouri U.S.A." *Mining Science and Technology* 9 (2): 181–85. https://doi.org/10.1016/S0167-9031(89)90272-7.

Xiao-li, Xu, Kang Zong-xin, Ji Ming, Ge Wen-xuan, and Chen Jing. 2009. "Research of Microcosmic Mechanism of Brittle-Plastic Transition for Granite under High

Temperature." *Procedia Earth and Planetary Science* 1 (1): 432–37. https://doi.org/10.1016/j.proeps.2009.09.069.

Xu, Xiao-li, Feng GAO, Xiao-ming SHEN, and He-ping XIE. 2008. "Mechanical Characteristics and Microcosmic Mechanisms of Granite under Temperature Loads." *Journal of China University of Mining and Technology* 18 (3): 413–17. https://doi.org/10.1016/S1006-1266(08)60086-3.

Yi, Zhang, and Hemanta Kumar Sarma. 2012. "Improving Waterflood Recovery Efficiency in Carbonate Reservoirs through Salinity Variations and Ionic Exchanges: A Promising Low-Cost 'Smart-Waterflood' Approach." In *Abu Dhabi International Petroleum Conference and Exhibition*. Society of Petroleum Engineers. https://doi.org/10.2118/161631-MS.

Yin, Jian-Hua, Robina H.C. Wong, K.T. Chau, David T.W. Lai, and Guang-Si Zhao. 2017. "Point Load Strength Index of Granitic Irregular Lumps: Size Correction and Correlation with Uniaxial Compressive Strength." *Tunnelling and Underground Space Technology* 70 (November): 388–99. https://doi.org/10.1016/j.tust.2017.09.011.

Zare Naghadehi, M., R. KhaloKakaie, and S. R. Torabi. 2010. "The Influence of Moisture on Sandstone Properties in Iran." *Proceedings of the Institution of Civil Engineers - Geotechnical Engineering* 163 (2): 91–99. https://doi.org/10.1680/geng.2010.163.2.91.

Zhang, LianYing, XianBiao Mao, and AiHong Lu. 2009. "Experimental Study on the Mechanical Properties of Rocks at High Temperature." *Science in China Series E: Technological Sciences* 52 (3): 641–46. https://doi.org/10.1007/s11431-009-0063-y.

Zhao, Zhihong, Jun Yang, Dafeng Zhang, and Huan Peng. 2017. "Effects of Wetting and Cyclic Wetting–Drying on Tensile Strength of Sandstone with a Low Clay Mineral Content." *Rock Mechanics and Rock Engineering* 50 (2): 485–91. https://doi.org/10.1007/s00603-016-1087-9.

Zhou, Yaneng, and Jeen-Shang Lin. 2014. "Modeling the Ductile–brittle Failure Mode Transition in Rock Cutting." *Engineering Fracture Mechanics* 127 (September): 135–47. https://doi.org/10.1016/j.engfracmech.2014.05.020.

Appendix

Table 5: Summary table of the effect of saturation and aging on all the rock types investigated.

Rock Type	Condition	Qualitative Change in UCS (Comparing the kernel diagrams relative to baseline UCS trends)	Quantitative Change in UCS (%)
Indiana Limestone	SB	Minimal to no appreciable change in the trend post-saturation	(12)
	SW	Water-weakening indicated by shift in the trend towards the left of the diagram	(12)
	SO	Kernel diagram showing similar trend as the baseline UCS	Inconclusive
	AB	No apparent change in strength	Heterogeneity of the sample led to inconclusive results
	AW	No change in the trend as shown by the kernel diagram	-
	AO	No change shown by the trend in the kernel diagram	-
Desert Pink Limestone	SB	No change in the trend as shown by the kernel diagram	(4)
	SW	Relatively larger shift towards the left as compared to Indiana Limestone due to its larger porosity	(24)
	SO	Kernel diagram showing similar trend as the baseline UCS	Inconclusive
	AB	Slight shift towards the left but inconclusive due to sample heterogeneity	Similar comments as Indiana Limestone
	AW	Slight shift towards the right indicating strengthening.	9
	AO	Kernel diagram shifts towards the right, indicating strengthening	16
Berea Buff Sandstone	SB	Kernel diagram shifts towards the right, indicating strengthening	13
	SW	Clear water-weakening as observed by the shift in kernel diagram towards the left	(19)
	SO	A large shift towards the left illustrating strong weakening due to crude oil saturation	(20)
	AB	A flatter kernel plot is reported after aging which seems to cause a strength retention	(0)
	AW	Bi-modal behavior shown after aging. Water causes the strength to deteriorate and hence the shift in the kernel diagrams towards the left. Temperature opposes the water-weakening effect and thus we see a smaller second peak tending towards higher strength.	(10)
	AO	First peak towards the left illustrates weakening. A smaller second peak towards the right indicates strengthening due to temperature. Overall weakening of the rock sample is observed	(10)
Berea Grey Sandstone	SB	Trend shifts towards the right but relatively less as compared to Berea Buff	4
	SW	A larger shift towards the left observed owing to greater amount of clay swelling minerals relative to Berea Buff sample	(25)
	SO	No appreciable change post-oil saturation pointing towards clay swelling mechanism responsible for the weakening	(2)
	AW	Similar observations as for the Berea Buff sample	(11)
	AO	Similar to the Berea Buff sample. The second peak is less developed indicating lower affinity towards strengthening	(14)

S stands for saturation, A stands for aging; B – Brine, W – distilled water, O – Crude Oil

Table 6: Correlation between various internal/external factors and geomechanical properties.

Rock	Parameters Studied			Factors Investigated									Relationship				Reference
	UCS	*E*	*TS*	*ρ*	*Φ*	*Saturation Degree*	*Water Content*	*Moisture Content*	*Water Absorption*	*Surface Tension*	*Strain Rate*	*Dielectric Constant*	*Exponential*	*Power*	*Negative Exponential*	*Negative Power*	
Sandstone	x							x							x		(Hawkins and McConnell 1992)
			x								x			x			(Jung et al. 2001)
	x					x									x		(M. L. Lin et al. 2005)
		x				x									x		
Limestone			x									x	x				(Vutukuri 1974)
			x							x			x				
	x			x									x				(Vasarhelyi 2005)
Siltstone	x						x								x		(Erguler and Ulusay 2009)
		x					x								x		
			x				x								x		
	x			x									x				
	x				x											x	
	x								x							x	
Mudstone	x						x								x		(Lashkaripour and Ajalloeian 2000)
	x						x								x		(Erguler and Ulusay 2009)
		x					x								x		
			x				x								x		
	x			x									x				
	x				x											x	
	x								x							x	

Table 7: Investigations on the impact of fluid saturation on geomechanical parameters.

Study	Rock Type	Tests Conducted	Φ (%)	Saturation Method	% UCS Loss	% Young's Modulus Loss	% Tensile Strength Loss
(Price 1960)	Markham Sandstone	UCS	6	Air dry (Moisture content 38-62%)	-	-	-
	Parkgate rock Sandstone		10		45		
	Pennant Sandstone		2.5		45		
	Darley Dale Sandstone		19.5		45		
(Mann and Fatt 1960)	Boise Sandstone	Compression test	26.5	Water saturated using vacuum desiccator	-	15.1	-
	Berea Sandstone		20.5			6.33	
	Bandera Sandstone		20			19	
(Colback and Wiid 1965)	Quartzitic Shale	Triaxial and UCS	0.3	Water saturated	50	-	-
	Quartzitic Sandstone		15		50		
(Dube and Singh 1972)	Sandstone	Brazilian Disc	0.7-3.2	Relative Humidity's	-	-	11 - 48.6
(Parate 1973)	Limestone	Compression test and Brazilian Disc	4	Water saturated using vacuum desiccator	37.5	16.7	-
(Eeckhout and Peng 1975)	Beatrice Mine Shale	Compression test	1-3	Relative humidity environments	-	59.5-74.7	-
	Matthews Mine Shale					55-59	
	Armco Mine Shale					9.5-49.5	
(Bell 1978)	Fell Sandstone	UCS, Point load, and Brazilian Disc	6.5-20.7	Water saturated using vacuum desiccator	8.2-53	-	-
(White and Mazurkiewicz 1989)	Bituminous coal	UCS	-	Water saturated (Moisture content 12%)	12.2-21.1	31.1-34.3	-
(Ojo and Brook 1990)	Low Close Sandstone	Point load, Tensile strength, and UCS	-	Water saturated	37.5	-	51
	Woodkirk Sandstone				37.5		-

Table 8: Investigations on the impact of fluid saturation on geomechanical parameters (Continued).

Study	Rock Type	Tests Conducted	Φ (%)	Saturation Method	% UCS Loss	% Young's Modulus Loss	% Tensile Strength Loss
(Hadizadeh and Law 1991)	Sandstone	UCS	1.5	-	45	36	-
(Dyke and Dobereiner 1991)	Waterstone	UCS	22.3	Relative humidity environments	36.8	30.8	-
	Bunter Sandstone		21.1		20.8	25	
	Penrith Sandstone		12.3		23	11	
(Hawkins and McConnell 1992)	Bristish Sandstone	UCS	-	Water saturated	8.2-78.1	2.5-70	-
(Anwar et al. 1998)	Sandy Shale-1	UCS and Uniaxial tensile strength	-	Water saturated	75	94	83
	Sandy Shale-2				81	66.7	80
	Shale (Non-laminated)				67	73	75
	Shale (laminated)				68	75	89
	Sandstone				51	45	41
(Lashkaripour and Ajalloeian 2000)	Mudstone	UCS	-	Water saturated	Up to 93.4	-	-
	Mud Shale				Up to 90.4		
	Clay Shale				Up to 94		
(Vasarhelyi 2005)	Miocene Limestone	UCS and Brazilian Disc	11-52.2	Water saturated	2-74	0-53	0-77
(Lin et al. 2005)	Sandstone	UCS	11.5-24.6	Water saturated using vacuum desiccator	16-86	57-60	-
(Silva et al. 2008)	Beringen Shale	UCS	2.4-7.5	Water saturated using vacuum desiccator	80	60	-
(Shakoor and Barefield 2009)	Sandstone	UCS	4.1-12.7	Water saturated	20-70	-	-

Table 9: Investigations on the impact of fluid saturation on geomechanical parameters (Continued).

Study	Rock Type	Tests Conducted	Φ (%)	Saturation Method	% UCS Loss	% Young's Modulus Loss	% Tensile Strength Loss
(Erguler and Ulusay 2009)	Siltstone	UCS, Brazilian Disc, and Needle penetration	5.3-42.1	Water saturated using vacuum desiccator	56-90.2	35-87.5	42.9-95.5
	Mudstone		2.1-48.1		44.7-88.7	20-93	29-93.1
	Marl		6.1-53.9		61.2-81.4	57.1-76.5	19.6-91.7
(Török and Vásárhelyi 2010)	Travertine	UCS	2.1-13.1	Water saturated	0.7-31.8	-	-
(Huang et al. 2010)	Longyou Sandstone	UCS and SHPB	17	Water saturated	51.6	-	-
(Gajic et al. 2011)	Struganik limestone	UCS	1.1-3.3	Water saturated	10	-	-
(Rajabzadeh et al. 2012)	Limestone	UCS	0.2-9.7	Water saturated	15-71	-	-
(Karakul and Ulusay 2013)	Sandstone	Brazilian Disc	2.7-16.2	Water saturated using vacuum desiccator	-	-	63
	Limestone		0.5-15.4				16
(Verstrynge et al. 2014)	Brusselian ferruginous sandstone	UCS and controlled creep test	21-30	Water saturated with vacuum desiccator	Up to 40	-	-
	Diestian ferruginous sandstone		22-45		50-59		

Vitae

Name: Mohammad Rasheed Khan

Nationality: Pakistani

Date of Birth: 8/30/1992

Email: taharashid@hotmail.com

Address: House B-90, Block-5, Gulshan-e-Iqbal, 75300, Karachi, Sindh, Pakistan.

Academic Background: Master of Science in Petroleum Engineering

Publications:

Tariq, Zeeshan, Mohamed Mahmoud, Hasan Al-Yousef, and **Mohammad Rasheed Khan**. "Carbonate Rocks Resistivity Determination using Dual and Triple Porosity Conductivity Models." *Petroleum.* (In Press).

Khan, Mohammad Rasheed, Sami Alnuaim, Zeeshan Tariq, and Abdulazeez Abdulraheem. "Machine Learning Application for Oil Rate Prediction in Artificial Gas Lift Wells." In SPE Middle East Oil and Gas Show and Conference. Society of Petroleum Engineers, 2019.

Khan, Mohammad Rasheed, Ahmed Sadeed, Abdul Asad, Zeeshan Tariq, and Muhammad Tauqeer. "Maximizing Oil Recovery in a Naturally Fractured Carbonate Reservoir Using Computational Intelligence based on Particle Swarm Optimization." In PAPG/SPE Pakistan Section Annual Technical Conference and Exhibition. Society of Petroleum Engineers, 2018.

Khan, Mohammad Rasheed, Zeeshan Tariq, and Abdulazeez Abdulraheem. "Machine Learning Derived Correlation to Determine Water Saturation in Complex Lithologies." In SPE Kingdom of Saudi Arabia Annual Technical Symposium and Exhibition. Society of Petroleum Engineers, 2018.

Tariq, Zeeshan, Mohamed Mahmoud, Hasan Al-Yousef, and **Mohammad Rasheed Khan**. "Non-Archie Rock Characterization Using Triple Porosity Conductivity Model in Carbonate Reservoirs." In SPE Kingdom of Saudi Arabia Annual Technical Symposium and Exhibition. Society of Petroleum Engineers, 2018.

Tariq, Zeeshan, Mohamed Mahmoud, Amjed Hassan, **Mohammad Rasheed Khan**, and Ahmed Sadeed. "Carbonate

Rock Resistivity Index Measurement Using Equivalent Rock Model." In SPE Kingdom of Saudi Arabia Annual Technical Symposium and Exhibition. Society of Petroleum Engineers, 2018.

Tariq, Zeeshan, Abdulazeez Abdulraheem, **Mohammad Rasheed Khan**, and Ahmed Sadeed. "New Inflow Performance Relationship for a Horizontal Well in a Naturally Fractured Solution Gas Drive Reservoirs using Artificial Intelligence Technique." In Offshore Technology Conference Asia. Offshore Technology Conference, 2018.

Munawar, Muhammad Dawood, Dandina Rao, and **Mohammad Khan**. "Evaluation of Gas Assisted Gravity Drainage (GAGD) Using CO 2 in a Limestone Formation through Compositional Simulation." In SPE/PAPG Pakistan Section Annual Technical Conference and Exhibition. Society of Petroleum Engineers, 2017.

Tariq, Zeeshan, Sami Alnuaim, Abdulazeez Abdulraheem, and **Mohammad Rasheed Khan**. "New Methodology to Quantify Productivity of Vertical Wells in Naturally Fractured Solution Gas Drive Reservoirs with Dual Porosity and Dual Permeability." In PAPG/SPE Pakistan Section Annual Technical Conference and Exhibition. Society of Petroleum Engineers, 2016.

Shoaib, M., M. S. Qamar, **M. R. Khan**, A. Khan, S. Mumtaz, and A. Abbasi. "Tight Gas Reservoir (TGR)-In Place & Reserves Estimation and Economic Feasibility of Project." In SPE Middle East Oil & Gas Show and Conference. Society of Petroleum Engineers, 2015.

Educational Qualifications: **MSc. Petroleum Engineering** – 2019

King Fahd University of Petroleum & Minerals, Saudi Arabia.

B.E Petroleum Engineering – 2015

NED University of Engineering & Technology, Pakistan.